DEVELOPMENT AND MECHANISTIC STUDIES OF THE CHROMIUM TETRAMETHYLTETRAAZAANNULENE CATALYST SYSTEM FOR THE COPOLYMERIZATION OF CARBON DIOXIDE AND EPOXIDES

A Dissertation

by

SHAWN BRENDAN FITCH

Submitted to the Office of Graduate Studies
Texas A&M University
in partial fulfillment of the requirements for the degree of

DOCTOR OF PHILOSOPHY

May 2009

Major Subject: Chemistry

DEVELOPMENT AND MECHANISTIC STUDIES OF THE CHROMIUM TETRAMETHYLTETRAAZAANNULENE CATALYST SYSTEM FOR THE COPOLYMERIZATION OF CARBON DIOXIDE AND EPOXIDES

A Dissertation

by

SHAWN BRENDAN FITCH

Submitted to the Office of Graduate Studies
Texas A&M University
in partial fulfillment of the requirements for the degree of

DOCTOR OF PHILOSOPHY

Approved by:

Co-Chairs of Committee,	Donald J. Darensbourg
	Marcetta Y. Darensbourg
Committee Members,	Francois P. Gabbai
	Abraham Clearfield
	Terry S. Creasy
Head of Department,	David H. Russell

May 2009

Major Subject: Chemistry

ABSTRACT

Development and Mechanistic Studies of the Chromium Tetramethyltetraazaannulene Catalyst System for the Copolymerization of Carbon Dioxide and Epoxides.

(May 2009)

Shawn Brendan Fitch, B.S., Texas A&M University

Co-Chairs of Advisory Committee: Dr. Donald J. Darensbourg
Dr. Marcetta Y. Darensbourg

A prominent goal of scientists is to develop products and processes to meet the ever-growing needs of society. Today's needs include products that are economical, specialized, and made through processes with minimal impact on the environment. One such product that serves an important and widespread need is poly(bisphenol A carbonate) for its physical properties and ease of synthesis and processing. However, this polymer does not meet the growing need of being environmentally benign as production involves carcinogenic, chlorinated solvents and toxic monomers that can leach out from the polymer product.

An answer to this new demand is the development of a different process for the production of polycarbonate plastics utilizing carbon dioxide and epoxides. Carbon dioxide is an attractive monomer that is cheap and nontoxic, and its utilization signifies an important contribution to counteract global greenhouse emissions. The stability of carbon dioxide has posed a significant and complex challenge towards its utilization.

Epoxides are attractive since they are synthesized from a wide variety of olefins, both naturally occurring and those derived from petroleum. The exploration of catalysts to facilitate the coupling of epoxides to carbon dioxide to afford polycarbonates has been under investigation in the Darensbourg lab for fifteen years, and has lead to the development of several successful systems such as zinc bisphenoxides and chromium salens. This dissertation focuses on the development of another successful catalyst system, chromium tetramethyltetraazaannulene, and further elucidation of the mechanism by which polycarbonates are formed. Herein, aspects of the copolymerization process using this system will be discussed in detail, such as cocatalyst and pressure dependence, catalyst derivatization, and kinetic and mechanistic investigations. The end result of these investigations is the development of the most active chromium-based catalyst for the copolymerization of cyclohexene oxide and carbon dioxide and a better understanding of how the copolymer product is produced.

DEDICATION

I dedicate this dissertation to my mother and father. Without their guidance and inspiration, I would have never made it as far as I have come. They taught me the importance of goals and to work hard in order to achieve those goals. They provided me with the opportunities and experiences that built a broad base of knowledge, leadership, and responsibility, whether through Scouting, schooling, or hobbies. My mom taught me to be organized and analytical, while my dad taught me ingenuity, as well as sparking and nurturing my interest in chemistry. It is through them that I learned one of the most important lessons in life: You cannot push a chain; you have to pull it.

ACKNOWLEDGEMENTS

For as long as I can remember (and apparently before that, so my parents tell me) my interests have been in the field of science. Up until the 10th grade, Sea World and marine biology dominated my visions of the future. That was until Mrs. Anderson and high school chemistry. I have no idea if it was the mystique of chemical transformation, basic fundamental nature, or a combination with the "clandestine" stories from my father, a Fort Worth Police Officer working in the narcotics division with a passion for chemistry. No matter the cause, after my introduction to chemistry, I knew I had found my calling.

Once I began my journey in the field of chemistry, I met many mentors along the way. The first of which was my undergraduate advisor, Dr. John Hogg, who gave me my first impression of Texas A&M chemistry. He was a very enthusiastic man who met an untimely end, but during his tenure I was privileged to be one of the numerous students he inspired to pursue greatness. I learned the real value of chemistry once I began my undergraduate research experience under Professor Paul A. Lindahl, working with, then graduate student, Matt Bramlett. Matt taught me a great deal of common sense around the lab and with air sensitive chemistry and glove boxes. He and Brandon Hudder also taught me the importance of having fun while working to break up any moments of boredom and monotony that frequently occurred while watching *E. coli* grow, among other tedious biochemical assays.

Also during pursuit of my undergraduate degree, I made the decision to join Lambda Chi Alpha fraternity. I regard this decision as one of the best I have made in my life. Through this organization, I have made an incredible number of friends that have made a forever memorable impact on my life. To begin, David Swift, whom I met in the dorm a couple years before joining the fraternity, quickly became and has been ever since, my best friend and someone I can call on if ever I am in need of anything. Tim Pool could possibly be the person responsible for getting me involved in the fraternity, and despite his dropping out of chemistry and choosing to fly an Apache attack helicopter, I care for him very much and cannot hold it against him. I also cannot forget the numerous conversations with my big brother Aaron Atkin, a truly awesome person who has chosen to serve in ways concealed but to those with the proper authority. Throughout most of my graduate school tenure, I have had the privilege of getting to know someone who later became another great friend of mine, Jason Ewing. He taught me many things, including personal improvement through weight training and martial arts, as well as a greater interest in the electronic side of my hobbies. Other figures that have influenced my life in the fraternity are (but not limited to): Ryan Jenkins, Matt Gardner, Eric Berger, Jonathon Clites, Lane Enderby, Paul Segreto, Trey Marak, Christopher Stokes, Daniel Springer, Blake Spence, and my little bro, Matt Reid.

Graduate school has been everything but a cake walk. For the most part, it has the requirement of a normal job, expecting an exceptional amount of effort and thought, with select times requiring every ounce of attention and willpower. The graduate school experience has, however, been extremely rewarding to me. All throughout this time, I

have benefitted from discussions between group members regarding directions to take my research projects and likewise to theirs. I would like to thank my research advisors, Drs. Donald and Marcetta Darensbourg. Don has always provided fundamental directions when results were sluggish, while Marcetta has been present to challenge convention to ensure thorough investigation. I cannot extend enough appreciation to Jeremy Andreatta for his timeless discussions, both about research and otherwise, that have helped me gain a better knowledge of chemistry and the world around me. I would also like to thank the advice and friendship of Drs. Christine Thomas, Kayla Green, and Eric Frantz. They all helped to keep me on track and provide me with fresh new directions in which to take my research. I cannot forget the patience of Drs. Joseph H. Reibenspies and Nattamai Bhuvanesh for their continued patience in collecting X-ray crystal date and resolving structures. Many of the structures presented in this dissertation would not be possible if it were not for these crystal "gods". I must also thank my other fellow members of the DJD group: Adrianna Moncada, Osit "Pop" Karroonnirun, Ross Poland, and Sheng-Hsuan Wei for their numerous intellectual (and very often less serious) conversations, as well as the MYD research group. Two other people that made my graduate school experience much easier, and absolutely must not be left unmentioned, are Susan Winters and Sandy Manning. They have served as a both liaisons and translators for the departmental and bureaucratic intricacies of the department and university. Sue, you spoke of leaving many years ago and I said you could not quit (retire) until I was finished (as every new student requests). Now that I am finished, you are now free to go.

Last, but certainly not least, an extra special acknowledgement goes to my girlfriend of nearly three years, Tiffany Sweet. Ever since meeting her during my second year in graduate school, that part of my life has never felt so fulfilled, despite the seemingly insurmountable distance between us. You have been incredibly patient with the trials and tribulations that I have had to go through in these three long years, and one day I hope to be able to make your efforts worthwhile. I love you very much.

TABLE OF CONTENTS

CHAPTER Page

LIST OF FIGURES

Page

Page

Page

Page

Page

Page

LIST OF TABLES

Page

Page

CHAPTER I

INTRODUCTION

A brief discussion on carbon dioxide

In recent years, carbon dioxide has received much attention in both the scientific community and the general public. With atmospheric concentrations of CO_2 on the rise and the impending threat of 'global climate change', many scientists are looking for ways to reduce CO_2 emissions. In addition to these efforts, others are concentrating their efforts on capture and sequestration or utilization of this greenhouse gas for industrial and/or health and safety benefits. Carbon dioxide has found growing applications in refrigerants, water treatment, dry-cleaning, the food and agriculture industry, and chemical synthesis, either as a solvent, reagent, or for chemical separation.[1,2] Much of the attraction to carbon dioxide stems from its price and availability as well as its inherent properties of being nontoxic, nonflammable, noncorrosive, and having an easily obtainable supercritical state. The critical point for carbon dioxide lies at 31.1 °C and 72.8 bar, upon which there is no longer a distinction between the liquid and gaseous phases, as shown in Figure 1.

This dissertation follows the style and format of the *Journal of the American Chemical Society.*

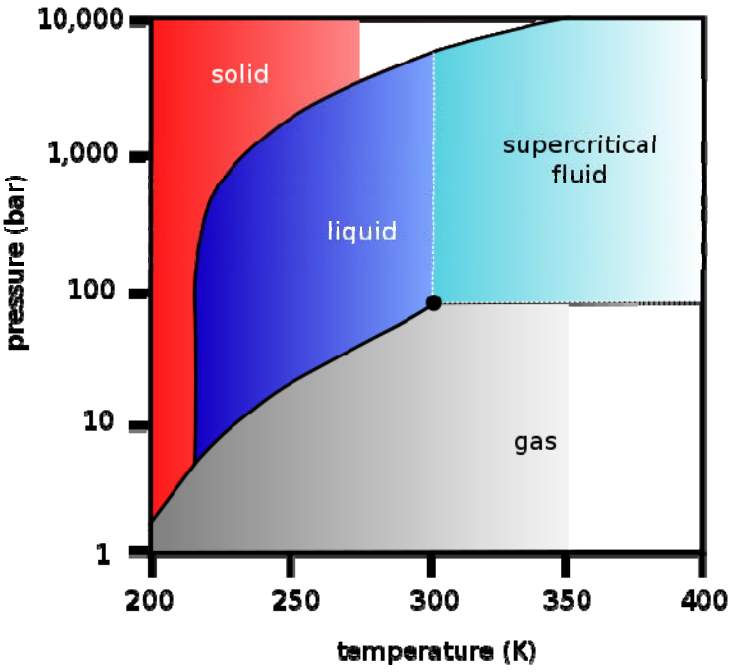

Figure 1. Phase diagram of carbon dioxide.

Aspects and concerns for polycarbonates currently produced industrially

For over a decade, our research efforts have focused on the utilization of carbon dioxide for a more environmentally benign route towards the production of polycarbonates. Currently, polycarbonate plastics comprise a large portion of the polymer industry and are produced industrially by the interfacial reaction between a caustic solution containing a diol, typically Bisphenol A, and phosgene in a chlorinated solvent (Figure 2). This route poses several human and environmental health concerns.[3] One such worry is with the use of large quantities of carcinogenic chlorinated solvents.

Dichloromethane is used to extract the polymer from the reaction and must be separated and disposed in a proper, costly manner. Additionally, the use of Bisphenol A due to its possible disruption of the human endocrine system is also an area of great concern.[3] Resent studies into the biological effects of Bisphenol A have led several governments to ban the use of Bisphenol A plastics in baby bottles and similar products. By far the most hazardous component in the production of poly(Bisphenol A carbonate) (PBPA) is phosgene, which exhibits extreme toxicity, and upon exposure, can result in pulmonary edema and death.

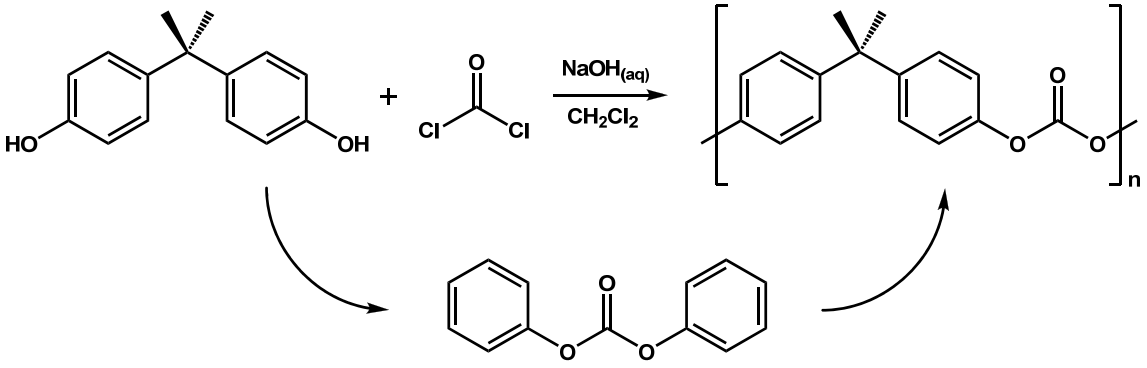

Figure 2. The step-growth condensation reaction of Bisphenol A and phosgene to produce poly(Bisphenol A carbonate) along with an alternate route using diphenyl carbonate.

An alternative and more widely used route to PBPA uses diphenyl carbonate instead of phosgene. This process eliminates the use of organic solvents by operating in a melt polymerization at 300 °C, with the reaction being driven by the removal of

phenol. This method produces a lower molecular weight polymer than the biphasic method but has the advantage of direct isolation of the polymer. Although this method is less hazardous than that of the interfacial process as it lack the use of phosgene and organic solvents, diphenyl carbonate is still often produced using phosgene and the recovered phenol from the polymerization reaction. Therefore, with the demand for polycarbonates expected to increase from 572,000 tonnes in 2007 to 694,000 tonnes by 2011 in the United States alone, new methods of production without the hazards of today's processes, must be explored.[4]

Poly(Bisphenol A carbonate) was first discovered in 1953 by Schell and Fox[5] and marketed by General Electric under the trade name Lexan® which, in 2007, has been sold to SABIC Innovative Plastics. This polymer is optically transparent and has an impact strength of up to 900 J/m, approximately 250 times stronger than common glass but only half the weight. It has a wide usable temperature range (-100 °C – 135 °C) with a glass transition temperature of 150 °C.[6] With properties very similar to those of poly(methyl methacrylate), the strength, clarity, and workability of PBPA make it useful for a variety of applications ranging from paneling used in windows and 'bullet-proof' glass, optical storage devices such as CDs and DVDs, lenses, and storage containers.

Background into the copolymerization of carbon dioxide and epoxides

A more environmentally benign route for the production of polycarbonates can be achieved through the alternating copolymerization of carbon dioxide and epoxides.

The reaction depicted in Figure 3 shows the coupling of an epoxide and CO_2 facilitated by a metal catalyst yielding three possible products: polycarbonate, polyether, and cyclic carbonate. Polycarbonate is formed by the alternating insertion of epoxide and CO_2. A polyether linkage is formed from the consecutive ring opening of epoxide while the cyclic carbonate byproduct is formed from backbiting of the polymer chain, producing a thermodynamically stable five-membered carbonate ring. This reaction can be performed using a variety of epoxides with cyclohexene oxide (CHO) and propylene oxide (PO) being the most common. Cyclohexene oxide is an alicyclic epoxide that provides a polymer with inadequate mechanical properties for current industrial needs, but its high reactivity and low propensity to form cyclic carbonate make it useful for academic investigation. Propylene oxide is an aliphatic, terminal epoxide, whose corresponding polycarbonate has found uses in industry as a binder for ceramics and in packaging. The propensity to form cyclic byproducts is much higher when propylene oxide is employed due to a low strain on the newly formed carbonate ring.[7] This is due to the inherent ring strain imposed by the chair conformation of the cyclohexylene ring onto the five-membered cyclic carbonate ring. The lack of steric restriction within propylene carbonate allows it to act as a thermodynamic sink, making the production of poly(propylene carbonate) difficult.

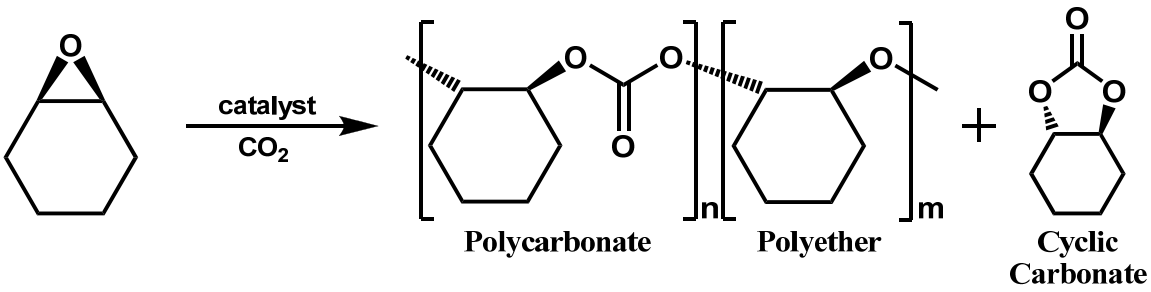

Figure 3. The reaction of epoxide and CO_2 to produce polycarbonate, polyether, and cyclic carbonate.

This copolymerization of carbon dioxide and epoxides has been studied for 40 years, beginning in 1969 when Inoue discovered a heterogeneous catalyst made from the mixture of diethyl zinc and water facilitated the copolymerization of propylene oxide and carbon dioxide to afford a polycarbonate product, but with very low activity (TOF < 1 h^{-1}), where activity is defined the moles of epoxide consumed per mole catalyst per hour (turnover frequency (TOF)).[8] The active species was unknown but thought it to be a mixture of zinc hydroxide and zinc oxide. Inoue then developed, in 1978, an aluminum tetraphenyl porphyrin complex as the first homogeneous catalyst capable of homopolymerizing epoxides and copolymerizing epoxides with CO_2, but was also plagued with low activities (TOF < 1 h^{-1}).[9] It was not until 1995 that Darensbourg and coworkers discovered the first homogeneous zinc-based catalyst system.[7] These zinc bisphenoxides (Figure 4) provided a significant increase in activity (TOF = 16 h^{-1}) over previously used catalyst systems for the copolymerization of CO_2 and cyclohexene oxide. The use of zinc β-diiminates (Figure 4) by Coates 1998 represent some of the

most active catalysts to date.[10] These catalysts exhibited TOFs with cyclohexene oxide generally around 800 and approaching 2,300 h^{-1}; however, their activity decreases quickly with time. In 2000, Holmes and coworkers found that a highly fluorinated, supercritical CO_2-soluble chromium tetraphenyl porphyrin complex proved active for copolymerization, achieving 173 turnovers per hour.[11] Darensbourg and coworkers in 2001 reported the use of chromium salens (salen = N,N'-bis(salicylidene) ethylenediamine) as highly active and robust catalysts for the copolymerization of CO_2 and CHO with activities reaching upwards of 1,150 per hour (Figure 4).[12] The development of these catalysts was spurred by the work of Jacobsen who found chromium salen complexes to be highly active for the asymmetric ring opening of epoxide.[13] Chromium has proven one of the most active metal for the copolymerization of CO_2 and epoxide when utilizing the salen ligand architecture.[14] The derivatization and study of the chromium salen system have been the primary focus of the Darensbourg group.

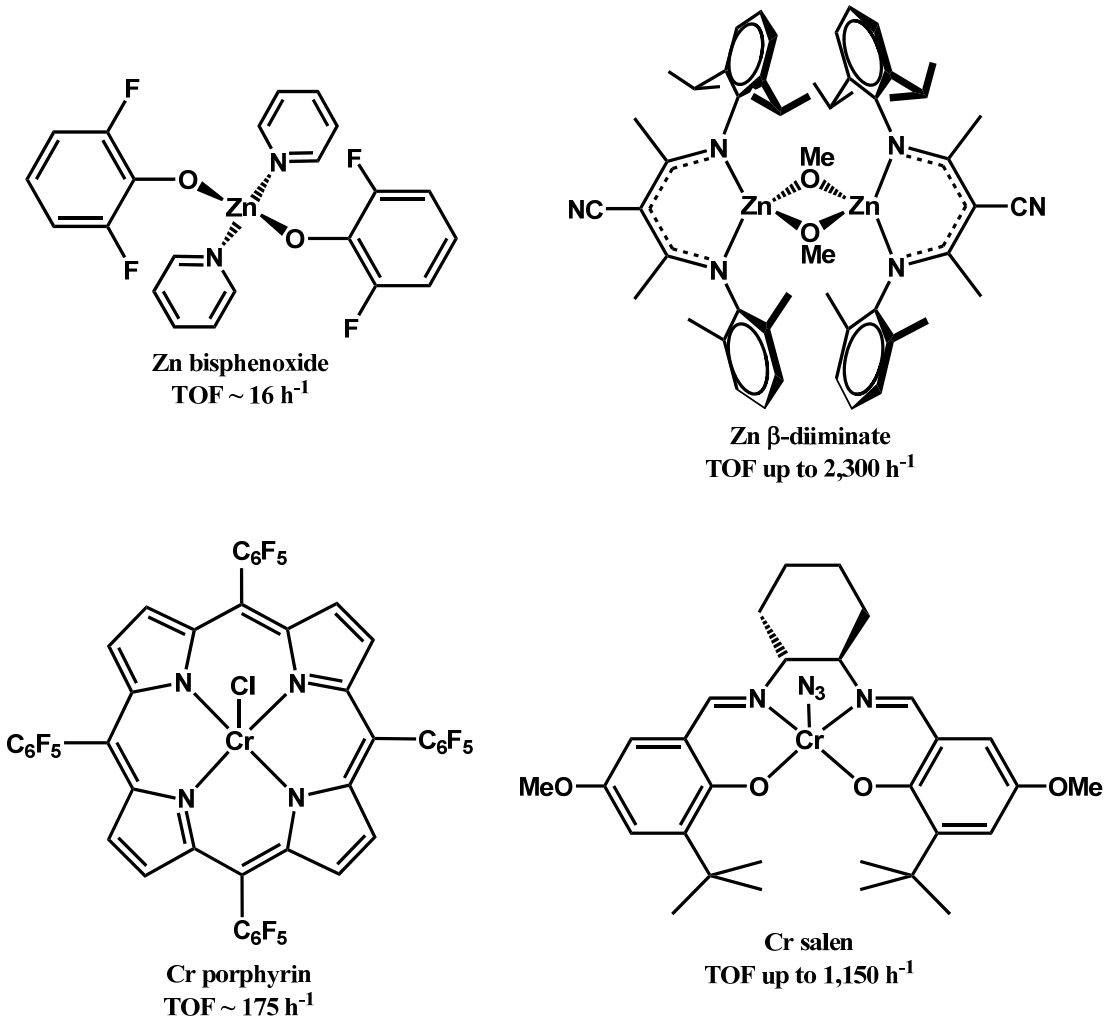

Figure 4. Active catalysts for the copolymerization of CO_2 and cyclohexene oxide.

A proposed mechanism for the chromium salen facilitated copolymerization of CO_2 and epoxide has been proposed by Darensbourg and coworkers.[14] The first step of this mechanism (Figure 5) is the addition of a nucleophilic cocatalyst, such as a neutral Lewis base or an anion, which binds to the metal center forming a six-coordinate "activated" complex. Once dissolved in epoxide, this species exists in equilibrium with

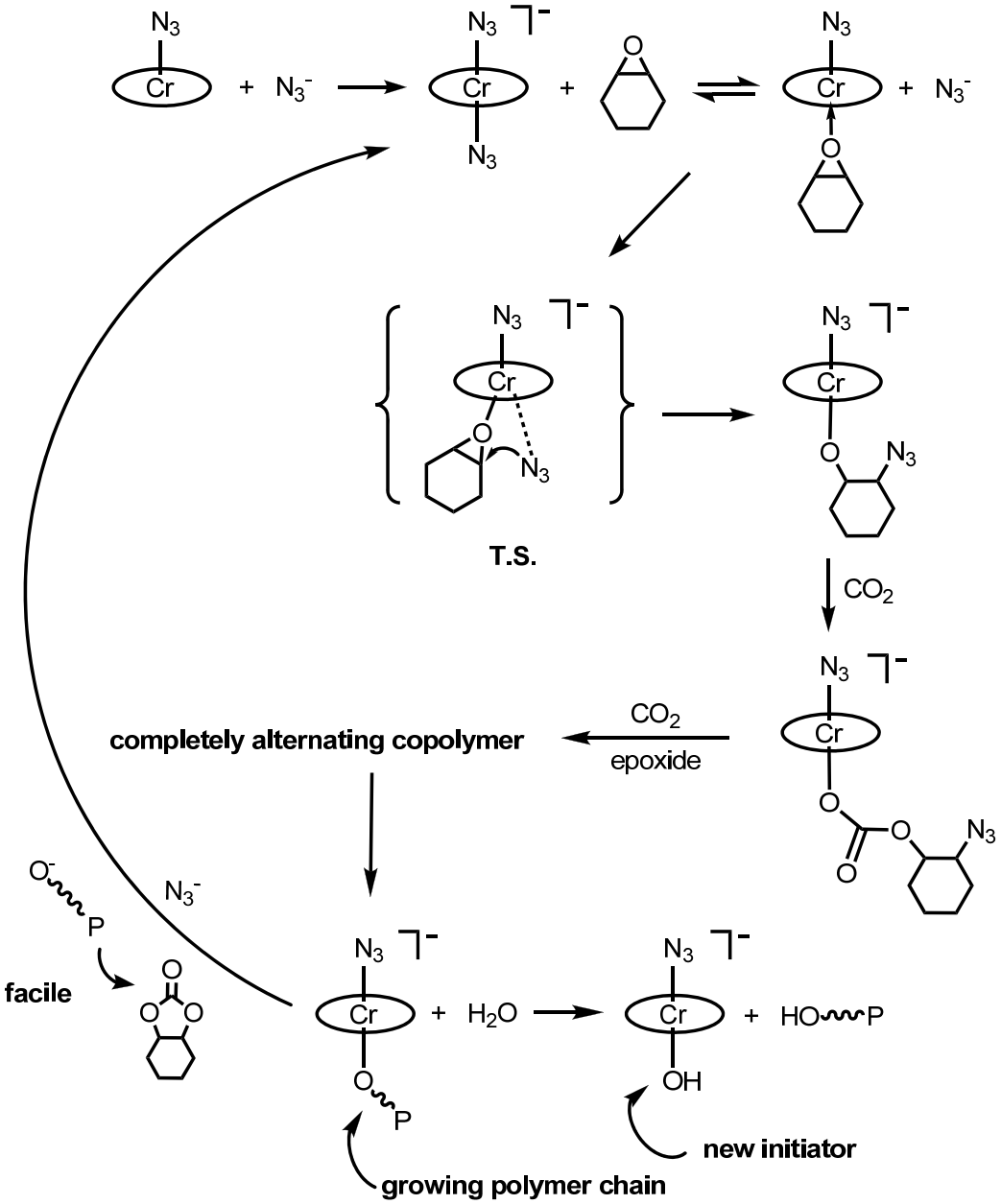

Figure 5. Demonstration of the proposed chromium salen catalyzed copolymerization mechanism of cyclohexene oxide and carbon dioxide.

a complex where one of the ancillary nucleophiles has been replaced by an epoxide molecule. For exemplary purposes, Figure 5 is shown with the azide (N_3^-) anion as the added cocatalyst and cyclohexene oxide as the epoxide. This hexa-coordination serves to lengthen the metal-nucleophile bond, allowing the activation and ring-opening of an incoming epoxide, thus forming a metal alkoxide complex. The metal-alkoxide active species can then undergo a rapid concerted insertion of CO_2, breaking the alkoxide bond and forming a new metal-carbonate linkage. Chain propagation then continues as another epoxide molecule is inserted followed by CO_2 insertion, forming a perfectly alternating polycarbonate copolymer.

In addition to the alternating growth of the copolymer chain, the sequence can be interrupted by the consecutive insertion of epoxide monomer, *vide supra*, resulting in an ether linkage in the polymer chain. As depicted in Figure 5, the polymer chain can also dissociate from the catalyst as a result of competitive binding from another nucleophile in the reaction mixture. The "free" polymer chain is then able to backbite upon itself, ejecting one equivalent of cyclic carbonate, as demonstrated in Figure 6, resulting in polymer chain degradation. If the nucleophilic attack at the chromium center is carried out by trace water or any other protic species in the system, chain transfer occurs resulting in polymer chain termination by protonation, leaving a chromium-hydroxide catalyst that can initiate the ring-opening of another epoxide monomer to start the

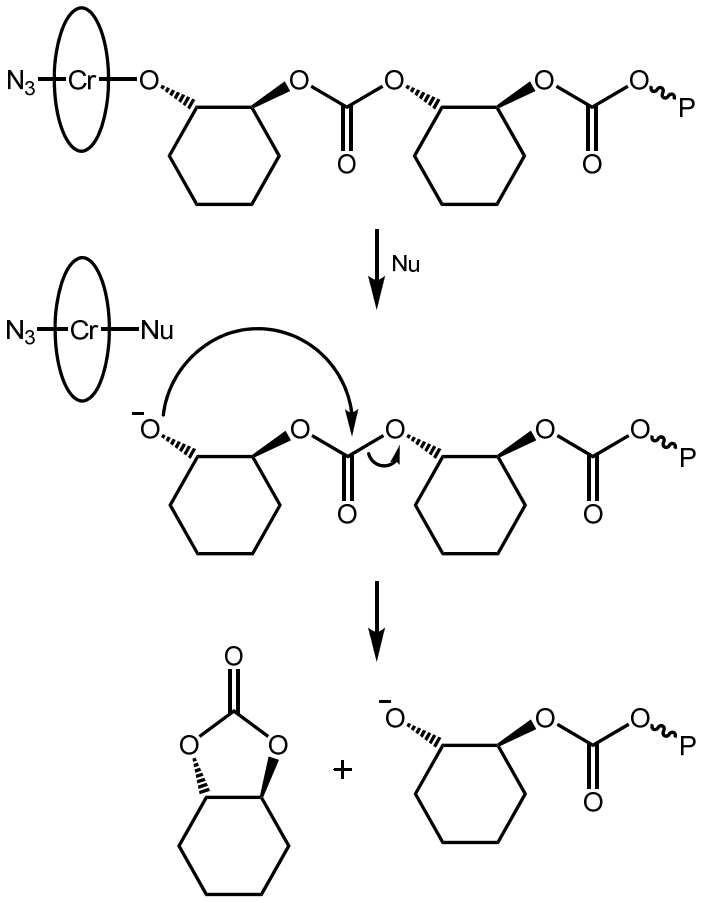

Figure 6. The proposed displacement and backbiting mechanism of the copolymer, resulting in degradation of the polymer chain.

growth of a new polymer chain (Figure 5). Both of the aforementioned detriments to the continuing growth of the polymer chain result in molecular weights far lower than theoretically calculated. Techniques such as nuclear magnetic resonance (NMR) and infrared (IR) spectroscopies as well as gel permeation chromatography (GPC) are imperative to the in depth study of the copolymerization reaction. Characteristic IR, ^{1}H and ^{13}C NMR spectra are shown in Figure 7 display the various products from the reaction between cyclohexene oxide and carbon dioxide. Stereochemical elucidation was provided by Nozaki using ^{13}C NMR to identify isotactic and syndiotactic tetrads within the polymer chain.[15] Despite the marked importance of the previously mentioned techniques, another spectroscopic apparatus has been instrumental to the mechanistic understanding of the copolymerization reaction made by the Darensbourg group. The convenience of attenuated total reflectance Fourier transform infrared spectroscopy (ATR-FTIR) has been utilized as part of a high pressure reaction vessel (Figure 8). This has afforded us the ability to monitor the copolymerization in situ, under the temperature and pressure conditions necessary, allowing for meticulous study of the catalyst and the products formed over the course of the reaction (Figure 9).

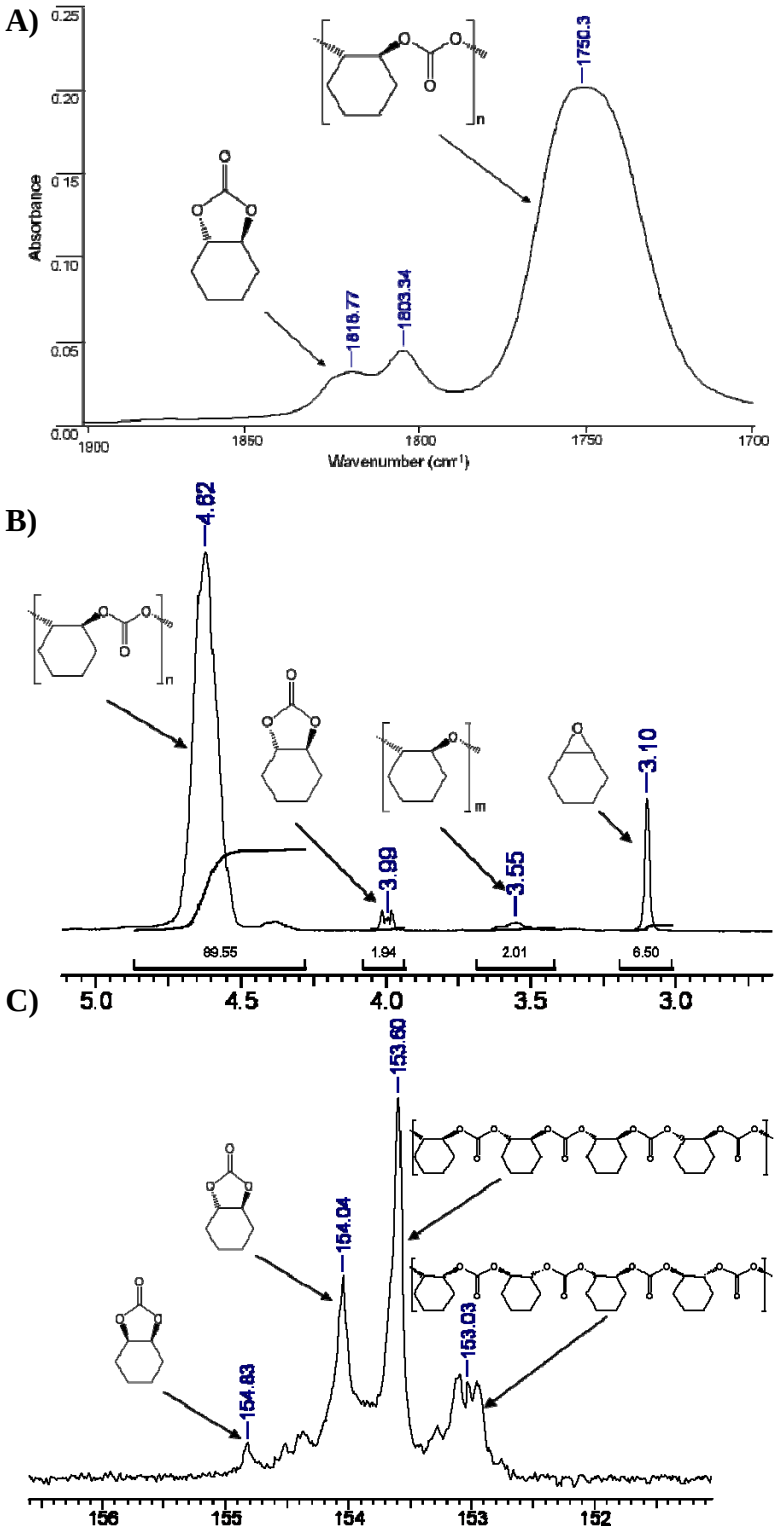

Figure 7.[16] Typical spectroscopic methods of characterization of the reaction between cyclohexene oxide and CO_2: a) Infrared, b) ^{1}H NMR, and c) ^{13}C NMR.

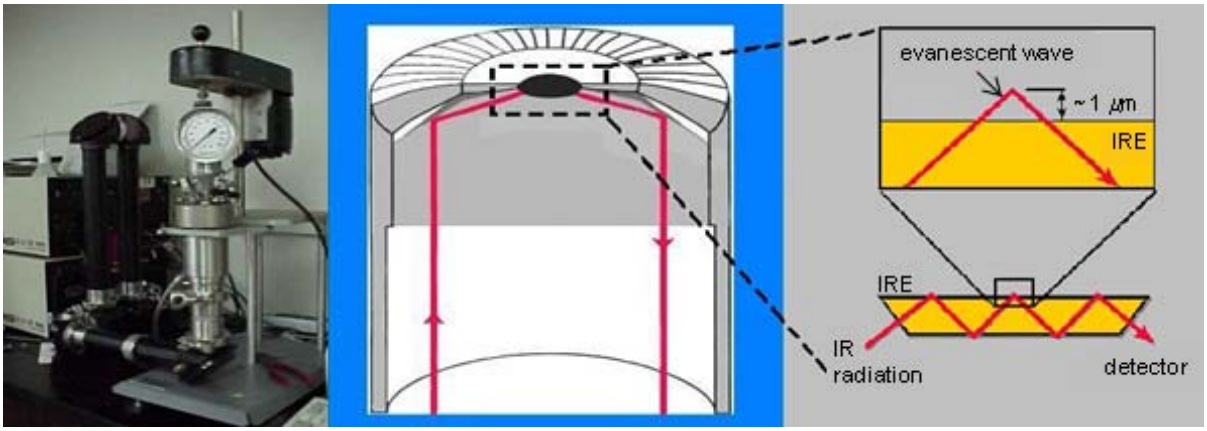

Figure 8. The ASI ReactIR 1000 system modified with a high pressure Parr® autoclave for the use of studying high pressure reaction systems (left) and a diagram illustrating ATR-FTIR (right).

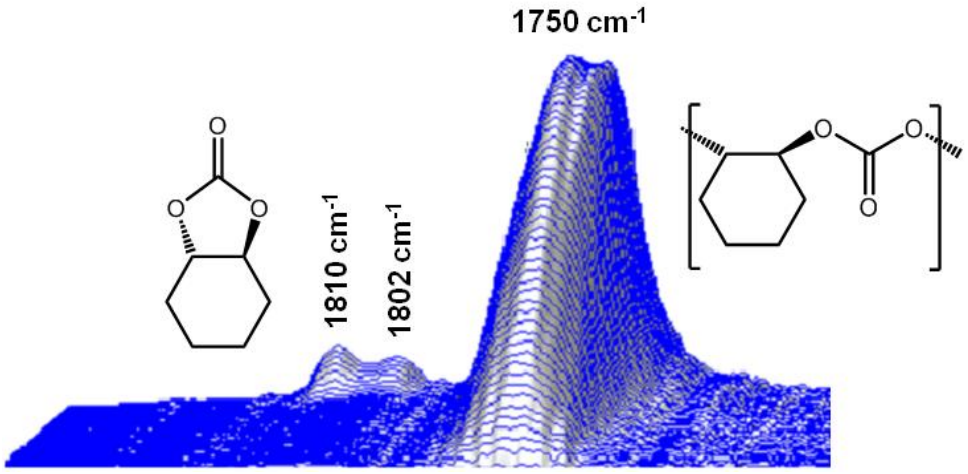

Figure 9. Typical infrared stack plot of the copolymerization of cyclohexene oxide and carbon dioxide displaying the $\nu_{C=O}$ stretches for poly(cyclohexylene carbonate) (1750 cm^{-1}) and cyclic cyclohexylene carbonate (1802 cm^{-1} and 1810 cm^{-1}).

Within the remainder of this dissertation, a new catalyst system for the copolymerization of carbon dioxide and epoxides will be discussed. This system is based on a ligand architecture similar to both the porphyrin and salen systems, but with distinct advantages over both. The topics discussed will range from catalyst system optimization to kinetic and mechanistic considerations unique to this system. Also to be discussed is the further enlightenment into the copolymerization mechanism previously inaccessible to similar square planar catalyst systems. It will be demonstrated that through the efforts of myself and others that this system has been developed to be more active, selective towards copolymer formation, and mechanistically insightful than many previously developed catalysts systems.

CHAPTER II

THE COPOLYMERIZATION OF CARBON DIOXIDE AND CYCLOHEXENE OXIDE CATALYZED BY TETRAMETHYLTETRAAZAANNULENE CHROMIUM CHLORIDE*

Information on previous porphyrin catalysts

It is well-known that coordinating ligands greatly influence the reactivity of metal complexes. Often times, inspiration for the design of a catalyst comes from what we know about systems that exist in nature. Metalloporphyrin complexes have been found to occur in nature in such systems as chlorophyll, giving plants their green pigment, and in red blood cells, where an iron heme manages the uptake and release of oxygen. The former system, chlorophyll, is of special interest to the copolymerization reaction as it is a biological example of carbon dioxide fixation in nature. In 1978, Inoue developed the first single-site catalysts for the copolymerization of carbon dioxide and epoxides, following the guidance of these natural systems.[9] These catalysts were based on a tetraphenylporphyrin (tpp) ligand framework chelated around an aluminum(III) center with ancillary initiating groups that include chloride, methyl, and various alkoxides (Figure 10). These aluminum porphyrinate complexes, enhanced by the

*Reproduced in part with permission from Darensbourg, D. J.; Fitch, S. B. *Inorg. Chem.* **2007,** *46,* 5474-5476.

addition of a phophonium or ammonium salt cocatalyst, were found to homopolymerize epoxides, lactides, and a number of lactones, as well as copolymerize epoxides with carbon dioxide.[17-23] This system, utilizing Al(tpp)Cl and $EtPh_3PBr$, was able to produce a copolymer from cyclohexene oxide and carbon dioxide with a M_n of 6,200 g mol^{-1} and a polydispersity (PDI) of 1.06 that contained >99% carbonate linkages. Despite the moderate, yet monodisperse, molecular weight polymers, the activity of the catalysts was quite low, only achieving 100 turnovers in 14 days (TOF = 0.3 h^{-1}).

Recently, Wang and coworkers were able improve upon the aluminum porphyrin system with the addition of a bulky Lewis acid.[24] Using an optimized system containing Al(tpp)Cl, Et_4NBr, and methylaluminum bis(2,6-di-*tert*-butyl-4-methylphenolate), in a 8:8:1 ratio, was able to produce a copolymer with a M_n of 5,800 g mol^{-1} and a PDI of 1.07 with 96.7% carbonate linkages. The bulky Lewis acid was attributed to aiding in the ring opening of the cyclohexene oxide monomer and ultimately achieving an activity (TOF) of 44.9 h^{-1} at 60 °C over the course of 9 hours. This work presents a significant increase over the previous Al(tpp)X work conducted by Inoue, but still leaves much to be desired when compared to other, more active systems.

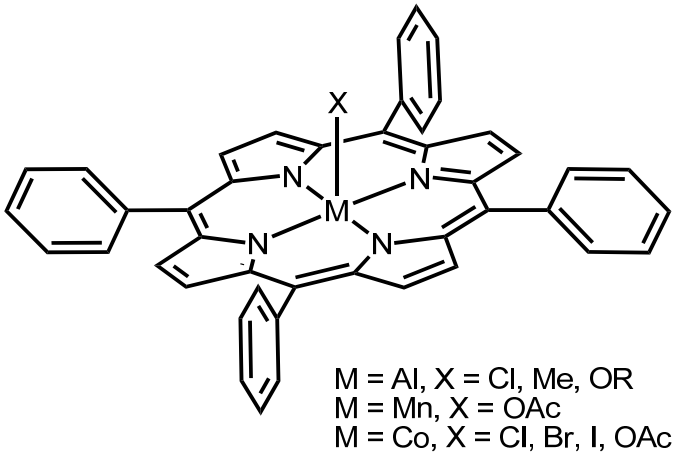

Figure 10. Porphyrin catalysts for the copolymerization of epoxides and carbon dioxide.

Inoue and coworkers, in 2003, developed a catalyst system related to their previous work with Al(tpp)X.[25] This tetraphenylporphyrin catalyst incorporated a manganese center with an acetate initiator (Figure 10). At 80 °C and under 50 atm CO_2, Mn(tpp)OAc was able to catalyze the copolymerization of carbon dioxide and cyclohexene oxide with an TOF of 16.3 h^{-1} to afford a polymer with 99% carbonate linkages and a M_n of 6,700 g mol^{-1} with a narrow polydispersity of 1.3. This catalyst was also able to produce copolymer, albeit at the lower activity of 3.3 h^{-1}, with 95% carbonate content, a M_n of 3,000 g mol^{-1}, and a PDI of 1.6 under only 1 atm of CO_2 pressure. Interestingly, Inoue found that upon the addition of a cocatalyst, such as PPh_3, pyridine, or N-methylimidazole (MeIm), decreased the rate of polymerization and decreased the carbonate content of the polymer. This is in contradiction to all other

catalysts with a similar architecture whose activities that greatly benefit from the presence of a cocatalyst.

In 2008, Wang and coworkers reported a cobalt porphyrin system capable of copolymerizing propylene oxide and carbon dioxide (Figure 10).[26] Many aspects of the copolymerization reaction were investigated, including: various reaction temperatures, CO_2 pressures, axial initiator (X) groups, cocatalysts, cocatalyst concentrations, and reaction times. They found Co(tpp)Cl with 1 equivalent of PPNCl to be the optimal catalyst system. This binary mixture, reacted with propylene oxide and 20 atm CO_2, was able to selectively (99%) produce a 48,000 g mol^{-1} number average molecular weight polymer containing 99% carbonate linkages and a PDI of 1.17 at only 25 °C in 5 hours to achieve a TOF of 188 h^{-1}. A decrease in the selectivity of polymer over cyclic carbonate was observed when either the reaction temperature or reaction time was increased. These phenomena are expected due to the increased opportunity for dissociation of the polymer chain followed by depolymerization via a backbiting mechanism to produce cyclic propylene carbonate.

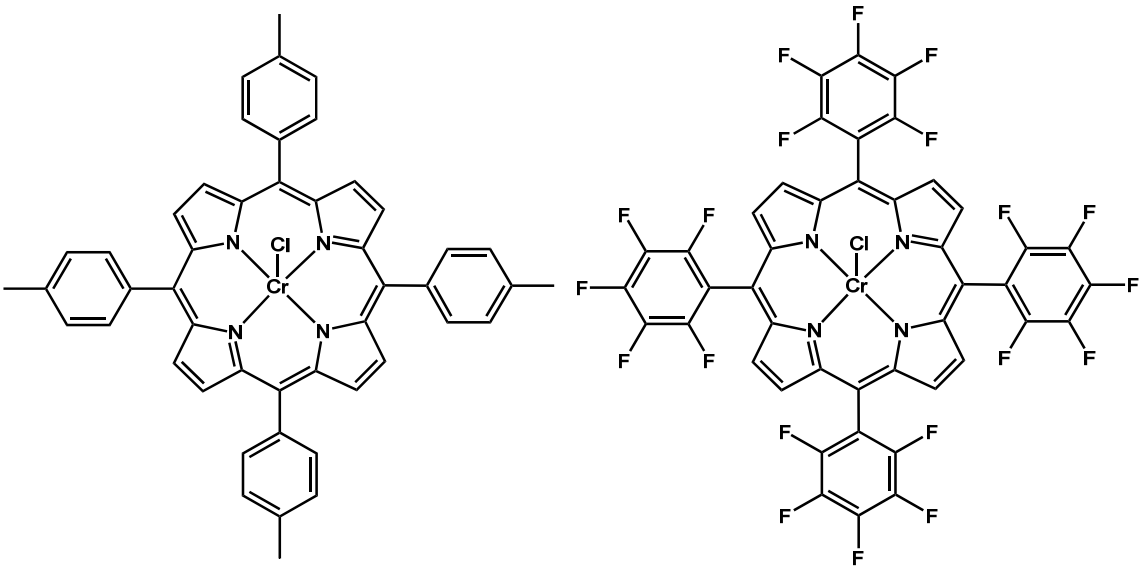

Figure 11. Chromium tetra-*p*-tolylporphyrin chloride (left) and $scCO_2$-soluble, highly fluorinated, chromium pentafluorotetraphenylporphyrin chloride (right) catalysts for the copolymerization of cyclohexene oxide and carbon dioxide.

Porphyrin complexes incorporating a chromium center have also shown catalytically active for the coupling of carbon dioxide and epoxides. In 1995, Kruper and Dellar were investigating the coupling of carbon dioxide and various epoxides using Cr(tpp)Cl as a catalyst to produce cyclic carbonates (Figure 11).[27] In their investigation, the reaction of cyclohexene oxide and 50 atm CO_2 in the presence of 4-10 equivalents of (4-dimethylamino)pyridine (DMAP) at 80 °C yielded a 97% selectivity towards alternating copolymer. Conversely, the same reaction conditions employing propylene oxide produced a 95% yield of cyclic propylene carbonate.

Improving on the work of Kruper and Dellar, Holmes and coworkers explored a way to fix the solubility issues associated with metalloporphyrin complexes. In 2000, Holmes reported that a highly fluorinated chromium porphyrin was active for the copolymerization of cyclohexene oxide and carbon dioxide.[11] The chromium tetrakis(pentafluorophenyl)porphyrin catalyst shown in Figure 11 was found to be soluble in liquid and supercritical CO_2 with the ability to produce copolymer at 110 °C and 225 atm CO_2 ($scCO_2$) with properties on par other aluminum porphyrin catalysts,[24] achieving a TOF of 173 h^{-1} in the presence of 8-10 equivalents of DMAP as a cocatalyst.

On the history of salen catalysts

A simple tetradentate chelating ligand known universally as salen, named from the abbreviation of its starting materials, salicylaldehyde and ethylenediamine. The salen ligand was first discovered in 1933 by Pfeiffer and coworkers and often generated in situ followed by the addition of a metal salt or prepared as a pure organic compound by the condensation of salicylaldehyde and ethylenediamine.[28,29] Salen serves as a biological mimic to many porphyrin-containing systems. There also exist many variations with diverse substituents that affect the solubility, electronic, and steric effects of the ligand, but a more in-depth discussion on this area will me made later in this section.

In contrast to the extensive investigations conducted for the Al(tpp)X catalyst system, far less has been reported on analogous aluminum salen complexes. Instances of

aluminum salen complexes acting as catalysts for the coupling of carbon dioxide and epoxides were reported in 2002 by He and coworkers.[30,31] In their investigations, they looked at altering the reaction temperature, times, and using various cocatalysts, including Lewis bases, such as MeIm, pyridine, and tri-*n*-butylamine, and quaternary ammonium salts such as $^{n}Bu_4NX$ (where X = Cl, Br, I). It was found that the binary mixture of Al(salen)Cl (Figure 12, where R^1, R^2 = H), a tetra-*n*-butylammonium salt cocatalyst, and ethylene oxide under supercritical CO_2 (150 atm) would selectively produce cyclic ethylene carbonate with an activity ranging from 2,200-2,400 h^{-1} at 110 °C in 1 hour.

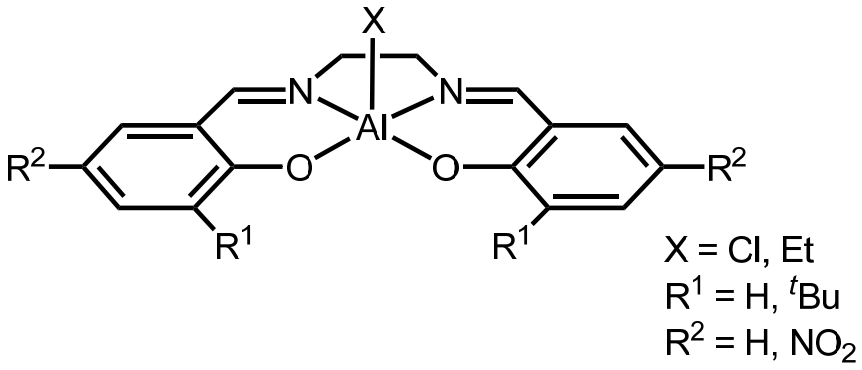

Figure 12. Skeletal representation of Al(salen)X complexes used as catalysts for the coupling of carbon dioxides and epoxides.

In 2004, Darensbourg and coworkers also presented efforts to produce polycarbonate using aluminum salen complexes.[14] It was found that more electron-

withdrawing substituents on the phenolate moieties and the initiating group resulted in an increase in catalytic activity for the copolymerization of cyclohexene oxide and carbon dioxide. Al(salen)Cl (Figure 12, where R^1 = ^{t}Bu and R^2 = NO_2), utilizing 1 equivalent of $^n Bu_4NN_3$ as a cocatalyst, was able to catalyze the copolymerization reaction at 80 °C and under 50 atm CO_2, achieving an activity of 35.3 turnovers per hour towards the formation of a polymer that contained >99% carbonate linkages. These results are confirmed by a similar study in a recent report by Inoue.[32]

Due to the greater industrial demand for poly(propylene carbonate), much of the recent literature has focused on catalysts for the copolymerization of propylene oxide with carbon dioxide. Several notable advances in catalyst design stand out for their innovation and further insight into the copolymerization mechanism. In 2006, Nozaki and coworkers explored the addition of piperidinium moieties to the *ortho* position of the phenolate rings of cobalt salen (Figure 13).[33] This system was designed to reduce the amount of cyclic propylene carbonate during the copolymerization by proton transfer from the piperidinium group to the anionic end group of the polymer chain as it is dissociated from the metal center via the chain transfer mechanisms discussed earlier. The neutral polymer chain is then much less likely to backbite upon itself, thereby preserving its integrity. Selectivities towards narrowly disperse, high molecular weight polymers of up to 99% over cyclic carbonate were achieved with this catalyst system.

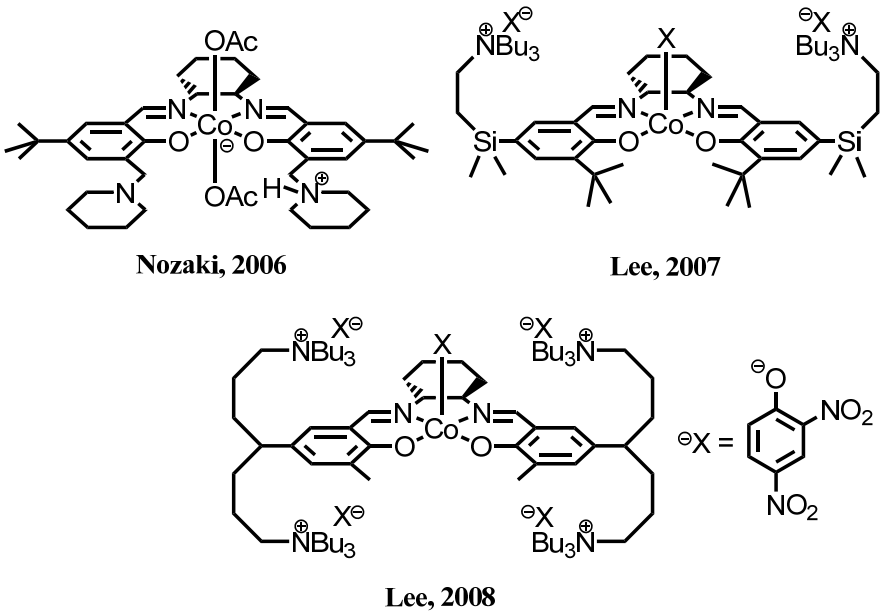

Figure 13. Cobalt salen catalysts developed for the copolymerization of propylene oxide and carbon dioxide by Nozaki and Lee.

Expanding on the work of Nozaki, Lee and coworkers investigated modifying a cobalt salen complex to incorporate pendant alkyl chains with terminal quaternary alkyl ammonium functionalities extending from the *para* position of the phenolate rings (Figure 13). Their first of such catalysts, reported in 2007, contained pendant chains attached to the ligand through a silane linkage.[34] This catalyst has the advantage of keeping the chain-growing carbonate unit in close proximity to the metal center through Coulombic interaction between the quaternary ammonium cation anchored on the ligand framework and the anionic growing polymer chain. The "herding" of the polymer chain back to the metal center to continue the copolymerization reaction allows for high

activities, low catalyst loadings, the ability for higher reaction temperatures, and a greater selectivity for polymer over cyclic carbonate. Lee and coworkers were able to obtain activities of 3,500 h^{-1} with a monomer to catalyst loading of 25,000:1, carried out at 90 °C, and selectivity towards polymer formation of 90%. The difference between the two systems is that Nozaki's catalyst was designed to protonate and terminate the polymer chain should it dissociate from the metal center, while Lee's catalyst allows the dissociated polymer chain to re-coordinate to the metal center and continue the copolymerization reaction to achieve polymer molecular weights 10-fold higher than with Nozaki's catalyst for the same reaction time.

In 2008, Lee and coworkers improved upon their previous catalyst system by incorporating four ammonium moieties into the ligand architecture (Figure 13).[35] This catalyst was able to achieve an astonishing 26,000 turnovers per hour with a monomer to catalyst loading of 50,000:1, producing a number average molecular weight (M_n) of over 200 kg mol^{-1} and >99% selectivity towards polymer formation. The highest molecular weight (M_n = 296 kg mol^{-1}) was obtained using a catalyst loading ratio of 100,000:1 and allowed a one hour reaction time. It was found that this drastic increase in activity and polymer molecular weight is attributable to the increased number of alkyl ammonium groups attached to the catalyst. These herding ability of these groups allowed the for the copolymerization reaction involving propylene oxide to be run at much higher temperatures without the predicament of cyclic carbonate formation, inaccessible to other catalyst systems. Lee also found this catalyst to be highly recyclable with no significant loss in activity through a silica gel separation technique.

In 1996, Jacobsen and coworkers reported on a highly active catalyst system for the asymmetric ring-opening of epoxides.[13] At the core of the system was a Cr(salen)Cl catalyst. In addition to the chromium complex's ability to rapidly, efficiently, and selectively ring open epoxides to form chiral 1,2-diols, Jacobsen received a patent in 2000, outlining the ability of chromium salen to catalyze the copolymerization of carbon dioxide and epoxides.[36] This inspirational work has directed the primary research focus of the Darensbourg group to further understand the chromium salen system and how it can be improved upon.

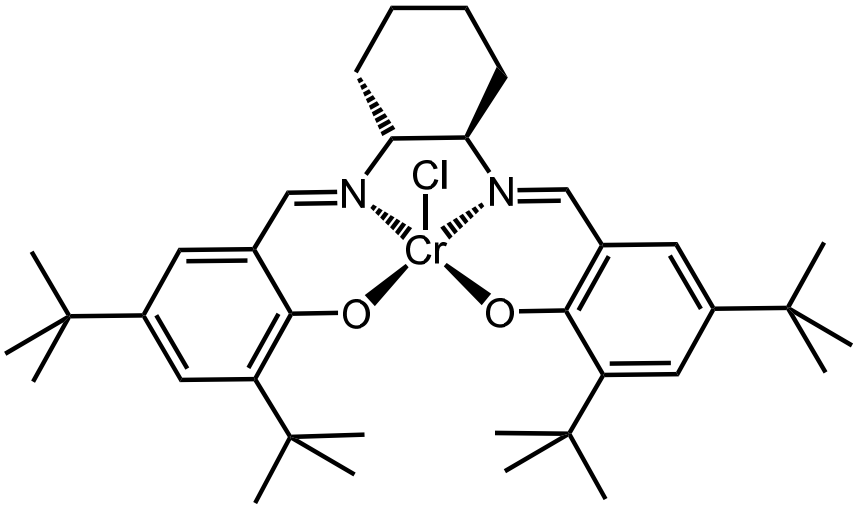

Figure 14. Skeletal representation of a typical chromium salen used to catalyze the copolymerization of cyclohexene oxide and carbon dioxide.

Darensbourg and Yarbrough reported the first mechanistic investigation into the chromium salen catalyst system in 2002.[12] Using the chromium salen catalyst shown in Figure 14, they were able to form poly(cyclohexylene carbonate) from cyclohexene oxide under 60 atm of carbon dioxide at a M_n of 8,900 g mol^{-1} and a polydispersity of 1.2 with a TOF of 10.4 h^{-1} at 80 °C. Through the utilization of infrared and NMR spectroscopy, they found the catalyst to be highly selective towards the formation of a polymer product with a near quantitative CO_2 incorporation. The mechanism proposed by Darensbourg and Yarbrough involved an equilibrium between a cocatalyst-bound and an epoxide-bound chromium complex. The epoxide is then ring-opened by the nucleophilic cocatalyst. This resulted in the newly formed chromium-alkoxide species able to rapidly insert a molecule of carbon dioxide, thereby giving one full turnover of the catalyst. Following the work of Mang and Holmes[11] on the chromium porphyrin system, the addition of MeIm resulted in a 3-fold increase in catalytic activity to 32.2 h^{-1}. Further investigation into this system found a significant increase in the ability of the chromium salen system to copolymerize cyclohexene oxide and carbon dioxide with the addition of anionic cocatalysts.[14] The greater nucleophilicity of an anion compared to that of a neutral Lewis base proved essential to achieving high catalytic activity. In order to increase the effectiveness of the anion, cocatalysts with non-interacting cations were chosen to study, chiefly PPN^+X^- salts (PPN = bis(triphenyl-phosphoranylidene)ammonium). The optimum chromium salen catalyst, aided by $PPNN_3$ as a cocatalyst, was able to achieve a TOF of 1,150 h^{-1}. The utilization of anionic cocatalysts lead to a more detailed proposed mechanism, one that is widely

accepted today (Figure 15). The first step involves the chromium-nucleophile bond being lengthened through the trans influence of the anionic cocatalyst, allowing for greater ease in epoxide ring-opening.

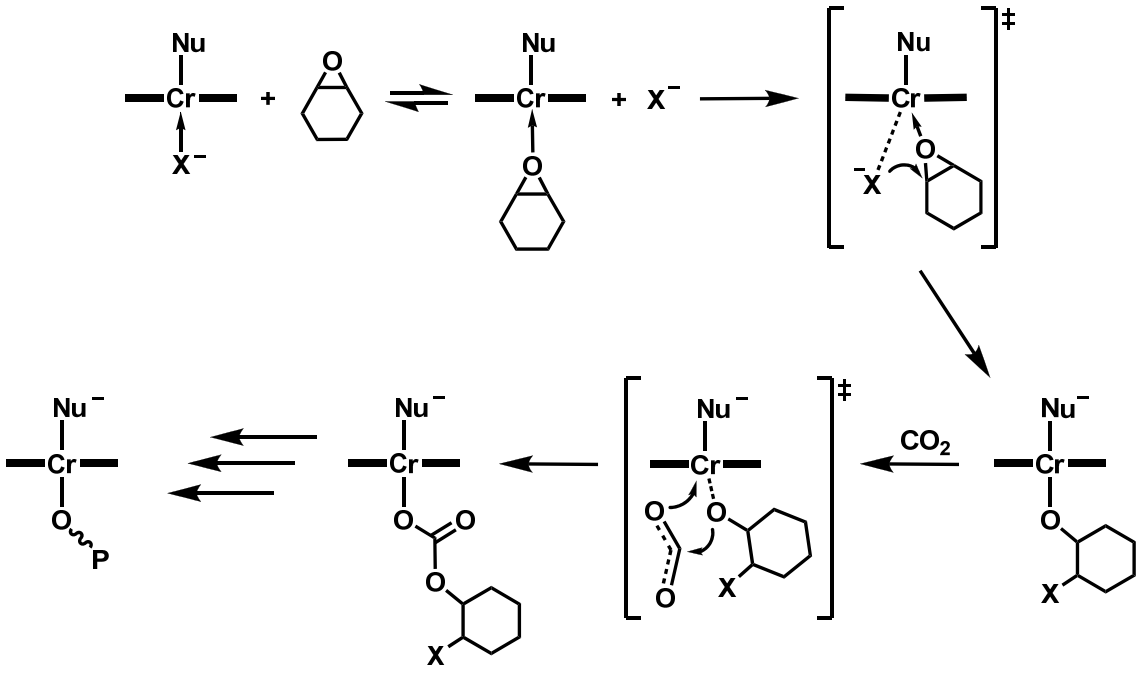

Figure 15. Proposed mechanism for the alternating insertion of cyclohexene oxide and carbon dioxide.

Background information on the tetramethyltetraazaannulene ligand system

The highly active and robust nature of the chromium salen complexes for the copolymerization of carbon dioxide and epoxides has spurred interest in other systems that resemble the salen ligand architecture, but may vary slightly in their steric and

electronic nature. One such example is the acacen (*N,N'*-bis(acetylacetone)-1,2-ethylenediamine) system, studied extensively through binding assays and solid state structures by Frantz, utilizing a manganese metal center (Figure 16).[37,38]

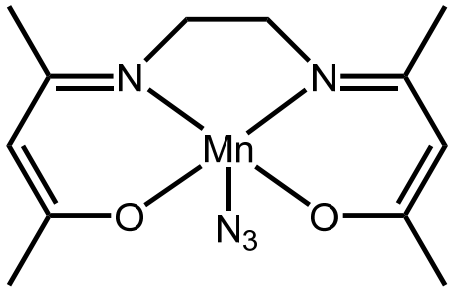

Figure 16. Mn(acacen)N_3 complex relevant to the copolymerization of carbon dioxide and epoxide.

A second alternative system to salen being developed in the Darensbourg laboratories is based on the ligand architecture of 5,14-dihydro-6,8,15,17-tetramethyldibenzo[*b*,*i*][1,4,8,11]tetraazacyclotetradecine (tetramethyltetraazaannulene, tmtaa) and is the primary focus of this dissertation. The tmtaa ligand bears several similarities to the porphyrin framework. Both ligands are macrocyclic and contain a planar four-nitrogen donor core. Upon deprotonation, they are both completely conjugated, dianionic systems. Tmtaa has been extensively studied as a porphyrin mimic since porphyrin metal complexes are found in many important biological systems such as hemoglobin, chlorophyll, and vitamin B_{12}.[39,40] Many differences also exist

between the two ligand systems. Porphyrins are 16-membered planar rings and $18e^-$ Hückel aromatic systems with completely delocalized electron density. This gives rise to the general insolubility of porphyrins. Tmtaa, on the other hand, is saddle-shaped due to the steric interaction between the aromatic hydrogens and the hydrogens of the methyl groups, restricting the $16e^-$ Hückel antiaromatic system from delocalizing its electron density throughout the macrocycle.[39-41] This non-planar distortion along with the isolated aromatic stabilization of the benzene rings places the majority of electron density on the iminato portions of the ligand and gives rise to a high solubility in common organic solvents. This is apparent by the carbon-nitrogen distances of the ligand. The iminato carbon-nitrogen distance exhibits a great deal of double-bond character with a distance of 1.343(3) Å while the phenylene diamine carbon-nitrogen bonds are much more single-bond in nature with a distance of 1.404(2) Å, as compared to the normal bond lengths for carbon-nitrogen double and single bonds 1.29 and 1.47 Å, respectively.[41] Another considerable advantage over porphyrin, in addition to a vast increase in solubility, is the 10-fold reduction in cost to synthesize the tmtaa ligand.

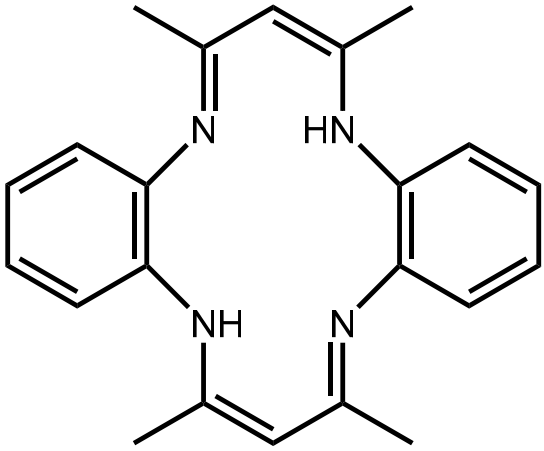

Figure 17. Skeletal representation of H_2tmtaa.

The tmtaa system has some similarities to the salen ligand. As with the tmtaa ligand, salen is tetradentate, dianionic when deprotonated, and support a square pyramidal geometry around a metal center. Differences are evident in that salen possesses an N_2O_2 mixed donor set compared to the N_4 donor set of tmtaa. Salen is comparatively planar while tmtaa has the aforementioned saddle-shaped macrocyclic structure.

The tmtaa ligand has some other unique characteristics. It has a core size of 1.902 Å, which is 0.1 Å smaller than that of a porphyrin ring. This small core size of the ligand combined with the ionic radius of the bound metal force the nitrogen bonding orbitals to twist upward. This results in an even more pronounced saddle-shaped distortion, compared to the free ligand, and the metal lies above the N_4 plane. The degree of distortion depends on the radius of the metal ion, which correlates with its d^n

electronic configuration. For a given oxidation state, more electron-rich metals have a smaller radius, causing the metal to lie closer to the N_4 plane and the saddle shape of the ligand almost disappears. This forced out-of-plane distortion from the ligand favors a metal bound in a square pyramidal geometry. Table 1 shows four metal tmtaa complexes along with their respective metal ionic radii, metal-nitrogen distances, and out-of-plane distances of the metal.[42-44] The disappearance of the metal-N_4 distortion and lessening of the saddle shape are easily observed as the metal center gains electrons and becomes smaller in size, exemplified in the cobalt complex shown in Table 1, where the out-of-plane distortion has decreased 3-fold. In the case of Ni(tmtaa) (not shown), the distortion entirely disappears. This permits later transition metals to bind a sixth ligand in a *trans*-octahedral geometry. For d^0 and d^1 metals, the out-of-plane distortion is the greatest. For example, in Zr(tmtaa)Cl_2, the zirconium lies 1.071(2) Å above the N_4 plane.[43] This distance is great enough to allow the chloride ions to bind *cis* to each other in an overall trigonal prismatic arrangement.

Table 1. Selected Structural Parameters and Solid State Structures of Several Tmtaa Metal Complexes.

	Ti(tmtaa)Cl	**V(tmtaa)Cl**	**Fe(tmtaa)Cl**	**Co(tmtaa)I**
M^{3+} (Å)	0.81	0.78	0.738	0.718
M-N (Å)	2.06(8)	2.009(10)	2.002	1.901
M-N_4 (Å)	0.785(2)	0.644(2)	0.6	0.234
	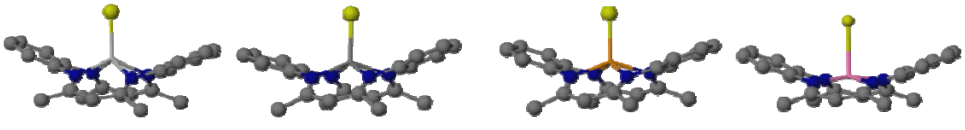			

The tmtaa ligand was first synthesized by Jäger[45] in 1969 followed by a more widely used, modified synthesis published by Goedken and coworkers in 1973.[46,47] The latter consists of a condensation reaction between two equivalents of 2,4-pentanedione and two equivalents of *ortho*-phenylenediamine around a square planar metal template. $Ni(OAc)_2 \cdot 4H_2O$ is most commonly used as the template metal due to its price and availability. The square planar template allows for the formation of the macrocycle by positioning the ketone and amine functionalities in the correct orientation to undergo a condensation reaction in a 2:2 ratio. Without the presence of the templating metal, the dominant product would be the result of a double condensation of a 1:1 diketone to diamine to form 1,5-benzodiazapine. The Ni(tmtaa) macrocycle can then be demetallated through the addition of anhydrous hydrogen chloride gas, forming a tetra-protonated dicationic ligand tetrachloronickelate salt. Ion exchange must then occur to avoid reinsertion of the nickel into the macrocycle. This is achieved by the addition of a salt containing a large, non-coordinating anion such as ammonium hexafluorophosphate. The bis(hexafluorophosphate) salt of the ligand can then be neutralized by the addition of an amine base such as triethylamine, producing a golden-yellow microcrystalline precipitate of the free tmtaa ligand, H_2tmtaa.

Building on the success of the chromium porphyrin and chromium salen catalyst systems, the analogous chromium tetramethyltetraazaannulene complex is the basis of this dissertation. This complex was reported by Cotton and coworkers in 1990.[48] The straightforward synthesis entails refluxing the free ligand with anhydrous chromium trichloride and two equivalents of triethylamine in benzene overnight, resulting in an

intensely colored burgundy solution containing the product, Cr(tmtaa)Cl (**1**) in near quantitative yield.

Experimental

Methods and materials. Unless otherwise specified, all manipulations were carried out on a double manifold Schlenk vacuum line under an atmosphere of argon or in an argon-filled Glovebox. Methanol (EMD Chemicals), ethanol (Pharmco-Aaper), 2,4-pentanedione (Aldrich), *o*-phenylenediamine (Aldrich), nickel acetate tetrahydrate (Fisher), chromium(III) chloride (Strem), ammonium hexafluorophosphate (Oakwood), hydrochloric acid (EMD Chemicals), sodium chloride (EMD Chemicals), sulfuric acid (EMD Chemicals), and sodium azide (Aldrich) were used without further purification. Triethylamine (EMD Chemicals) was stored over sodium hydroxide and freshly distilled before use. Bis(triphenylphosphoranylidene)ammonium chloride was recrystalized from methylene chloride/ether. Bis(triphenylphosphoranylidene)ammonium azide was synthesized from a published literature procedure.[49] Methylene chloride, benzene, ethyl ether, and hexanes were freshly purified by an MBraun Manual Solvent System packed with Alcoa F200 activated alumina desiccant. Cyclohexene oxide (TCI) was freshly distilled from CaH_2 prior to use. Bone dry carbon dioxide (Scott Specialty Gases) was supplied in a high pressure cylinder equipped with a liquid dip-tube. Unless otherwise stated, all other reagents were used without further purification. ^{1}H and ^{13}C NMR spectra were acquired on using a Varian Inova 300 MHz superconducting NMR

spectrometer. Infrared spectra were recorded on using a Bruker Tensor 27 FTIR spectrometer. Molecular weight determinations were carried out on a Viscotek Gel Permeation Chromatograph equipped with refractive index, right-angle and low-angle light scattering detectors.

Synthesis of (6,8,15,17-tetramethyldibenzo[*b*,*i*][1,4,8,11]tetraazacyclo-tetradecinato) nickel (Ni(tmtaa)). The synthesis of Ni(tmtaa) was performed following the published procedure.[47] 1,2-phenylenediamine (60 g, 0.555 mol) and nickel acetate tetrahydrate (69 g, 0.247 mol) were refluxed in 700 mL methanol for 30 minutes, resulting in a dark blue solution. A color change to a dark aqua green was observed upon the addition of 2,4-pentanedione (57 mL, 0.555 mol). The reaction was allowed to reflux for 3 days. The solution was then cooled and the dark purple, microcrystalline product was collected by vacuum filtration and air dried (38.4 g, 39.7% yield). ^{1}H NMR ($CDCl_3$, 300 MHz): δ 6.60 (s, 8H), 4.84 (s, 2H), 2.06 (s, 12H). ^{13}C {^{1}H} NMR ($CDCl_3$, 75 MHz): δ 155.44, 147.25, 121.83, 120.85, 111.11, 22.02.

Synthesis of 5,14-dihydro-6,8,15,17-tetramethyldibenzo[*b*,*i*][1,4,8,11]-tetraazacyclotetradecine (H_2tmtaa). The neutral ligand, H_2tmtaa, was synthesized following the established literature procedure.[47] Anhydrous hydrogen chloride gas (generated by sulfuric acid slowly added to sodium chloride) was bubbled through a suspension of Ni(tmtaa) (20 g, 50 mmol) in absolute ethanol (500 mL) overnight with vigorous stirring. The tetrachloronickelate salt of the ligand precipitates as a blue-white solid. The mixture is cooled at -4 °C and filtered, washed with a minimal amount of cold absolute ethanol, and air dried. The demetallated ligand salt is then dissolved in a

minimal amount of water. Ammonium hexafluorophosphate (25 g, 0.153 mol) was added to the aqueous solution to exchange the $NiCl_4^{2-}$ anion with two PF_6^{1-} counterions. The bis(hexafluorophosphate) ligand salt precipitates from the aqueous solution as a white solid, which is filtered, washed with water, and dried in air. The salt is dissolved in a minimal amount of methanol and upon neutralization with a slight excess of triethylamine (14 mL, 0.1 mol) a color change from pale yellow to golden yellow along with the precipitation of a microcrystalline product of the same color was observed. The product was isolated by filtration, washed with methanol, and dried in air to yield 15.9 g of H_2tmtaa (92% yield). ^{1}H NMR ($CDCl_3$, 300 MHz): δ 12.58 (s, 2H), 6.98 (s, 8H), 4.87 (s, 2H), 2.13 (s, 12H). ^{13}C {^{1}H} NMR ($CDCl_3$, 75 MHz): δ 158.92, 138.45, 123.09, 122.87, 97.93, 20.91.

Synthesis of (6,8,15,17-tetramethyldibenzo[*b,i*][1,4,8,11]tetraazacyclo-tetradecinato) chromium chloride (Cr(tmtaa)Cl) (1). The chromium complex, Cr(tmtaa)Cl (**1**), was synthesized according to the published literature procedure.[48] H_2tmtaa (1 g, 2.9 mmol) and anhydrous chromium(III) chloride (0.46 g, 2.9 mmol) were refluxed in 400 mL benzene and 2 equivalents of triethylamine (0.8 mL, 5.8 mmol) for 3 days. The dark burgundy solution was then filtered to remove triethylammonium chloride and any unreacted chromium chloride. The filtrate was minimized in vacuo and the product precipitated upon the addition of hexanes. After being allowed to settle, the supernatant was decanted and the precipitate isolated. The product was dried in vacuo, transferred to an argon-filled glove box, and weighed to determine yield (0.91 g, 73%

yield). X-ray quality crystals were obtained by the slow diffusion of hexanes into a solution of the complex in benzene. MS: 394.12 $(M\text{-}Cl)^+$ (calc. 394.12).

Copolymerization of cyclohexene oxide and carbon dioxide. High pressure measurements of the copolymerization processes were carried out using a stainless steel Parr autoclave modified with a SiComp window to allow for attenuated total reflectance infrared spectroscopy (ASI ReactIR 1000). The catalyst and cocatalyst were dissolved in 10 mL of dichloromethane, allowed to stir for 30 minutes, and then dried in vacuo. The "activated" catalyst/cocatalyst mixture was then dissolved in 20 mL of neat cyclohexene oxide and injected into the autoclave via injection port and cannula, after which a single 128-scan background spectrum was collected. The autoclave was then charged with 35 bar carbon dioxide and a single 128-scan spectrum was taken every 2 minutes during the reaction period. Profiles of the absorbances at 1750 cm^{-1} (polycarbonate) and 1810 cm^{-1} (cyclic carbonate) vs. time were recorded after baseline correction. After cooling and venting of the autoclave, the reaction mixture was extracted with dichloromethane. The solution was dried overnight under a stream of compressed air to remove excess dichloromethane. The polymer residue was then dissolved in a minimum amount of dichloromethane and slowly added to a stirred beaker containing acidified methanol (1 M HCl in MeOH) to remove the catalyst and cyclic carbonate and precipitate the polycarbonate product. The supernatant solution containing the catalyst, cyclic carbonate, and any remaining cyclohexene oxide was decanted and the purified polymer dried in vacuo overnight at 60 °C. The dried polymer was collected and weighed to determine yield and the corresponding TONs and TOFs.

The highest catalytic activities were obtained from crystalline catalyst. All other activities reported herein are for comparative purposes only. The polymers were analyzed by ^{1}H NMR where the amount of ether linkages was determined by integrating the peaks corresponding to the methine protons of polyether at ~3.45 ppm and polycarbonate at ~4.6 ppm.

X-ray structure studies. A Leica microscope, equipped with a polarizing filter, was used to identify suitable crystals from a sample of crystals from the same habit. The representative crystal was coated in a cryogenic protectant, such as paratone, and affixed to a nylon sample loop attached to a copper mounting pin. The mounted crystals were then placed in a cold nitrogen stream (Oxford) maintained at 110 K on either a Bruker SMART 1000, GADDS, or APEX 2 three circle goniometer. The X-ray data were collected on either a Bruker CCD, GADDS, or an APEX 2 diffractometer and covered more than a hemisphere of reciprocal space by a combination of three (or nine in the case of the GADDS) sets of exposures; each exposure set had a different φ angle for the crystal orientation and each exposure covered 0.3° in ω. Crystal data and details on collection parameters are given in Table 1. The crystal-to-detector distance was 5.0 cm for all crystals. Crystal decay was monitored by repeating the data collection for 50 initial frames at the end of the data set and analyzing the duplicate reflections; and found to be negligible. The space group was determined based on systematic absences and intensity statistics.[50] The structure was solved by direct methods and refined by full matrix least-squares on F^2. All non-H atoms were refined with anisotropic displacement parameters. All H atoms attached to C and N atoms were placed in idealized positions

and refined using a riding model with aromatic C-H = 0.93 Å, methyl C-H = 0.96 Å, amine N-H = 0.86 Å and with fixed isotropic displacement parameters equal to 1.2 (1.5 for methyl H atoms) times the equivalent isotropic displacement parameter of the atom to which they are attached. The methyl groups were allowed to rotate about their local 3-fold axis during refinement.

For all structures: data reduction, SAINTPLUS (Bruker[50]); program used to solve structures, SHELXS (Sheldrick[51]); program used to refine structures, SHELXL-97 (Sheldrick[52]); molecular graphics and preparation of material for publication, SHELXTL-Plus version 5.0 (Bruker[53]) and XSEED (Barbour[54]).

Results and discussion

The synthesis of Cr(tmtaa)Cl (**1**) was accomplished by reacting $CrCl_3$ with H_2tmtaa and triethylamine in a 1:1:2: ratio in benzene. In an attempt to grow single crystals, hexane was allowed to slowly diffuse in the filtered benzene solution for 2 weeks at room temperature followed by 2 weeks at 4 °C. Single crystals of complex **1** were obtained in large yield and subjected to X-ray structure analysis. The solid state unit cell obtained from the analysis contained two molecules of **1**, each existing as a five-coordinate square pyramidal species, along with one interstitial benzene molecule and half of a disordered hexane molecule.

Table 2 lists crystal data and details of the data collection. A thermal ellipsoid representation of complex **1** is shown in Figure 18 along with selected bond distances

and angles listed in Table 3. The structure of **1** exhibits the characteristic saddle shape inherent to complexes incorporating the tmtaa ligand, brought about from the steric interaction between the methyl and aromatic protons. Figure 18 also illustrates the out-of-plane distortion of the chromium center relative to the four nitrogen donor plane, where the chromium atom resides 0.4235 Å above the donor core. The pocket on the underside of the complex is not, however, too constrained to bind a substrate to the open site on the metal center, forming an octahedral species. This was shown by Hao and coworkers by reversibly cleaving the chromium-chromium quadruple bonded dimer of $[Cr(tmtaa)]_2$ with the addition of pyridine.[55] The solid state X-ray crystal structure depicted a monomeric complex with pyridine bound to both the apical position and the cavity on the underside of the chromium in a *trans* binding motif. This demonstrated that the binding of a nucleophilic cocatalyst, being much less sterically encumbered than pyridine, should be expected to occur in the same manner as in the chromium salen catalysts.

Table 2. X-ray Crystallographic Data for Complex **1**.

Empirical formula	$C_{21.2}H_{22.8}Cl_{0.8}Cr_{0.8}N_{3.2}$
Formula wt, g/mol	392.39
Temp (K)	110(2)
Wavelength	0.71073
Crystal system	triclinic
Space group	P-1
a (Å)	12.6158(10)
b (Å)	13.5543(11)
c (Å)	15.9732(12)
α (deg)	84.2930(10)
β (deg)	73.2590(10)
γ (deg)	64.4110(10)
Cell volume ($Å^3$)	2358.1(3)
Z	5
Density (calcd) ($Mg \cdot m^{-3}$)	1.382
Absorb coeff (mm^{-1})	0.612
Obsd no. of reflcns	27342
No. of unique reflcns ($I > 2\sigma$)	10953
GooF	1.011
R,[a] % [$I > 2\sigma$]	4.19
R_w,[a] % [$I > 2\sigma$]	10.46

[a] $R = \sum||F_o| - |F_c||/\sum|F_o|$. $R_w = \{[\sum w(F_o^2 - F_c^2)^2]/[\sum w(F_o^2)^2]\}^{1/2}$.

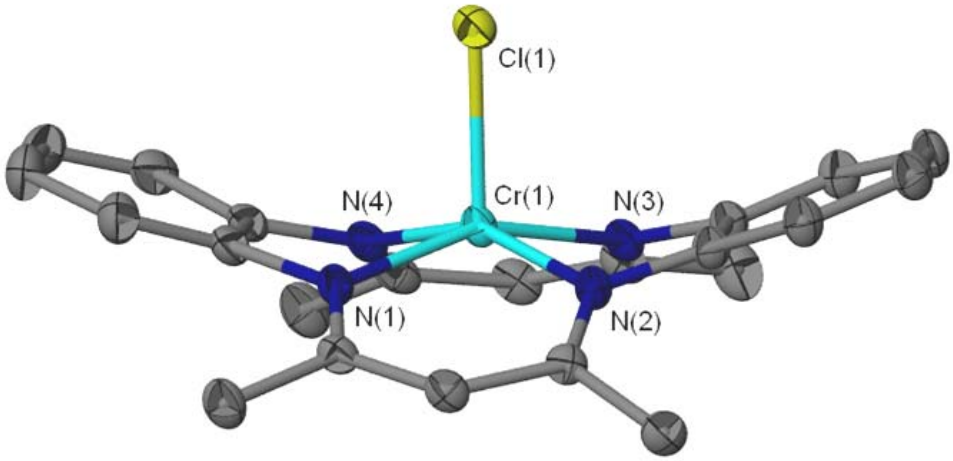

Figure 18. Thermal ellipsoid representation of complex **1**, Cr(tmtaa)Cl, shown (50% probability) with hydrogens and interstitial solvent molecules removed for clarity.

Table 3. Selected Bond Distances (Å) and Bond Angles (deg) of Complex **1**.

Cr – N1 (Å)	1.9881(18)
Cr – N2 (Å)	1.9745(17)
Cr – N3 (Å)	1.9900(18)
Cr – N4 (Å)	1.9716(17)
Cr – Cl (Å)	2.2607(7)
N1 – Cr – N2 (deg)	92.98(7)
N2 – Cr – N3 (deg)	81.76(7)
N3 – Cr – N4 (deg)	92.96(7)
N1 – Cr – N4 (deg)	81.78(7)
Cr – N_4 (Å)	0.4235

Following previous work with the chromium salen system, it was shown early in their application as catalysts that the rate of copolymerization was greatly increased in the presence of a nucleophilic cocatalyst.[12,56] In order to gain a better understanding of how complex **1** will interact with an added cocatalyst, a binding study was performed. To carry out this study, stock solutions of complex **1** and cocatalyst were prepared. Sequential additions of cocatalyst were added to a number of vials containing a constant amount of complex **1** . The cocatalyst was chosen to be an anionic azide salt with a non-interacting cation, in this case, tetra-n-butylammonium, for their significance to the chromium salen system.[56] The azide anion also provides a convenient handle in the infrared region of the electromagnetic spectrum, allowing for precision monitoring via infrared spectroscopy. The hypothesis was for the addition of 1 equivalent of cocatalyst to bind to the chromium center, forming the mixed chloride-azide six-coordinate complex (**B**) in Figure 19. As the titration continues, further addition of azide cocatalyst could form an equilibrium process between the mixed species (**B**) and a species where the chloride from complex **1** has been displaced by an additional equivalent of azide to form a diazide complex (**C**). Table 4 outlines the specifics of the of the cocatalyst binding study.

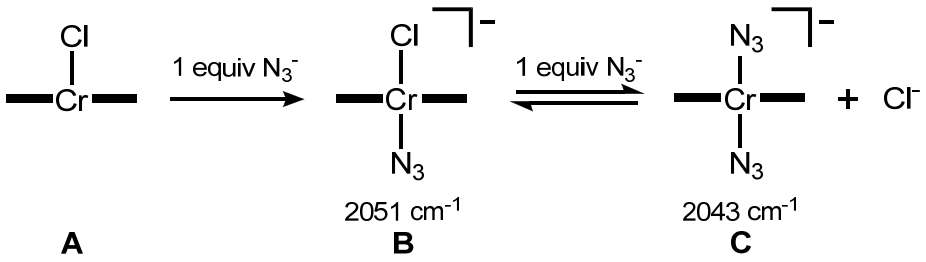

Figure 19. Demonstration of azide cocatalyst binding to complex **1** and the infrared stretching frequencies associated with each six-coordinate complex.

After the solutions were prepared and care taken to ensure the correct concentrations with respect to each sample, the solutions were analyzed by FTIR spectroscopy. Upon assaying Vial 4, which contained NBu_4N_3 in a 5 mM concentration, an absorbance band corresponding to the free azide anion was observed at 2005 cm^{-1}. The spectra of Vials 3 and 5 through 13 are shown as a stack plot in Figure 20. As can be seen in the figure, complex **1** does not have any vibrational stretching modes in this area of the infrared. When half an equivalent of azide is introduced, a stretching band is observed at 2051 cm^{-1}, corresponding to the presence of the Cl-Cr-N_3 mixed species (**B**) shown in Figure 19. This stretching band continues to grow in intensity as the cocatalyst concentration reaches 1 equivalent. Upon increasing the azide concentration to 1.5 and 2 equivalents, a shift in the absorbance band is observed from 2051 to 2043 cm^{-1}. This shift is attributable to the chloride being displaced by the additional azide, resulting in the formation of the diazide species (**C**) shown in Figure 19, thus lowering the stretching energy owed to the trans influence of the second bound azide molecule.

Table 4. Parameters for the Binding Study Between Complex **1** and Tetra-n-butylammonium Azide Cocatalyst.

Vial	Cr(tmtaa)Cl		NBu_4N_3		CH_2Cl_2
1	stock 86 mg	25 mM			8 mL
2	stock		200 mg	50 mM	14 mL
3	1 equiv (0.4 mL)	5 mM			1.6 mL
4			1.0 equiv (0.2 mL)	5 mM	1.8 mL
5	1 equiv (0.4 mL)	5 mM	0.5 equiv (0.1 mL)	2.5 mM	1.5 mL
6	1 equiv (0.4 mL)	5 mM	1.0 equiv (0.2 mL)	5 mM	1.4 mL
7	1 equiv (0.4 mL)	5 mM	1.5 equiv (0.3 mL)	7.5 mM	1.3 mL
8	1 equiv (0.4 mL)	5 mM	2.0 equiv (0.4 mL)	10 mM	1.2 mL
9	1 equiv (0.4 mL)	5 mM	2.5 equiv (0.5 mL)	12.5 mM	1.1 mL
10	1 equiv (0.4 mL)	5 mM	3.0 equiv (0.6 mL)	15 mM	1.0 mL
11	1 equiv (0.4 mL)	5 mM	4.0 equiv (0.8 mL)	20 mM	0.8 mL
12	1 equiv (0.4 mL)	5 mM	6.0 equiv (1.2 mL)	30 mM	0.4 mL
13	1 equiv (0.4 mL)	5 mM	8.0 equiv (1.6 mL)	40 mM	0.0 mL

At 2.5 equivalents of azide cocatalyst, the presence of free azide is apparent, confirming that complex **1** has been saturated at 2 equivalents of cocatalyst. As the azide concentration is further increased to 3, 4, 6, and 8 equivalents, the chromium-azide stretching band remains constant, while the intensity of the free azide band continued to increase. The slight increase in the chromium-azide stretching frequency and the activity from 2070-2170 cm^{-1} is due to a concentration effect as the ionic strength of the solutions was increased as more cocatalyst was added. In order to more clearly visualize the cocatalyst binding trend, peak profiles were plotted versus cocatalyst equivalents for

both the chromium-azide and free azide stretching bands (Figure 21). From this plot, one can easily see the rapid growth of the free azide absorbance band after 2 equivalents of cocatalyst was reached.

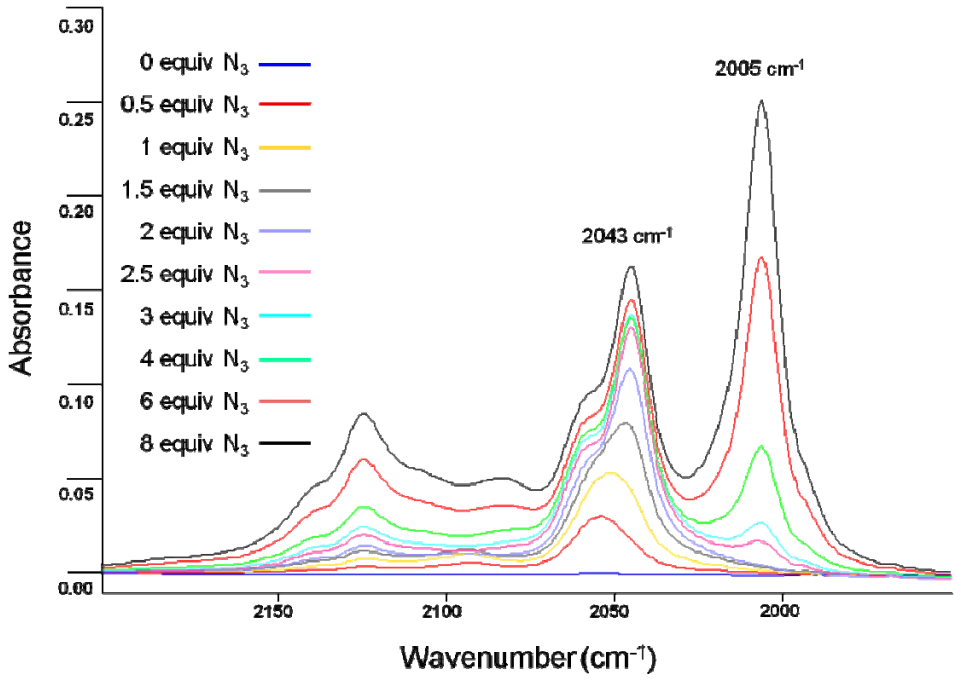

Figure 20. Infrared spectra from the titration of complex **1** with NBu_4N_3.

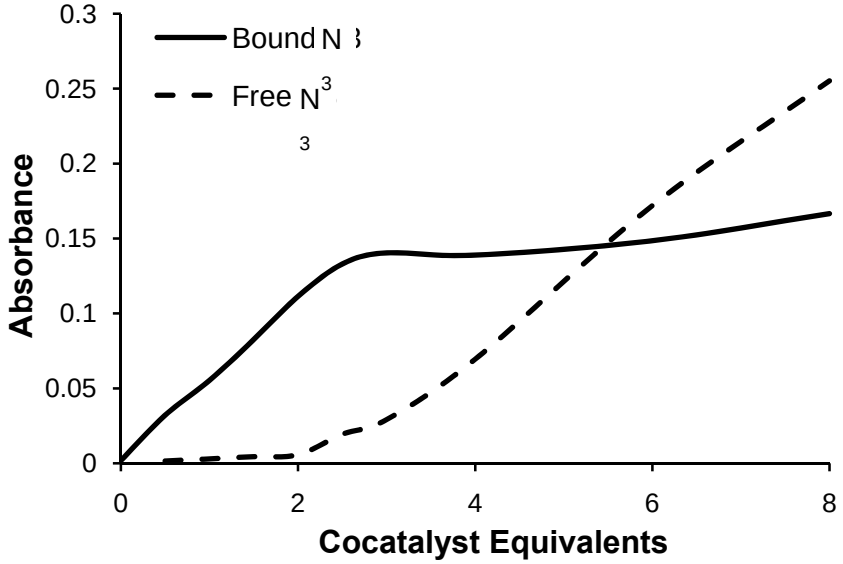

Figure 21. Plot of the peak profiles for the stretching frequencies for azide bound to complex **1** (——) and free azide (- - -) vs. equivalents of NBu_4N_3 cocatalyst.

Thus far, the latter part of the hypothesized cocatalyst binding behavior shown in Figure 19 has not been clarified. To address whether an equilibrium exists between the binding of chloride versus azide, a solution was made containing complex 1 and 2 equivalents of NBu_4N_3 cocatalyst. An analysis of the sample by FTIR spectroscopy confirms earlier observations for the presence of a chromium diazide species and no absorbances indicating the presence of free azide. A large excess (~10 equiv) NBu_4Cl was added to the sample in an attempt to displace the bound azide molecules, thus establishing the presence of an equilibrium. Upon examination by FTIR spectroscopy, the absorbance corresponding to free azide in solution remained absent, implying a large

equilibrium constant and a reaction that is not easily reversible, demonstrating complex **1**'s affinity for the azide anion.

Building from the azide cocatalyst titration study, complex **1** was found to readily convert to the anionic diazide species when 2 equivalents of NBu_4N_3 were added. Since this behavior is in sync with what is known about the copolymerization mechanism, employing this complex as a catalyst was the next logical progression in the study of the chromium tetramethyltetraazaannulene system. A series of polymerizations were conducted using complex **1** as a catalyst and $PPNN_3$ as a cocatalyst. The PPN (bis(triphenylphosphoranylidene)ammonium) cation is more non-interacting, more easily dried due to its hydrophobicity, and has shown to yield a slightly more active catalyst system with chromium salen catalysts over their tetraalkylammonium analogues.[14,56] The purpose of these polymerizations is to examine complex **1**'s ability to copolymerize cyclohexene oxide and carbon dioxide using a range of cocatalyst concentrations. In each case, the catalyst and desired amount of $PPNN_3$ cocatalyst were dissolved 10 mL dichloromethane. After 30 minutes, the dichloromethane was removed in vacuo. This 'activation' step is necessary due to the relative insolubility of PPNX salts in neat cyclohexene oxide. All polymerizations were conducted at 80 °C and 35 bar CO_2 pressure. The reactions were allowed to proceed with monitoring of the absorbance bands at 1750 and 1810 cm^{-1} for polycarbonate and cyclic carbonate, respectively, over

the course of the reaction using in situ infrared spectroscopy until the polymer absorbance profile reached a plateau. At this time, the acquisition was halted, the CO_2 vented, the heating mantle removed, and the reactor allowed to cool. Figure 22 displays an overlay of the polymer peak profiles obtained from the copolymerization reactions using complex **1** as a catalyst at cocatalyst concentrations of 0.0, 0.5, 1.0, 1.5, 2.0, 3.0, 4.0, and 6.0 equivalents.

Interesting to note when looking at Figure 22 is the saturation in rate reached at 2 equivalents of $PPNN_3$ cocatalyst. This indicates that a maximum copolymerization rate is achieved at 2 equivalents of cocatalyst and no further rate enhancement is seen when higher concentrations are employed. This leveling of the polymerization rate is better observed in the plot of the polymer profile rates versus cocatalyst equivalents shown in Figure 23. These results are in good agreement with those of the binding study previously discussed *vide supra* where complex **1** preferentially bound 2 equivalents of azide anion over chloride.

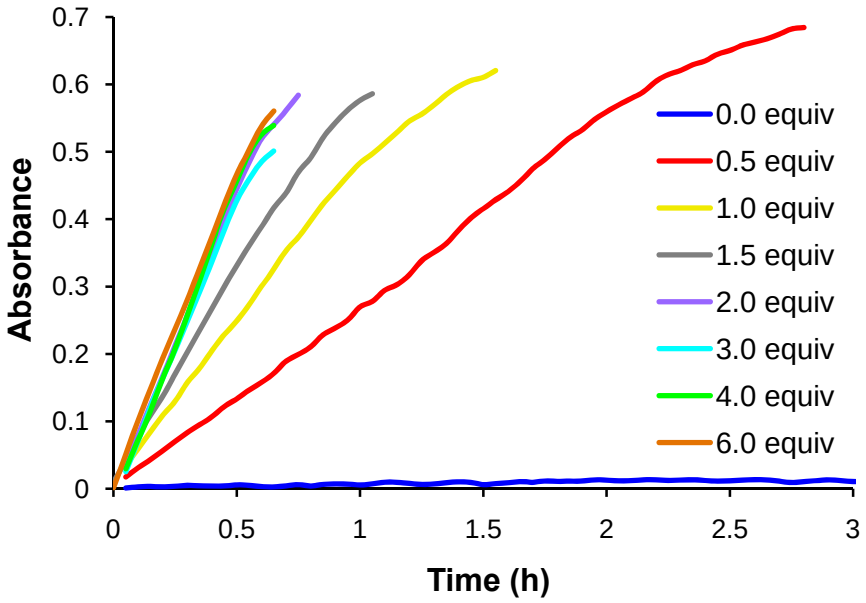

Figure 22. Polymer peak trace (~1750 cm^{-1}) overlay of copolymerizations conducted using complex **1** and various $PPNN_3$ cocatalyst loadings.

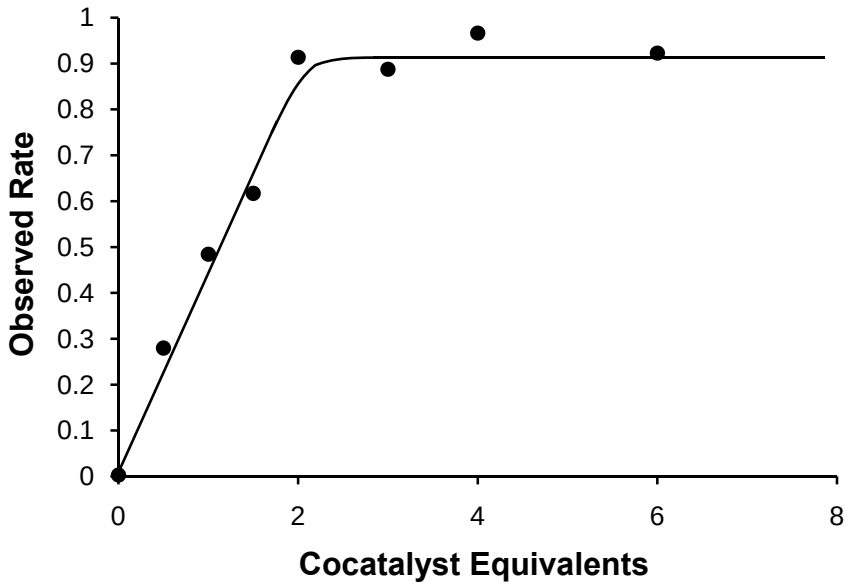

Figure 23. Plot of the peak profile slopes from the copolymerizations using complex **1** versus added equivalents of $PPNN_3$ cocatalyst.

The parameters and results from these copolymerizations conducted to study complex **1**'s dependence on cocatalyst are shown below in Table 5. From this table, one can see that despite the reaction times progressively getting shorter, there is a maximum difference of only 100 turnovers between the reactions that employed a cocatalyst. The highest activities were achieved with excess cocatalyst reached as high as 1,300 turnovers per hour. The polymer obtained when no cocatalyst was used was analyzed by ^{1}H NMR spectroscopy and determined to be almost exclusively polyether with less than 2% CO_2 incorporation. This polymer was subjected to GPC analysis and found to have a M_n of 33,300 g mol^{-1} and a broad polydispersity index of 1.6.

Table 5. The Effect of Varying Equivalents of $PPNN_3$ Cocatalyst on the Copolymerization.[a]

Equiv N_3	P_{CO_2} (bar)	Time (h)	TON[b]	TOF[c]	% carbonate[d]	M_n	PDI[e]
0	35	6	100	17	< 2	33,300	1.6
0.5	35	2.85	906	318		27,300	1.07
1	35	1.55	939	606		24,900	1.07
1.5	35	1.35	925	685		21,600	1.09
2	35	1.05	842	802	> 98	23,400	1.09
3	35	1	860	860		18,600	1.11
4	35	0.8	834	1025	> 94	14,500	1.08
6	35	0.7	912	1303		13,900	1.08

[a]Each experiment was performed using 20 mL cyclohexene oxide, 50 mg catalyst **1**, and the desired amount of $PPNN_3$ as a cocatalyst. [b]Mol epoxide consumed/(mol Cr). [c]Mol epoxide consumed/(mol Cr-hour). [d]Estimated by ^{1}H NMR. [e]M_n/M_w.

In contrast, selected purified polymers from reactions containing cocatalyst were determined to contain greater than 94% carbonate linkages. Complex 1 was able to produce narrowly controlled (PDI = 1.07-1.11) and moderately high molecular weight polymers that ranged from 13,900-27,300 g mol^{-1}. There was a decrease observed in the molecular weight of the polymer products as a greater cocatalyst concentration was employed. This is attributable to the greater amount of water and excess cocatalyst anions introduced with the increased quantity of cocatalyst, resulting in early chain transfer and termination. This trend is illustrated in Figure 24 below.

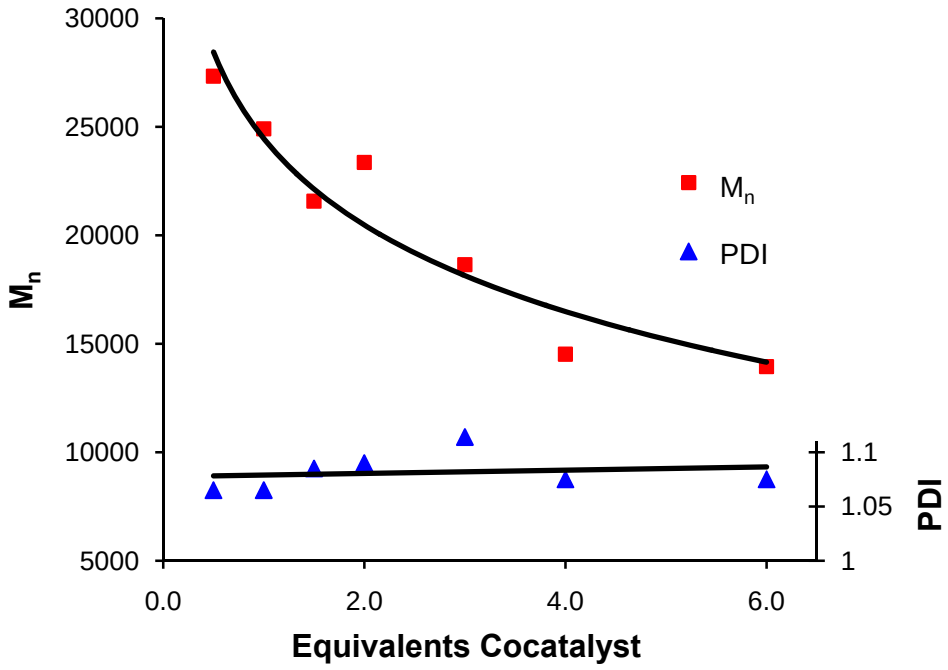

Figure 24. Plot of molecular weights and polydispersity indices of polymers obtained from the copolymerization of cyclohexene oxide and carbon dioxide using catalyst **1** and various equivalents of $PPNN_3$ cocatalyst.

Careful observation of the stack plots obtained from the in situ infrared monitoring during a copolymerization reaction when excess cocatalyst was used indicated an interesting and unexpected result. For the case with the chromium salen catalysts, when excess cocatalyst was employed, an absorbance band corresponding to cyclic cyclohexylene carbonate formation was more prominent than what was observed for the chromium tetraazaannulene system. For the copolymerization of cyclohexene oxide and carbon dioxide using catalyst 1 and 3 equivalents of $PPNN_3$ as a cocatalyst, formation of cyclic carbonate was negligible until the peak profile for copolymer formation reached plateau. This plateau is observed due to the increased viscosity of the reaction mixture, which, according to ^1H NMR spectroscopy, occurs when around 50% of the epoxide monomer has been converted to polymer. Once this plateau was reached, the cyclic carbonate absorption band began to increase in intensity (Figure 25). It is believed that the chromium tetraazaannulene system has a greater affinity for the growing polymer chain than analogous chromium salen catalysts. This preference towards copolymer formation is a significant advantage of the chromium tmtaa system over that of the chromium salens.

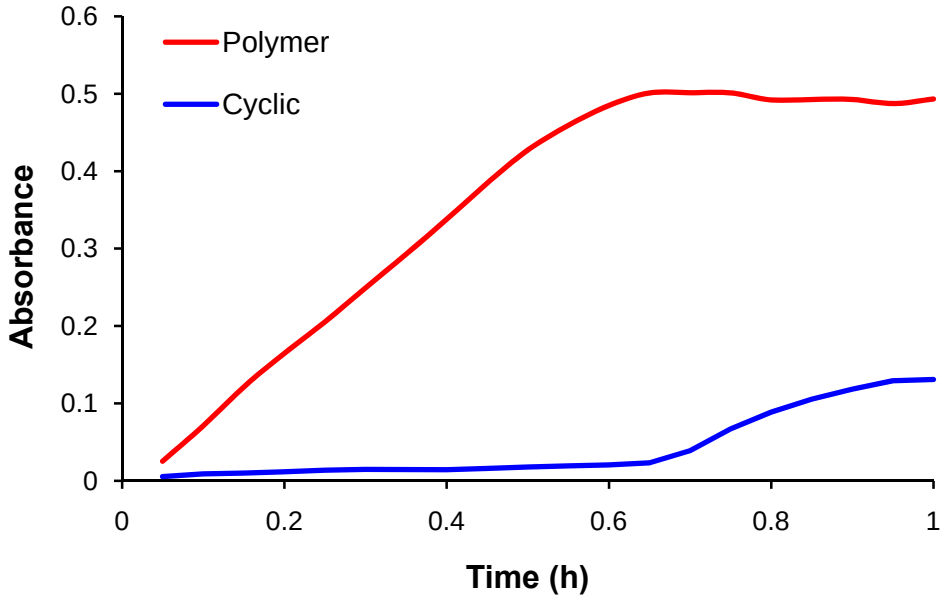

Figure 25. Infrared peak traces for polycarbonate and cyclic carbonate formation for the reaction of cyclohexene oxide and carbon dioxide using catalyst **1** and 3 equivalents of $PPNN_3$ as a cocatalyst.

Conclusions

A chromium tetraazaannulene complex (Cr(tmtaa)Cl, **1**) was introduced as a possible catalyst for the copolymerization of cyclohexene oxide and carbon dioxide. Interest in this complex as a possible catalyst was spurred by its similarities to both the chromium porphyrin and chromium salen catalytic systems. The ν_{N_3} stretching vibrational mode of was utilized to probe the behavior or complex **1** in the presence of $PPNN_3$. It was found that at 2 equivalents, the azide anion not only coordinated to the sixth coordination site of complex **1**, but displaced the apical chloride ligand to form a chromium diazide species. Copolymerizations conducted with cyclohexene oxide and

carbon dioxide using complex **1** as a catalyst and varying amounts of $PPNN_3$ cocatalyst found that a maximum rate was achieved at 2 equivalents of cocatalyst with TOFs as high as 1,300 h^{-1}. The moderately high molecular weight copolymers produced contained a near quantitative percentage of carbonate linkages and an average polydispersity less than 1.1. Complex **1** also proved to exhibit a higher affinity for the growing polymer chain compared to analogous salen catalysts, only producing consequential amounts of cyclohexylene carbonate after the copolymerization reaction had reach completion, even in the presence of an excess of $PPNN_3$ cocatalyst.

CHAPTER III

KINETIC AND MECHANISTIC ASPECTS OF TETRAMETHYLTETRAAZAANNULENE CHROMIUM CHLORIDE AS A CATALYST FOR THE COPOLYMERIZATION OF CARBON DIOXIDE AND EPOXIDES*

Introduction

To fully understand the success of the chromium tetramethyltetraazaannulene catalyst system, various efforts were made to more fully understand the characteristics that give rise to its activity and advantages over other catalyst systems. These efforts include studies to probe the kinetic and mechanistic aspects of the copolymerization reaction including the dependence on cocatalyst type and quantity, the effects of various carbon dioxide pressures and kinetic investigations in both neat cyclohexene oxide and in the presence of a cosolvent. Additionally, modifications to the ligand architecture to adjust its electronic characteristics, and the copolymerization of epoxides other than cyclohexene oxide were studied. These studies are in direct comparison to work previously conducted on the chromium salen system to understand its intricacies and to achieve optimization of the catalytic system.[12,14,56-61]

---

*Reproduced in part with permission from Darensbourg, D. J.; Fitch, S. B. *Inorg. Chem.* **2008,** *47,* 11868-11878.

Like porphyrin complexes, compounds incorporating the salen ligand are planar, resulting in low solubility. To overcome this problem, aromatic or alkyl groups are often added to the ligand periphery. Common solubilizing substituents for the porphyrin ligand are phenyl or ethyl groups. For the salen ligand, the addition of *tert*-butyl groups to its phenolate moieties has become a frequent practice. Aside from solely acting to increase the solubility of the complex, alkyl substituents such as the *tert*-butyl group are also able to donate electron density to the metal center of the complex. Conversely, electron-withdrawing substituents, such as chloride, can also be incorporated onto the salen ligand and are able to afford an increased solubility over the underivatized salen ligand. Other sources for complex alteration include ligand backbones other than ethylenediamine and various nucleophiles attached to the chromium-metal center. A summary of usual locations of derivatization to the chromium salen architecture are

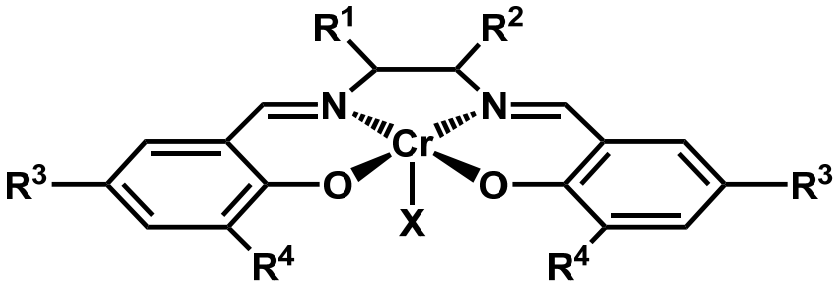

R^1, R^2 = H, -C_4H_4-, (1*R*,2*R*)-C_4H_8-
R^2 = H, ^{t}Bu, OMe
R^3 = H, ^{t}Bu

Figure 26. Generalized skeletal representation of chromium salen catalysts described in Table 6.

shown in Figure 26 while the effects the derivatizations had on the copolymerization reaction of cyclohexene oxide and carbon dioxide are listed in Table 6 below.[58]

Table 6. Copolymerization of Cyclohexene Oxide and CO_2 Catalyzed by Cr(salen)X Complexes.[a]

Complex	R^1	R^2	R^3	R^4	X	TON[b]	TOF[c]	% carbonate
A	H	H	H	H	Cl	270	11.2	92
B	H	H	^{t}Bu	^{t}Bu	Cl	857	35.7	99
C	-C_4H_4-		Cl	Cl	Cl	90	3.8	15
D	-C_4H_4-		H	H	Cl	383	15.9	97
E	-C_4H_4-		^{t}Bu	^{t}Bu	Cl	868	36.2	99
F	(1*R*,2*R*)-C_4H_8-		^{t}Bu	^{t}Bu	Cl	851	35.5	99
G	(1*R*,2*R*)-C_4H_8-		OCH_3	^{t}Bu	Cl	1575	65.6	96
H	(1*R*,2*R*)-C_4H_8-		OCH_3	^{t}Bu	N_3	1966	81.9	>99

[a]Each experiment was performed using 20 mL cyclohexene oxide, 50 mg of catalyst, 2.25 equiv MeIm as a cocatalyst, 80 °C, and 55 bar CO_2 over 24 h. [b]Mol epoxide consumed/(mol Cr). [c]Mol epoxide consumed/(mol Cr-hour). [d]Estimated by ^{1}H NMR.

Several trends concerning the reactivity of chromium salen catalysts towards the copolymerization of cyclohexene oxide and carbon dioxide using 2.25 equivalents of *N*-Methylimidazole (MeIm) as a cocatalyst are revealed in Table 6. A three-fold increase in activity (TOF) was achieved from the underivatized chromium salen catalyst (**A**) upon the addition of *tert*-butyl groups to the phenolate portions of the ligand (**B**). This increase is likely due to the combination of the increased solubility of the complex and the electron-donation to the metal center from the alkyl substituents. Complexes **C**-**E** also confirm an increase in polymerization activity as the phenolate substituents increase

in electron-donating ability from the electron-withdrawing chlorides to the unsubstituted ligand to the donating alkyl groups. Substitution of a better donating methoxy group (**G**) in place of the *tert*-butyl (**F**) at the R^3 position resulted in another two-fold increase in activity. Exchange of the metal-bound nucleophile (X) from chloride (**G**) to the slightly more nucleophilic azide anion (**H**) produced a further increase in TOF from 65.6 to 81.9 h^{-1}, further supporting the proposition that the more electron density that can be put toward the chromium center, the greater the catalytic activity. This trend was not observed, however, when the ligand backbone was changed from ethylene (**B**) to an electron-withdrawing phenylene (**E**) to an electron-donating cyclohexylene backbone (**F**), with each resulting in a negligible change in activity.

Further advancements, and perhaps the most profound, toward optimization of the chromium salen catalyst system were achieved through the implementation of cocatalysts with more nucleophilic character.[56] As shown in Table 6 above, when *N*-MeIm was used as a cocatalyst, the maximum achieved TOF was 81.9 h^{-1}. The employment of phosphines as cocatalysts gave a significant increase in catalytic activity, with turnovers of up to 346 per hour when three equivalents of tricyclohexylphosphine were used. The activity was further doubled upon the application of anionic cocatalysts, such as PPNCl and $PPNN_3$, which utilize a bulky, non-interacting cation and are able to donate an essentially "free" anion to the metal center of the catalyst. When just one equivalent of $PPNN_3$ was used as a cocatalyst, the catalyst was able to perform 760 turnovers per hour. The use of these anionic cocatalysts have provided the highest activities yet attainable with the chromium salen catalyst system. Unrelated to cocatalyst

development, further enhancements to the catalytic activity were achieved by adjusting the carbon dioxide pressure of the copolymerization reaction. All of the polymerizations described above were performed under 55 bar carbon dioxide. It was found by simply lowering the reaction pressure to 35 bar, thereby creating a more concentrated reaction mixture, the activity of the system was increased to 1,150 h^{-1}.[14,60] These results are summarized in Table 7, which illustrates the various cocatalysts' effects on the catalytic activity along with a brief synopsis of the effects of ligand, nucleophile substitution, and pressure dependence.

Table 7. The Effect of Varying R^3, Nucleophile (X), Cocatalyst, and CO_2 Pressure on the Copolymerization of Cyclohexene Oxide and CO_2 Using the Chromium Salen Catalyst System.[a]

R^{3} [b]	X	Cocatalyst (equiv)	P_{CO_2} (bar)	TOF[c]	% carbonate[d]	M_n	PDI[e]
^{t}Bu	Cl	none	55	10.4	80		
^{t}Bu	Cl	MeIm (2.25)	55	35.5	99	8,900	1.2
OMe	Cl	MeIm (2.25)	55	65.6	>99		
OMe	N_3	MeIm (2.25)	55	81.9	>99	23,000	1.6
OMe	N_3	PCy_3 (3)	55	346	>99		
OMe	N_3	$PPNN_3$ (1)	55	760	>99		
OMe	N_3	$PPNN_3$ (1)	35	1150	>99	50,000	1.1

[a]Each experiment was performed using 20 mL cyclohexene oxide, 50 mg catalyst , and the desired cocatalyst and CO_2 pressure. [b]Catalyst is outlined in Figure 26 where R^1 and R^2 are cyclohexylenediamine and R^4 is a *tert*-butyl group. [c]Mol epoxide consumed/(mol Cr-hour). [d]Estimated by ^{1}H NMR. [e]M_n/M_w.

The scope of this chapter is to communicate the further investigation and optimization of the tetramethyltetraazaannulene chromium catalyst system as it pertains to ligand substitution, nature of cocatalyst, and the system's dependence on temperature and pressure. Copolymerizations were performed both in situ and in neat cyclohexene oxide to determine the corresponding kinetic parameters in order to gain a more full understanding of the chromium tetramethyltetraazaannulene system and will be discussed in detail. The studies presented mirror the work previously conducted using the chromium salen system as a guide, with the goal of direct comparison between the two. Exploring the capabilities of the chromium tmtaa system through the employment of different epoxides with the hope of forming an assortment of polycarbonates and discerning their inherent properties will also be reviewed.

Experimental

Methods and materials. Unless otherwise specified, all manipulations were carried out on a double manifold Schlenk vacuum line under an atmosphere of argon or in an argon-filled Glovebox. Methanol (EMD Chemicals), absolute ethanol (Pharmco-Aaper), 2,4-pentanedione (Aldrich), 4,5-diamino-*o*-xylene (TCI), 4,5-dichloro-1,2-phenylenediamine (TCI), nickel acetate tetrahydrate (Fisher), chromium(III) chloride (Strem), ammonium hexafluorophosphate (Oakwood), and sodium azide (Aldrich), sodium chloride (EMD Chemicals), sulfuric acid (EMD Chemicals), sodium bromide (Fisher), sodium cyanide (Aldrich), sodium hydroxide (EMD Chemicals), hydrochloric

acid (EMD Chemicals), and pentafluorobenzoic acid (Aldrich) were used without further purification. Triethylamine (EMD Chemicals) was stored over sodium hydroxide and freshly distilled before use. Bis(triphenylphosphoranylidene)ammonium chloride was recrystalized from methylene chloride/ether. Bis(triphenylphosphoranylidene)-ammonium azide was synthesized from a published literature procedure.[49] Methylene chloride, benzene, tetrahydrofuran, acetonitrile, hexane, and ethyl ether were freshly purified by an MBraun Manual Solvent System packed with Alcoa F200 activated alumina desiccant. The synthesis of H_2tmtaa was conducted using published procedures.[47] Cyclohexene oxide (TCI) was freshly distilled from CaH_2 (Alfa Aesar) prior to use. Acetone (Pharmco-Aaper) was freshly distilled from sodium carbonate (EMD Chemicals) prior to use. Bone dry carbon dioxide (Scott Specialty Gases) was supplied in a high pressure cylinder equipped with a liquid dip-tube. Unless otherwise stated, all other reagents were used without further purification. ^{1}H and ^{13}C NMR spectra were acquired on using a Varian Inova 300 MHz or 500 MHz superconducting NMR spectrometers. Infrared spectra were recorded on using a Bruker Tensor 27 FTIR spectrometer. Molecular weight determinations were carried out on a Viscotek Gel Permeation Chromatograph equipped with refractive index, right-angle and low-angle light scattering detectors.

Synthesis of (6,8,15,17-tetramethylbis-4,5-dichlorobenzo[*b,i*][1,4,8,11]-tetraazacyclotetradecinato) nickel (Ni(tmtaaCl$_4$)). The synthesis of Ni(tmtaaCl$_4$) was conducted following the published procedure for Ni(tmtaa).[47] 4,5-dichloro-1,2-phenylenediamine (10 g, 56.5 mmol) and nickel acetate tetrahydrate (7.03 g, 28.3 mmol)

were refluxed in 80 mL methanol for 30 minutes, resulting in a dark blue solution. A color change to a dark aqua green was observed upon the addition of 2,4-pentanedione (6 mL, 58.4 mmol). The reaction was allowed to reflux for 3 days. The solution was then cooled and the dark purple, microcrystalline product was collected by vacuum filtration and air dried (3.46 g, 22.7% yield). X-ray quality crystals were obtained through slow evaporation from THF. ^{1}H NMR ($CDCl_3$, 500 MHz): δ 6.61 (s, 4H), 4.81 (s, 2H), 1.99 (s, 12H). ^{13}C {^{1}H} NMR ($CDCl_3$, 125.7 MHz): δ 156.44, 146.68, 124.22, 121.43, 112.28, 22.17.

Synthesis of (6,8,15,17-tetramethylbis-4,5-dimethylbenzo[*b*,*i*][1,4,8,11]-tetraazacyclotetradecinato) nickel (Ni(omtaa)). The synthesis of Ni(omtaa) was modified from the published procedure for Ni(tmtaa).[47] 4,5-diamino-*o*-xylene (10 g, 73.42 mmol) and nickel acetate tetrahydrate (9.13 g, 36.7 mmol) were refluxed in 100 mL methanol for 30 minutes, resulting in a dark blue solution. A color change to a dark aqua green was observed upon the addition of 2,4-pentanedione (8 mL, 78 mmol). The reaction was allowed to reflux for 3 days. The solution was then cooled and the dark purple, microcrystalline product was collected by vacuum filtration and air dried (5 g, 30% yield). ^{1}H NMR ($CDCl_3$, 500 MHz): δ 6.44 (s, 4H), 4.75 (s, 2H), 2.03 (s, 24H). ^{13}C {^{1}H} NMR ($CDCl_3$, 125.7 MHz): δ 154.80, 145.27, 129.44, 122.00, 110.41, 22.07, 19.62.

Synthesis of 5,14-dihydro-6,8,15,17-tetramethylbis-4,5-dichlorobenzo[*b*,*i*]-[1,4,8,11]tetraazacyclotetradecine (H_2tmtaaCl_4). The neutral ligand, H_2tmtaaCl_4, was

synthesized by modifying established literature procedures.[47,62,63] Anhydrous hydrogen chloride gas (generated by sulfuric acid slowly added to sodium chloride) was bubbled through a suspension of Ni(tmtaaCl_4) (3.46 g, 6.42 mmol) in dry acetone (70 mL) overnight with vigorous stirring. The tetrachloronickelate salt of the ligand precipitates as a blue-white solid. The mixture is cooled at -4 °C and filtered, washed with a minimal amount of cold acetone, and air dried. The demetallated ligand salt is then dissolved in a minimal amount of water. Ammonium hexafluorophosphate (3.14 g, 19.3 mmol) was added to the aqueous solution to exchange the $NiCl_4^{2-}$ anion with two PF_6^{1-} counterions. The bis(hexafluorophosphate) ligand salt precipitates from the aqueous solution as a white solid, which is filtered, washed with water, and dried in air. The salt is dissolved in a minimal amount of methanol and upon neutralization with a slight excess of triethylamine (1.8 mL, 13 mmol) a color change from pale yellow to golden yellow along with the precipitation of a microcrystalline product of the same color was observed. The product was isolated by filtration, washed with methanol, and dried in air to yield 0.14 g of H_2tmtaaCl_4 (4.5% yield). X-ray quality crystals were obtained through slow evaporation from hexanes. ^{1}H NMR ($CDCl_3$, 500 MHz): δ 12.28 (s, 2H), 6.93 (s, 4H), 4.85 (s, 2H), 2.09 (s, 12H). ^{13}C {^{1}H} NMR ($CDCl_3$, 125.7 MHz): δ 159.22, 137.61, 125.92, 123.29, 99.41, 20.99.

Synthesis of 5,14-dihydro-6,8,15,17-tetramethylbis-4,5-dimethylbenzo[*b*,*i*]-[1,4,8,11]tetraazacyclotetradecine (H_2omtaa). The neutral ligand, H_2omtaa, was synthesized following the established literature procedure.[63] Anhydrous hydrogen chloride gas (generated by sulfuric acid slowly added to sodium chloride) was bubbled

through a suspension of Ni(omtaa) (1.81 g, 3.96 mmol) in dry acetone (80 mL) overnight with vigorous stirring. The tetrachloronickelate salt of the ligand precipitates as a blue-white solid. The mixture is cooled at -4 °C and filtered, washed with a minimal amount of cold acetone, and air dried. The demetallated ligand salt is then dissolved in a minimal amount of water. Ammonium hexafluorophosphate (1.94 g, 11.9 mmol) was added to the aqueous solution to exchange the $NiCl_4^{2-}$ anion with two PF_6^{1-} counterions. The bis(hexafluorophosphate) ligand salt precipitates from the aqueous solution as a white solid, which is filtered, washed with water, and dried in air. The salt is dissolved in a minimal amount of methanol and upon neutralization with a slight excess of triethylamine (1.1 mL, 7.92 mmol) a color change from pale yellow to golden yellow along with the precipitation of a microcrystalline product of the same color was observed. The product was isolated by filtration, washed with methanol, and dried in air to yield 0.55 g of H_2omtaa (30.4% yield). ^{1}H NMR ($CDCl_3$, 300 MHz): δ 12.55 (s, 2H), 6.75 (s, 4H), 4.80 (s, 2H), 2.19 (s, 12H), 2.10 (s, 12H). ^{13}C {^{1}H} NMR ($CDCl_3$, 75 MHz): δ 158.63, 136.17, 130.94, 124.04, 97.38, 20.86, 19.50.

Synthesis of (6,8,15,17-tetramethylbis-4,5-dichlorobenzo[*b,i*][1,4,8,11]-tetraazacyclotetradecinato) chromium chloride (Cr(tmtaaCl$_4$)Cl, 2). The chromium complex, Cr(tmtaaCl_4)Cl (**2**), was synthesized by modifying the published literature procedure for complex **1**.[48] H_2tmtaaCl_4 (0.14 g, 0.29 mmol) and anhydrous chromium(III) chloride (0.046 g, 0.29 mmol) were refluxed in 75 mL benzene and 2 equivalents of triethylamine (0.1 mL, 0.7 mmol) for 5 days. The dark burgundy solution was then filtered to remove triethylammonium chloride and any unreacted chromium

chloride. The filtrate was minimized in vacuo and the product precipitated upon the addition of hexanes. The supernatant was decanted and the precipitate isolated. The product was dried in vacuo, transferred to an argon-filled glove box, and weighed to determine yield (0.127 g, 77% yield). Anal. calcd (%) for $C_{22}H_{18}Cl_5CrN_4 \cdot 2H_2O$: C, 43.77; H, 3.67; N, 9.28; found: C, 44.15; H, 4.45; N, 8.78.

Synthesis of (6,8,15,17-tetramethylbis-4,5-dimethylbenzo[*b,i*][1,4,8,11]-tetraazacyclotetradecinato) chromium chloride (Cr(omtaa)Cl, 3). The chromium complex, Cr(omtaa)Cl (**3**), was synthesized by modifying the published literature procedure for complex **1**.[48] H_2omtaa (0.5 g, 1.25 mmol) and anhydrous chromium(III) chloride (0.2 g, 1.26 mmol) were refluxed in 200 mL benzene and 2 equivalents of triethylamine (0.35 mL, 2.5 mmol) for 3 days. The dark burgundy solution was then filtered to remove triethylammonium chloride and any unreacted chromium chloride. The filtrate was minimized in vacuo and the product precipitated upon the addition of hexanes. The supernatant was decanted and the precipitate isolated. The product was dried in vacuo, transferred to an argon-filled glove box, and weighed to determine yield (0.511 g, 84% yield). X-ray quality crystals were obtained through slow diffusion of hexanes into a benzene solution of the complex. Anal. calcd (%) for $C_{26}H_{30}ClCrN_4 \cdot 2H_2O$: C, 59.82; H, 6.56; N, 10.73; found: C, 59.88; H, 6.66; N, 10.19.

Synthesis of PPNX (X = Br, CN, or pentafluorobenzoate ($OBzF_5$)). The syntheses were modified as previously reported in the literature for $PPNN_3$.[49] PPNCl was stirred overnight with 1 equivalent of NaX in absolute ethanol. The solution was

filtered and the filtrate dried in vacuo. The salt was recrystallized from dichloromethane and ether, filtered, and dried in vacuo.

Copolymerization of cyclohexene oxide and carbon dioxide. High pressure measurements of the copolymerization processes were carried out using a stainless steel Parr autoclave modified with a SiComp window to allow for attenuated total reflectance infrared spectroscopy (ASI ReactIR 1000 in situ probe). The catalyst and cocatalyst were dissolved in 10 mL of dichloromethane, allowed to stir for 30 minutes, and then dried in vacuo. The "activated" catalyst/cocatalyst mixture was then dissolved in 20 mL of neat cyclohexene oxide and injected into the autoclave via injection port and cannula, after which a single 128-scan background spectrum was collected. The autoclave was then charged with 35 bar carbon dioxide and a single 128-scan spectrum was taken every 2 minutes during the reaction period. Profiles of the absorbances at 1750 cm^{-1} (polycarbonate) and 1810 cm^{-1} (cyclic carbonate) vs. time were recorded after baseline correction. After cooling and venting of the autoclave, the reaction was extracted with dichloromethane. The solution was dried overnight under a stream of compressed air to remove excess dichloromethane. The polymer residue was then dissolved in a minimum amount of dichloromethane and slowly added to a stirred beaker containing acidified methanol to remove the catalyst and precipitate the polycarbonate product. The supernatant solution containing the catalyst, cyclic carbonate, and any remaining cyclohexene oxide was decanted and the purified polymer dried in vacuo overnight. The dried polymer was collected and weighed to determine yield and the corresponding TONs and TOFs. The highest catalytic activities were obtained from crystalline catalyst.

All other activities reported herein are for comparative purposes only. The polymers were analyzed by ^{1}H NMR where the amount of ether linkages was determined by integrating the peaks corresponding to the methine protons of polyether at ~3.45 ppm and polycarbonate at ~4.6 ppm. Molecular weight determinations were carried out on a Viscotek Gel Permeation Chromatograph equipped with refractive index, right-angle light scattering, and low-angle light scattering detectors.

For the copolymerizations conducted for the purposes of cocatalyst comparison, the same procedure outlined above was used. The various PPNX salts used include azide, chloride, cyanide, bromide, and pentafluorobenzoate. In each run, 50 mg of **1** as catalyst with either 1 or 2 equivalents PPNX cocatalyst were used along with 20 mL cyclohexene oxide and 35 bar of carbon dioxide, maintained at 80 °C throughout the reaction.

Investigations to determine how chloro- and methyl- substitutions affect the electronic nature, and ultimately catalyst activity, of the ligand system were carried out at 80 °C with catalyst, 2 equivalents of $PPNN_3$, 20 mL of cyclohexene oxide, and 35 bar of carbon dioxide. The amount of catalyst was adjusted to maintain a constant monomer-to-initiator ratio (M/I = 1,700), therefore, 66 mg and 57 mg of **2** and **3** were used, respectively.

Copolymerizations for the pressure dependence studies were conducted at 80 °C using 50 mg of **1**, 2 equivalents of PPNCl, 20 mL of cyclohexene oxide, and the desired pressure of carbon dioxide.

The different epoxides attempted for the copolymerization reaction were treated in the same manner as previously prescribed, involving 50 mg of **1**, 2 equivalents of PPNCl, 20 mL of epoxide, and 35 bar carbon dioxide. The reaction temperature varied depending on the epoxide used.

In situ copolymerizations were conducted using the same procedure outlined above with the exception that the reaction mixture was comprised of 75 mg of **1**, 2 equivalents of $PPNN_3$, 10 mL of cyclohexene oxide, and 10 mL of dichloromethane in order to keep all reaction products in solution. The reactions were carried out at 35 bar carbon dioxide and a range of temperatures. Reaction rates were obtained as the slope of the log of the disappearance of monomer over time from the polymer and cyclic peak profiles. The observed rates were then applied to the Eyring and Arrhenius equations in order to determine the activation parameters.

Copolymerizations for the kinetic study of **1** utilizing an anionic cocatalyst in neat epoxide were carried out at the desired temperature using 50 mg catalyst, 2 equivalents of $PPNN_3$, 20 mL cyclohexene oxide, and 35 bar carbon dioxide. A best fit line was applied to the first few minutes of each polymer and cyclic carbonate profiles of each polymerization and used to determine their respective initial rates. These initial rates were appertained to the Arrhenius equation in order to calculate the energies of activation for polycarbonate and cyclic carbonate formation.

X-ray structure studies. A Leica microscope, equipped with a polarizing filter, was used to identify suitable crystals from a sample of crystals of the same habit. The representative crystal was coated in a cryogenic protectant, such as paratone, and affixed

to a nylon sample loop attached to a copper mounting pin. The mounted crystals were then placed in a cold nitrogen stream (Oxford) maintained at 110 or 293 K on either a Bruker SMART 1000, GADDS, or APEX 2 three circle goniometer. The X-ray data were collected on either a Bruker CCD, GADDS, or an APEX 2 diffractometer and covered more than a hemisphere of reciprocal space by a combination of three (or nine in the case of the GADDS) sets of exposures; each exposure set had a different φ angle for the crystal orientation and each exposure covered 0.3° in ω. Crystal data and details on collection parameters are given in Table 1. The crystal-to-detector distance was 5.0 cm for all crystals. Crystal decay was monitored by repeating the data collection for 50 initial frames at the end of the data set and analyzing the duplicate reflections; and found to be negligible. The space group was determined based on systematic absences and intensity statistics.[50] The structure was solved by direct methods and refined by full matrix least-squares on F^2. All non-H atoms were refined with anisotropic displacement parameters. All H atoms attached to C and N atoms were placed in idealized positions and refined using a riding model with aromatic C-H = 0.93 Å, methyl C-H = 0.96 Å, amine N-H = 0.86 Å and with fixed isotropic displacement parameters equal to 1.2 (1.5 for methyl H atoms) times the equivalent isotropic displacement parameter of the atom to which they are attached. The methyl groups were allowed to rotate about their local 3-fold axis during refinement.

For all structures: data reduction, SAINTPLUS (Bruker[50]); program used to solve structures, SHELXS (Sheldrick[51]); program used to refine structures, SHELXL-97

(Sheldrick[52]); molecular graphics and preparation of material for publication, SHELXTL-Plus version 5.0 (Bruker[53]) and XSEED (Barbour[54]).

Results and discussion

The tetramethyltetraazaannulene ligand (H_2tmtaa) was synthesized by the nickel template condensation of *o*-phenylenediamine with pentane-2,4-dione as described initially by Jaeger[64] and later modified by Goedken and coworkers.[46] The neutral H_2tmtaa ligand was isolated following removal of the dianionic tmtaa from Ni(tmtaa) by anhydrous HCl, precipitation as the PF_6^- salt affording $[H_4tmtaa][PF_6]_2$, and neutralization with triethylamine. The chromium(III) derivative was prepared following the literature procedure reported by Cotton and coworkers from H_2tmtaa and anhydrous chromium(III) chloride in refluxing benzene in the presence of 2 equivalents of triethylamine.[48] Other tetraazaannulene ligands were similarly prepared from the appropriately substituted *o*-phenylenediamine and their corresponding Cr(III) derivatives synthesized in an analogous manner to that described for Cr(tmtaa)Cl (**1**). Although

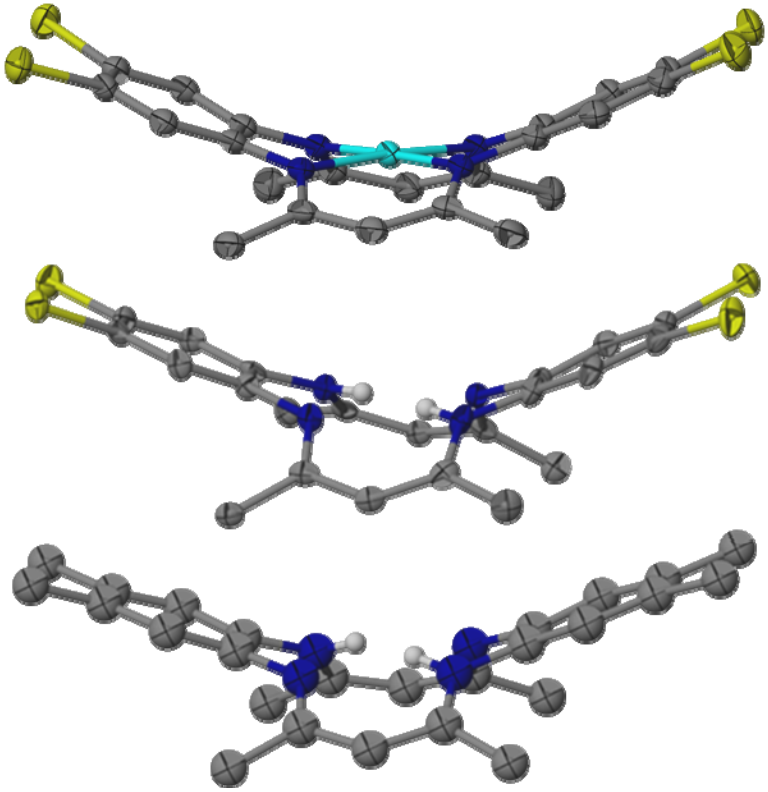

Figure 27. X-ray crystal structures of Ni(tmtaa)Cl_4 (top), H_2tmtaaCl_4 (middle), and H_2omtaa (bottom). Thermal ellipsoids are shown at the 50% probability level with hydrogens and solvent molecules omitted for clarity with the exception of the amine hydrogens.

most of the studies reported at this time involved complex **1**, other derivatives examined for catalytic activity include complexes **2** and **3**, i.e., Cr(tmtaaCl_4)Cl and Cr(omtaa)Cl, where the crystal data and structures of Ni(tmtaa)Cl_4, H_2tmtaaCl_4, and H_2omtaa are shown in Figure 27 and Table 8, respectively.

Table 8. Crystal Data and Structure Refinement for Ni(tmtaa)Cl_4, H_2tmtaaCl_4, and **3**.

	Ni(tmtaa)Cl_4·THF	**H_2tmtaaCl_4**	**Cr(omtaa)Cl (3)**
Empirical formula	$C_{26}H_{26}Cl_4N_4NiO$	$C_{22}H_{20}Cl_4N_4$	$C_{26}H_{30}ClCrN_4$
Formula wt, g/mol	611.02	482.22	485.99
Temp (K)	110(2)	110(2)	293(2)
Wavelength (Å)	0.71073	0.71073	0.71073
Crystal system	monoclinic	monoclinic	triclinic
Space group	C2/c	$P2_1/n$	P-1
a (Å)	14.0054(11)	9.644(4)	8.974(11)
b (Å)	25.033(2)	7.846(4)	12.227(15)
c (Å)	15.7345(13)	28.364(13)	13.150(16)
α (deg)	90	90	79.57(2)
β (deg)	113.8120(10)	98.908(4)	75.63(2)
γ (deg)	90	90	76.14(2)
Cell volume ($Å^3$)	5046.9(7)	2120.1(17)	1346(3)
Z	8	4	2
Density (calcd)	1.608	1.511	1.199
Absorb coeff (mm^{-1})	1.222	0.577	0.543
Obsd no. of reflcns	23839	21774	9863
No. of unique reflcns ($I > 2\sigma$)	5723	3744	4526
GooF	1.002	1.001	1.000
R,[a] % [$I > 2\sigma$]	6.83	9.11	8.00
R_w,[a] % [$I > 2\sigma$]	15.94	22.09	11.79

[a] $R = \sum||F_o| - |F_c||/\sum|F_o|$. $R_w = \{[\sum w(F_o^2 - F_c^2)^2]/[\sum w(F_o^2)^2]\}^{1/2}$.

The X-ray structures of H_2tmtaa and H_2omtaa have been reported elsewhere.[46,65,66] In the course of these studies, H_2tmtaaCl_4 and its precursor, Ni(tmtaa)Cl_4, were structurally characterized and found to be very similar with average carbon-chloride bond distances of 1.727 Å and 1.735 Å, respectively. In agreement with the observations that the metal center resides almost entirely within the donor plane in

Ni(tmtaa),[42] the nickel of Ni(tmtaa)Cl_4 deviates only slightly at 0.0589 Å. The three structures of the protonated, neutral ligands exhibit only minimal differences in bond distances and bond angles, with the largest distinction being the degree of distortion inherent to the saddle-shape. In order to quantify the magnitude of planar distortion, the angle between the phenylenediamine moieties were measured and found to be 133.5º, 136.2º, and 140.4º for H_2tmtaa, H_2tmtaaCl_4 and H_2omtaa, respectively. No obvious trend could be observed from these derivatives which could be merely a factor of crystal packing. The chromium(III) complex derived from H_2omtaa, complex **3**, has been fully characterized by X-ray crystallography. A thermal ellipsoid representation of complex **3** is shown in Figure 28 where the chromium center resides 0.4225 Å above the nitrogen donor plane, along with the atom labeling scheme. Table 9 lists comparative selected bond distances and bond angles for the closely related Cr(tmtaa)Cl and Cr(omtaa)Cl derivatives. As can been seen from this table, there exists only minor structural differences between these two complexes.

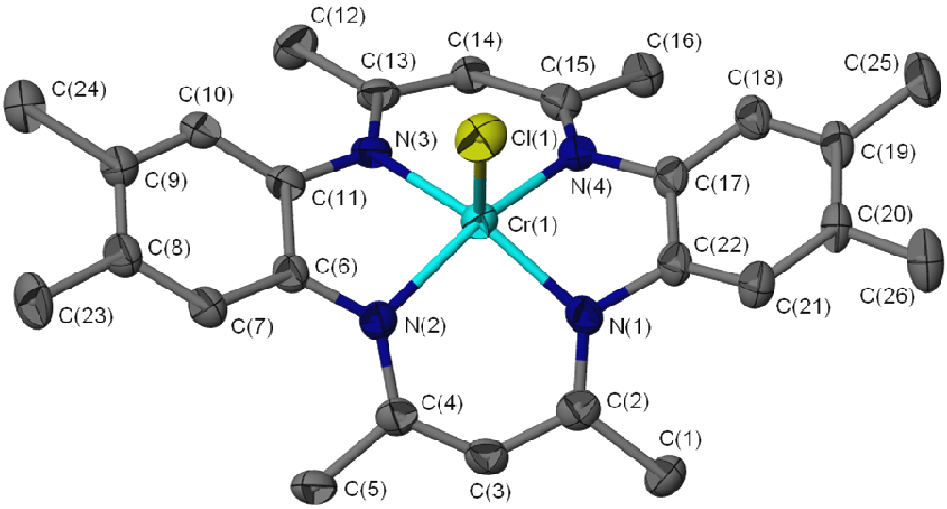

Figure 28. Thermal ellipsoid plot of **3** at 50% probability. Hydrogen atoms omitted for clarity.

Table 9. Selected Bond Distances and Angles for **1** and **3**.

	Cr(tmtaa)Cl (1)[a]	**Cr(omtaa)Cl (3)**
Cr – N1 (Å)	1.9881(18)	1.947(6)
Cr – N2 (Å)	1.9745(17)	2.000(6)
Cr – N3 (Å)	1.9900(18)	1.995(6)
Cr – N4 (Å)	1.9716(17)	1.957(7)
Cr – Cl (Å)	2.2607(7)	2.244(3)
N1 – Cr – N2 (deg)	92.98(7)	91.8(3)
N2 – Cr – N3 (deg)	81.76(7)	82.8(3)
N3 – Cr – N4 (deg)	92.96(7)	91.8(3)
N1 – Cr – N4 (deg)	81.78(7)	83.2(2)
Cr – N_4 (Å)	0.4235	0.4209

[a]Data taken from structure determination in ref. [67].

In a previous publication, the kinetic parameters for the copolymerization of cyclohexene oxide and propylene oxide with carbon dioxide employing Cr(salen)Cl as catalyst were reported.[12,57] In a later report, various cocatalysts (*N*-heterocyclic amines, phosphines, and salts containing anionic initiators) were compared for enhancing the effectiveness of the Cr(salen)Cl catalyst system and clearly established that greater catalytic activity is observed when employing salts possessing nucleophilic anions.[56] Hence, for the Cr(tmtaa)Cl catalytic studies, only anionic initiators were utilized. Despite its sensitivity to aerobic environments, the catalyst is very robust at polymerization conditions and does not appear to degrade over time, as evidenced by the constant rate of polymer formation observed from peak profiles obtained from in situ infrared monitoring of the copolymerization.

Copolymerization reactivity studies utilizing various PPNX salts as initiators. In efforts aimed at developing an optimal catalytic system, several anionic initiators were examined for their effectiveness as cocatalysts for the copolymerization of cyclohexene oxide and carbon dioxide in the presence of **1**. For this study the PPN(bis(triphenylphosphoranylidene)ammonium) salts were chosen due to their ease of being prepared anhydrously, and the non-interacting PPN cation provides an essentially free anion for interaction with the chromium center and ring-opening of the epoxide monomer. In the preliminary report covering the Cr(tmtaa)Cl catalyst utilizing $PPNN_3$ as a cocatalyst, maximum catalytic activity was observed when employing at least two equivalents of cocatalyst.[67] The same was found to be true for PPNCl. This is illustrated in Figure 2 by the copolymer peak profiles over time for the copolymerization

of cyclohexene oxide and carbon dioxide in the presence of **1** and the addition of one, two and four equivalents of PPNCl.

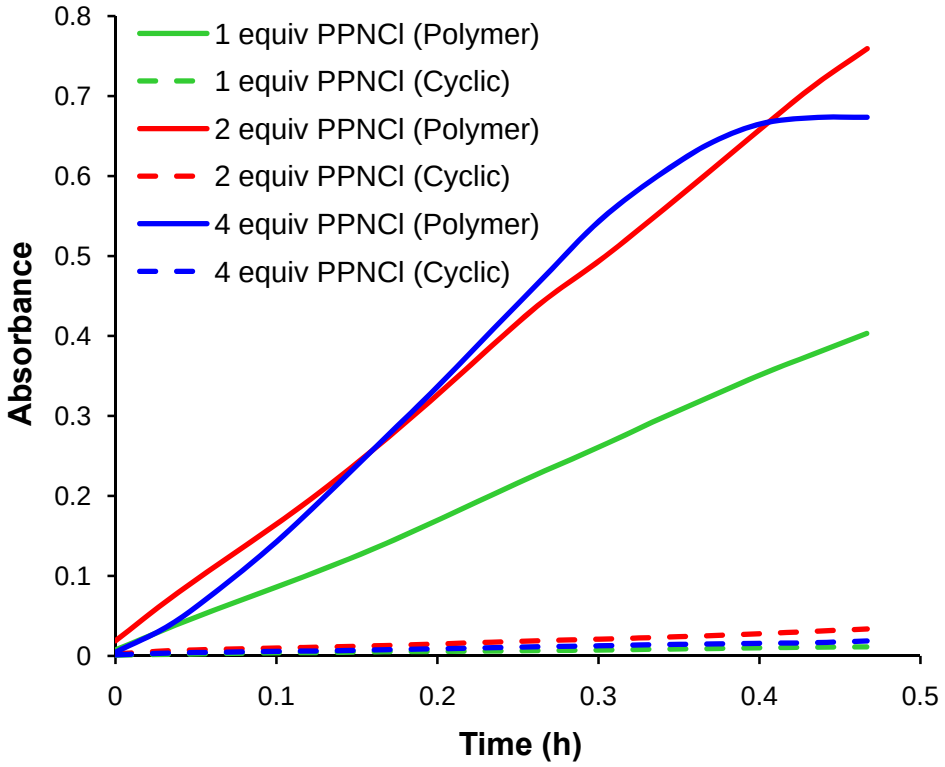

Figure 29. Reaction profiles indicating copolymer and cyclic carbonate formation with time for the copolymerization of cyclohexene oxide and CO_2 in the presence of **1** and 35 bar carbon dioxide at 80 ºC at various quantities of added PPNCl.

It was observed that upon titrating **1** with up to 8 equivalents of azide ions in methylene chloride the infrared bands assignable to metal-bound azides reached a maximum absorbance at two equivalents of azide ions, with further addition of azide ions remaining free in solution as revealed by an infrared band at 2005 cm^{-1}.[67] The $Cr(tmtaa)(N_3)_2^-$ anionic complex exhibits a strong asymmetric stretching vibration of N_3^-

at 2043 cm^{-1}, with a shoulder at 2057 cm^{-1}. Similar chromium(III)(salen) complexes, including the $Cr(salen)Cl_2^-$ species, have been fully characterized by X-ray crystallography.[68] Hence, it is assumed that Cr(tmtaa)Cl in the presence of excess chloride ions exists as $Cr(tmtaa)Cl_2^-$, which in the presence of epoxide monomer takes part in the equilibrium process depicted in Figure 30.

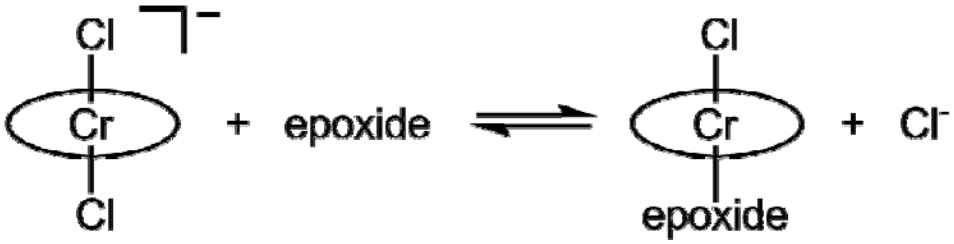

Figure 30. Equilibrium between epoxide and cocatalyst binding to the chromium center of the catalyst.

As is apparent from the reaction profiles in Figure 29, the catalytic activity for production of poly(cyclohexylene carbonate) dramatically increases when the concentration of PPNCl was increased from 1 to 2 equivalents, with only a negligible change upon further increase to 4 equivalents. The slight initiation period observed for the copolymerization reaction employing 4 equivalents of PPNCl can be attributed to competitive binding between the epoxide monomer and chloride ion. The TOFs when using 1 to 2 equivalents of PPNCl were 1,017 and 1,478 h^{-1}, respectively. Consistent with the initial report utilizing $PPNN_3$ as initiator, the production of cyclic carbonate is minimal throughout the reaction until the reaction mixture becomes highly viscous and

the epoxide monomer has been sufficiently depleted. At this point, the copolymerization process becomes limited by mass transfer and backbiting of the polymer chain to provide cyclic carbonate becomes more favorable.

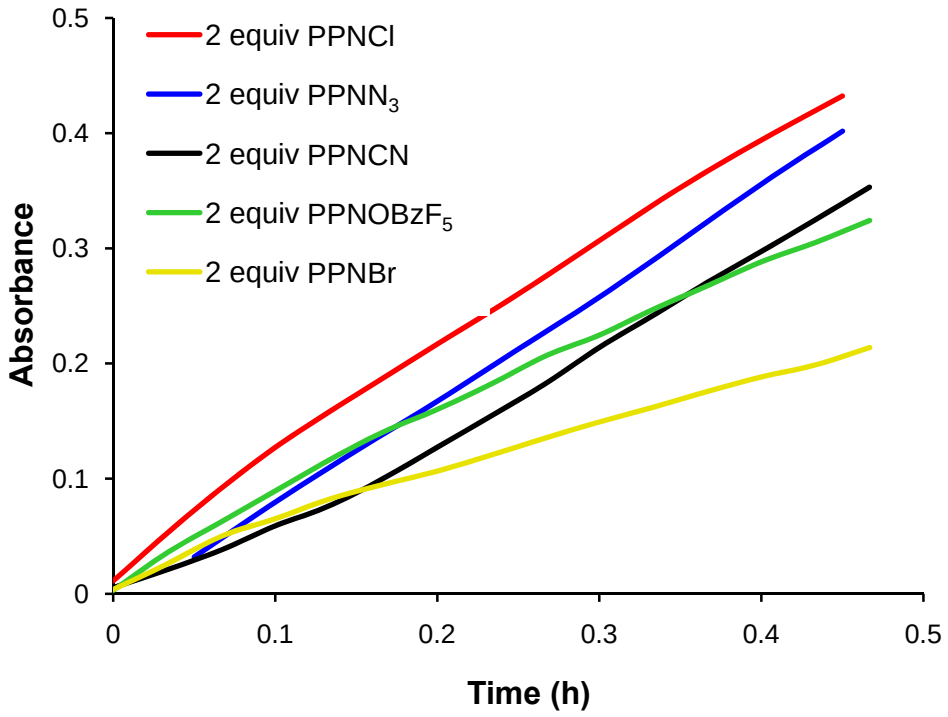

Figure 31. Reaction profiles of the copolymer formation with time for the copolymerization of CHO and CO_2 in the presence of Cr(tmtaa)Cl and 35 bar carbon dioxide at 80 ºC employing various PPNX salts as cocatalysts.

Figure 31 illustrates the reaction profiles for copolymer formation as a function of various PPNX salts present in 2 equivalents relative to **1**. Additionally, Table 10 lists the turnover frequency for this copolymerization process in the presence of both 1 and 2

equivalents of these PPNX salts. Comparatively, it is shown in the table that the chloride and azide anions gave the highest catalytic activity, followed closely by cyanide, while pentafluorobenzoate and bromide ion displayed the lowest activity of the initiators investigated herein. The pentafluorobenzoate anion has been previously reported to be a very efficient cocatalyst in the cobalt(III) salen catalysts for the copolymerization of propylene oxide and carbon dioxide.[69-71]

Table 10. Turnover Data for the Copolymerization of CHO and CO_2 Utilizing **1** as Catalyst and Either 1 or 2 Equivalents of Various PPN Salt Cocatalysts.[a]

	TOF (Time (h))	
PPNX	**1 Equiv**	**2 Equiv**
Cl	1,017[c] (0.5)	1,478[c] (0.5)
N_3	606 (1.55)	1,482[c] (0.5)
Br	542[c] (0.67)	795 (0.67)
CN	302 (0.5)	1,161[c] (0.5)
$OBzF_5$	415 (1.5)	656 (1.0)

[a]Copolymerization reactions were conducted with 50 mg of **1** as catalyst at 80 ºC and under 35 bar CO_2 pressure for the duration indicated. [b]Mol of epoxide consumed/mol of catalyst•h. [c]Runs were conducted using crystalline catalyst.

Copolymerization optimization through catalyst derivatization. Unlike chromium(III) salen complexes, which require the addition of substituents on the phenolate moieties to achieve sine qua non solubility, tmtaa complexes do not require such derivatization. These added ligand modifications, aside from altering solubility, also changed the electronic structure of the salen ligand, which concomitantly affected

the copolymerization activity of the catalyst. For the chromium salen catalyst system, it was found that the addition of electron-donating groups to the phenolate moieties and the ligand backbone increased the catalyst's activity towards the copolymerization of CHO and CO_2.[58] In order to further optimize the chromium(III) tmtaa system, ligands were synthesized with either electron-withdrawing chloro- or electron-donating methyl-groups on the phenylenediamine portions of the ligand framework. The expectation was for these substituents to affect the electron density around the chromium center, thereby influencing the activity of the catalyst.

As might be anticipated based on our earlier studies involving related Cr(salen)Cl catalysts, the TOF values for copolymerization of cyclohexene oxide and carbon dioxide with complexes Cr(tmtaa)Cl (**1**), Cr(omtaa)Cl (**3**), and Cr(tmtaaCl_4)Cl (**2**) under comparable reaction conditions at 80 ºC increase in the order **2** < **1** < **3**. That is, the catalytic activity increases as the nucleophilicity of the chromium(III) center increases, with TOF's at 80 ºC being 1,290 h^{-1} (**3**) > 943 h^{-1} (**1**) > 401 h^{-1} (**2**). Nevertheless, multiple runs employing various reaction conditions utilizing complexes **1** and **3** as catalysts in the presence of different anion initiators reveal only small differences in catalytic activity between these two chromium(III) derivatives. Hence, because of the greater ease of synthesizing and purifying complex **1**, this complex was employed in the more comprehensive studies of this catalytic system.

Epoxides and carbon dioxide coupling reactions as a function of carbon dioxide pressure. The effect of carbon dioxide pressure on the rate of copolymer formation as well as the extent of CO_2 incorporation, i.e., the percentage of ether linkages in thus formed polycarbonate was then explored when using complex **1** as a catalyst. It was noted in previous reports that the high epoxide affinity of Darensbourg's early generation zinc phenoxide catalysts required high carbon dioxide pressures to counteract the propensity for polyether formation over that of polycarbonate.[72-74] In contrast, the chromium(III) salen based catalysts were shown to be very ineffective at homopolymerizing epoxides into polyether, and hence did not require high concentrations of carbon dioxide to produce polycarbonates with greater than 95% carbonate linkages.[60] A similar situation was obvious when utilizing the Cr(tmtaa)Cl/PPNX catalyst system. That is, although the rate of copolymerization of cyclohexene oxide and CO_2 varied significantly with CO_2 pressure, at one atmosphere CO_2 pressure the copolymer produced contained 97% carbonate linkages as evident by ^{1}H NMR.

As seen in Figure 32, the reaction profiles for the copolymerization of cyclohexene oxide and CO_2 at 80 ºC over a range of CO_2 pressures. Supporting the observations from copolymerizations using Cr(salen)Cl,[60] the activity with **1** decreased at CO_2 pressures greater than 35 bar, attributable to the epoxide becoming diluted in the carbon dioxide-swelled reaction medium. The concentration of CO_2 dissolved in the cyclohexene oxide medium at atmospheric CO_2 pressure was rapidly depleted, thereby inhibiting continuation of the copolymerization process. Obviously, if maintained at one

atmosphere pressure of carbon dioxide, the copolymerization reaction would result in higher polycarbonate yield. Similar to what was noted in the case of the Cr(salen)X catalysts, as the CO_2 pressure was decreased the production of the cyclic carbonate byproduct increased.[60] The most notable instance of cyclohexylene carbonate formation was when the initial CO_2 pressure was one atmosphere. That is, at the higher CO_2 pressures the production of cyclic carbonate was negligible.

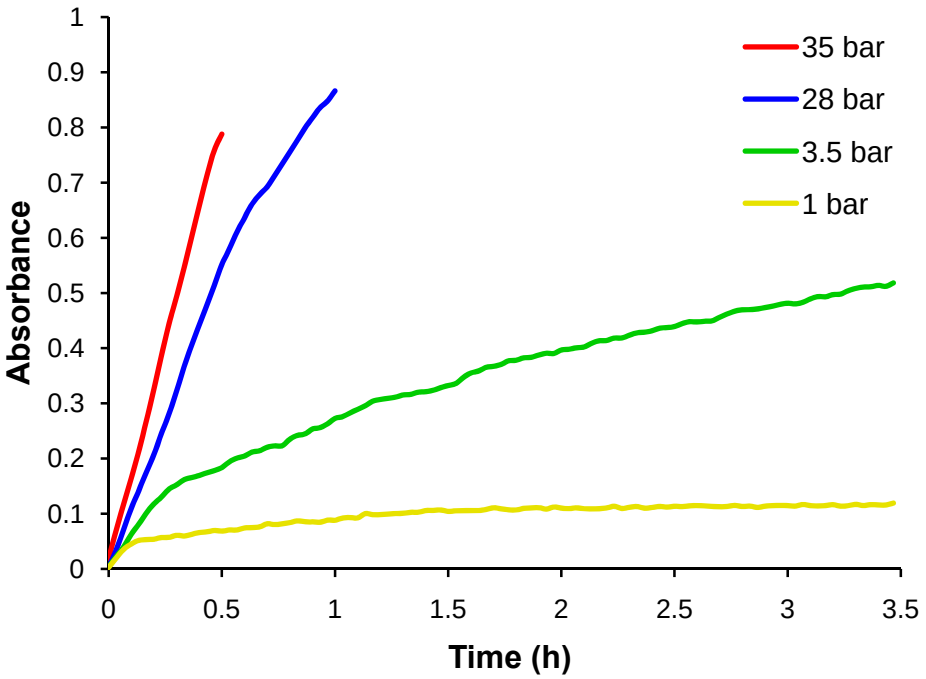

Figure 32. Effect of CO_2 pressure on the rate of polycarbonate formation from the coupling of CO_2 and cyclohexene oxide using **1** and 2 equivalents of PPNCl as a cocatalyst at 80 °C.

In situ kinetic studies of the cyclohexene oxide/carbon dioxide coupling reaction. The coupling reaction of cyclohexene oxide and carbon dioxide as catalyzed by the Cr(tmtaa)Cl/$PPNN_3$ catalyst system was monitored by in situ infrared spectroscopy in order to clearly define the kinetic parameters for this process. Since the reaction mixtures for polymerization reactions conducted in neat epoxide becomes denser and governed by mass transfer as the reaction progresses, accurate kinetic data for the process over extended time periods are impossible to obtain. Hence, in order to keep all components of the reaction in solution and to thwart any viscosity changes, instead of employing neat cyclohexene oxide as solvent, a 1:1 mixture of cyclohexene oxide and dichloromethane was employed in these studies. Because no appreciable rate enhanced was observed in excess of two equivalents of cocatalyst, all polymerization runs were performed employing 75 mg of **1** (1.74×10^{-4} moles) and 2 equivalents of $PPNN_3$ in 10 mL each of cyclohexene oxide and methylene chloride. These reactions were conducted over a 30 degree temperature range, each process resulting in an asymptotic rate profile for both copolymer (Figure 33) and cyclic carbonate formation (Figure 34). In all cases, the introduction of the cosolvent, methylene chloride, drastically increased the time needed for the complete conversion of epoxide to products. Observed reaction rate constants at each temperature were obtained for both copolymer and cyclic carbonate formation by fitting the data in plots of $\ln[A_\infty - A_t]$ vs time, where A_∞ and A_t correspond to the infrared absorbances for the copolymer (1750 cm^{-1}) and cyclic carbonate (1808 cm^{-1}) at time = infinity and time = t, respectively (Figure 35 and Figure 36). The respective rate constants are listed in Table 11.

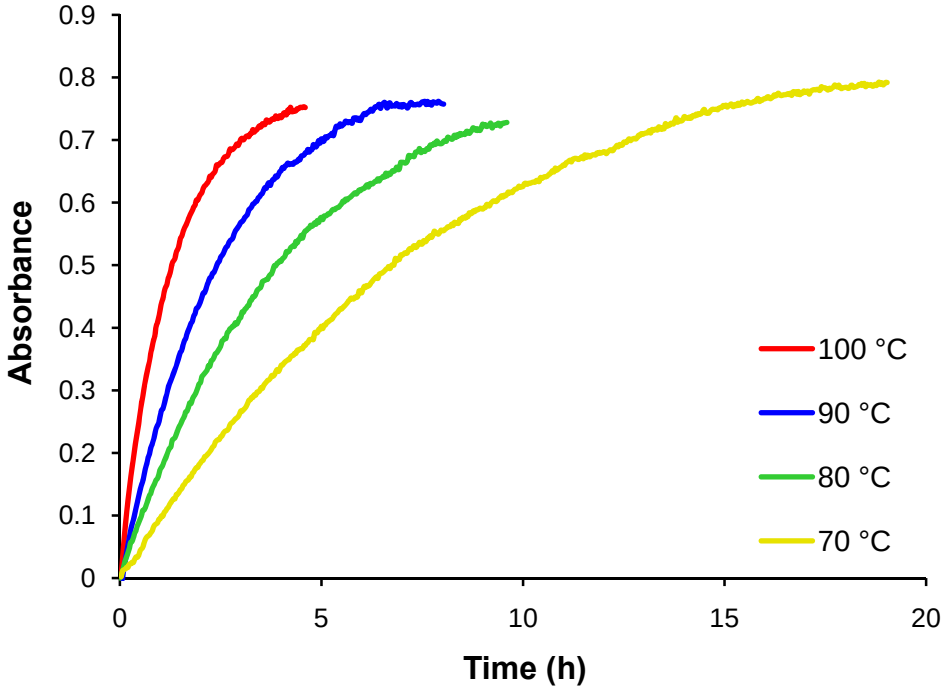

Figure 33. Kinetic traces recorded for the formation of poly(cyclohexylene carbonate) as a function of temperature in methylene chloride. Reaction conditions: 75 mg (1.74×10^{-4} mol) of **1** and two equivalents of $PPNN_3$ in 10 mL of cyclohexene oxide and 10 mL of methylene chloride and a CO_2 pressure of 35 bar.

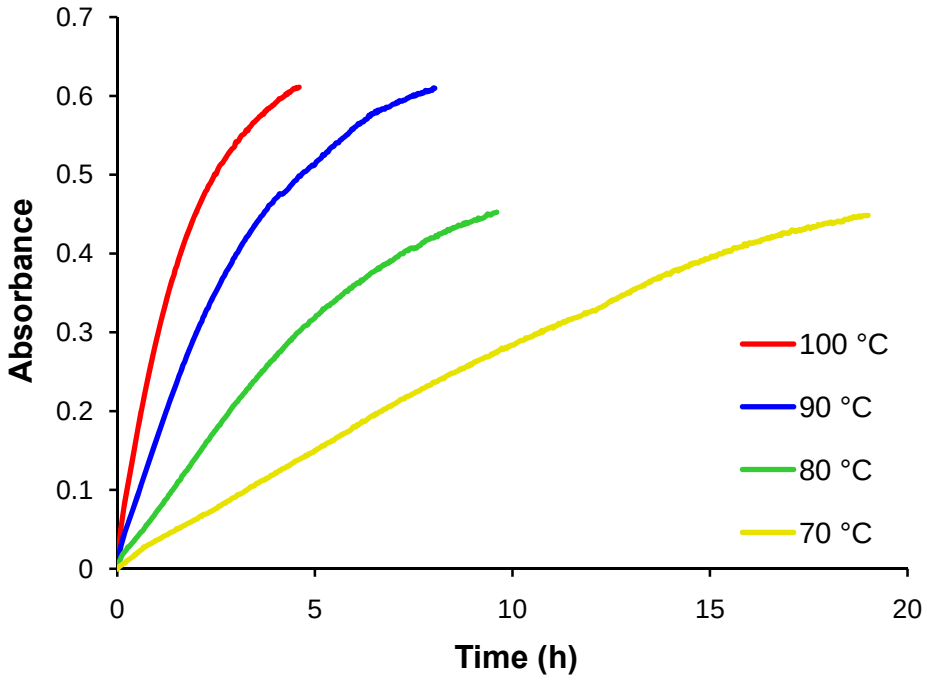

Figure 34. Kinetic traces recorded for the formation of poly(cyclohexylene carbonate) as a function of temperature in methylene chloride. Reaction conditions: 75 mg (1.74×10^{-4} mol) of **1** and two equivalents of $PPNN_3$ in 10 mL of cyclohexene oxide and 10 mL of methylene chloride and a CO_2 pressure of 35 bar.

Table 11. Temperature Dependent Rate Constants for the Coupling of Cyclohexene Oxide and Carbon Dioxide in Methylene Chloride.[a]

Temp. (°C)	k (M^{-1}-sec^{-1}) × 10^3	
	Copolymer	Cyclic Carbonate
70	3.45	1.37
80	8.44[b]	4.08[b]
90	12.9	7.31
100	21.0	13.6

[a]Reaction carried out in 10 mL of methylene chloride, 75 mg (1.74×10^{-4} mol) of **1**, 2 equivalents of $PPNN_3$, 10 mL of cyclohexene oxide, and a CO_2 pressure of 35 bar.
[b]Average value of two runs.

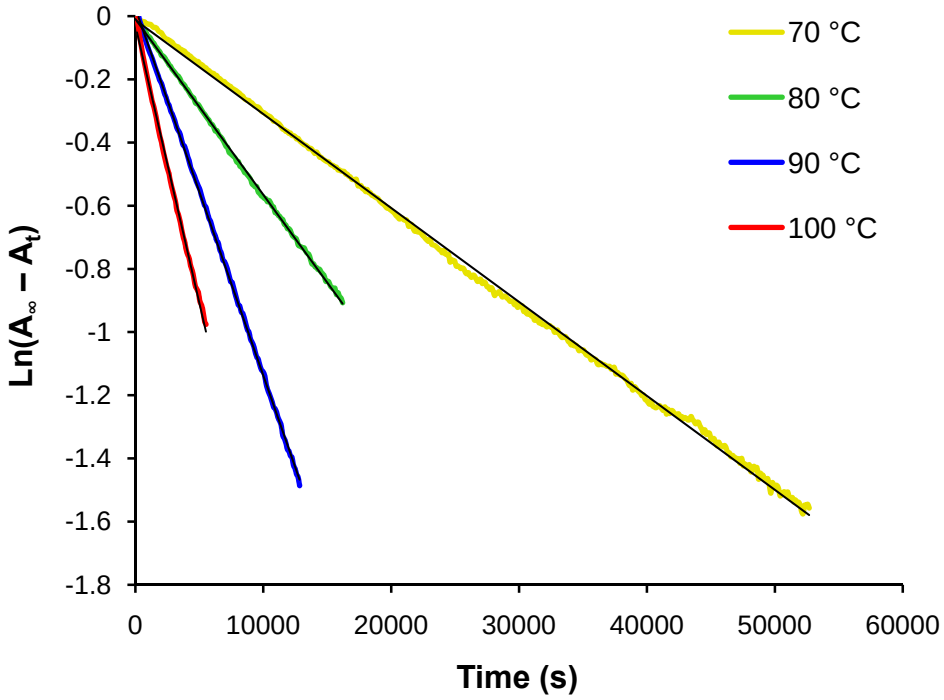

Figure 35. Plots of ln[A_∞-A_t] vs time as a function of time, where A_∞ and A_t are the infrared absorbances for the polycarbonate (1750 cm^{-1}) at time = infinity and time = t, respectively. R^2 values at the various temperatures (ºC) are: 70 (0.9990), 80 (0.9995), 90 (0.9998) and 100 (0.9973).

Eyring plots of the kinetic data provided in Table 11 are shown in Figure 37, with the calculated activation parameters listed in Table 12. As anticipated from the similarities in the reaction profiles provided in Figure 34, the $\Delta G^{\neq}$ for copolymer and cyclic carbonate formation in methylene chloride do not differ significantly at 80 ºC 115.6 and 117.6 kJ-mol^{-1}, respectively. Although, the enthalpy of activation for the production of copolymer (62.2 kJ-mol^{-1}) is less than that for cyclic carbonate production (77.3 kJ-mol^{-1}) as has been previously reported for chromium(III) and zinc(II) catalyst systems, it is offset by the more negative $\Delta S^{\neq}$ value.[12,57,73]

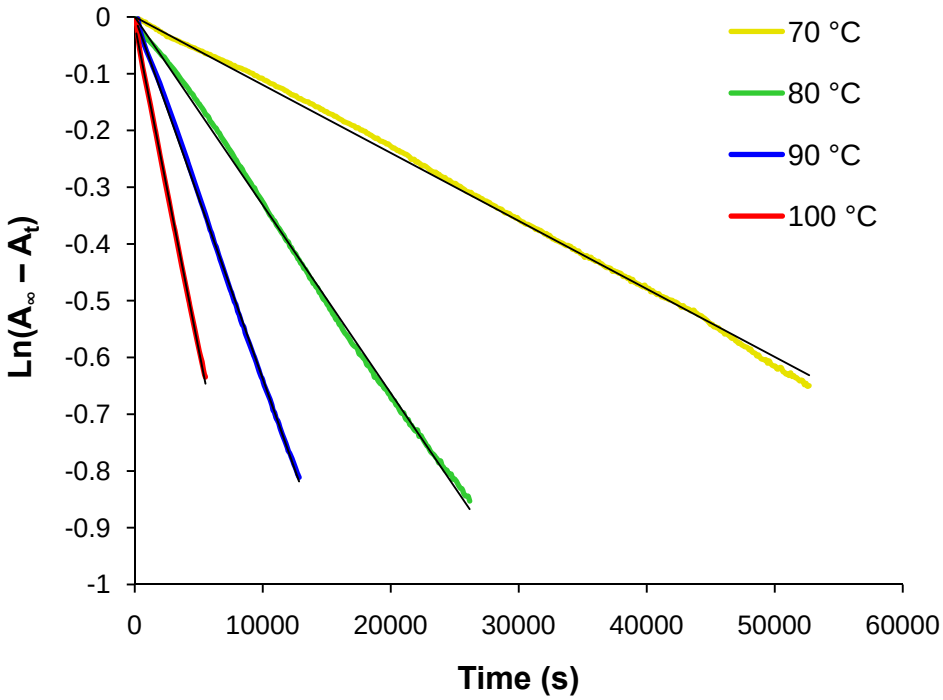

Figure 36. Plots of ln[A_∞-A_t] vs time as a function of time, where A_∞ and A_t are the infrared absorbances for the cyclic carbonate (1808 cm^{-1}) at time = infinity and time = t, respectively. R^2 values at the various temperatures (ºC) are: 70 (0.9980), 80 (0.9988), 90 (0.9995) and 100 (0.9992).

Table 12. Activation Parameters for the Coupling Reactions of Cyclohexene Oxide and Carbon Dioxide in Methylene Chloride.[a]

	Copolymer	**Cyclic Carbonate**
$\Delta H^{\neq}$ (kJ-mol^{-1})	62.2 ± 2.5	77.3 ± 5.7
$\Delta S^{\neq}$ (J-mol^{-1}-K^{-1})	-151.3 ± 6.9	-114.2 ± 16.0
$\Delta G^{\neq}$ (kJ-mol^{-1})	115.6	117.6
E_a(kJ-mol^{-1})	65.2	80.3

[a]$\Delta G^{\neq}$ value calculated at the typical reaction temperature of 80 ºC.

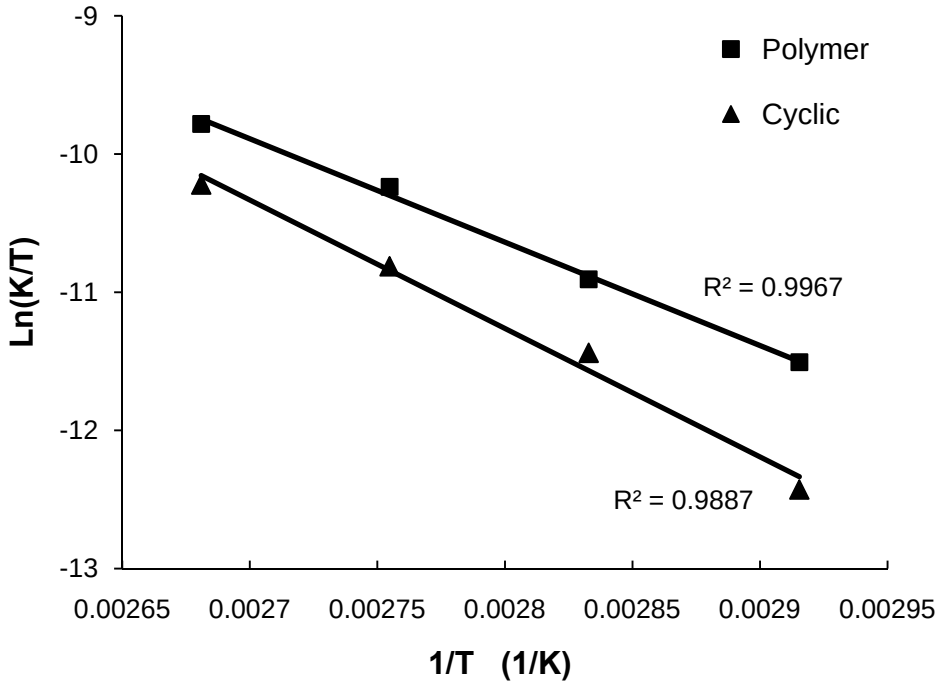

Figure 37. Eyring plot for the formation of polymer and cyclic carbonate.

Although the kinetic study presented above determined under homogenous solution conditions have proven to be insightful, the focus on a more environmentally benign route for the production of polycarbonates dictate the necessity of performing a comparable, albeit limited, investigation under solventless conditions. As mentioned earlier, because of the increase in viscosity during copolymer production in a neat carbon dioxide swollen cyclohexene oxide medium, it is only possible to quantitatively follow the reaction's progress during the early stages. Figure 38 depicts the reaction profiles for copolymer formation for processes carried out over the temperature range between 60-100 ºC. The reactions were monitored via in situ infrared spectroscopy

employing 50 mg (1.16×10^{-4}mol) of **1** and two equivalents of $PPNN_3$ in 20 mL of cyclohexene oxide at a CO_2 pressure of 35 bar. Initial rates for copolymer and cyclic carbonate were determined over the first few minutes of the processes. These rate data are tabulated in Table 13.

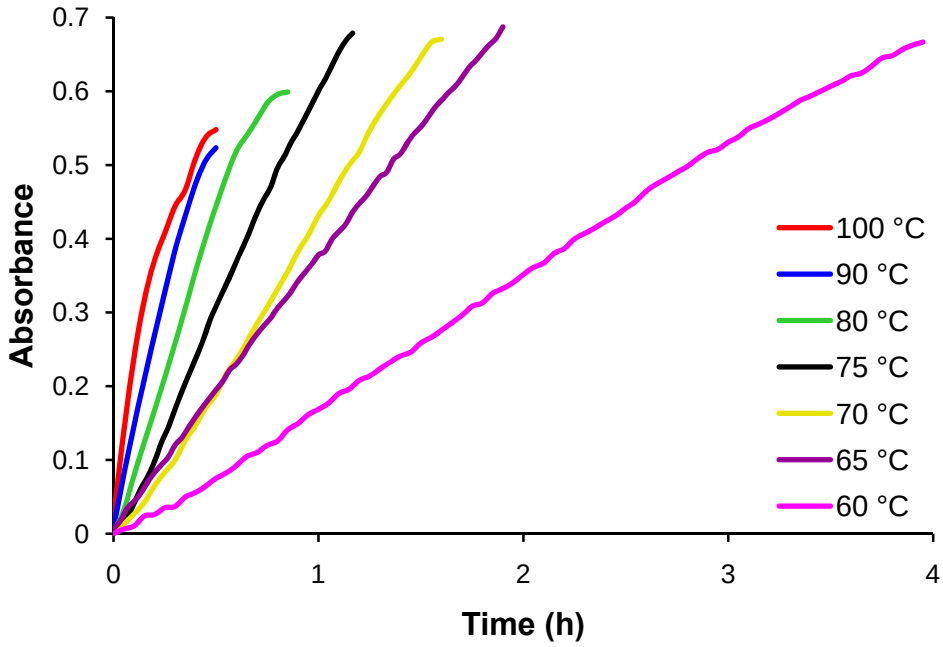

Figure 38. Effect of temperature on the rate of polycarbonate formation from the coupling of CO_2 and cyclohexene oxide using 50 mg (1.16×10^{-4} mol) of **1** and 2 equivalents of $PPNN_3$ catalyst system at a CO_2 pressure of 35 bar in pure cyclohexene oxide.

Table 13. Temperature Dependent Initial Rates for the Coupling of Cyclohexene Oxide and Carbon Dioxide in the Absence of a Cosolvent.[a]

Temp. (°C)	Initial rate (M/sec) × 10^5	
	Copolymer	**Cyclic Carbonate**
60	4.75	0.121
65	10.1	0.394
70	11.2	0.754
75	18	0.731
80	25.6	1.50
90	36.3	1.48
100	77.9	9.21

[a]Reactions carried out in 20 mL of cyclohexene oxide, 50 mg (1.16×10^{-4} mol) of **1**, and 2 equivalents of $PPNN_3$ at a CO_2 pressure of 35 bar.

Arrhenius plots for both copolymer and cyclic carbonate formation obtained from the initial rate data listed in Table 13 are provided in Figure 39. The calculated energies of activation for the two processes are 67.1 ± 4.2 and 91.2 ± 10.5 kJ-mol^{-1}, respectively. Comparison of the E_a values for copolymer production in a cosolvent (methylene chloride) and in the early stages of the reaction performed under solventless conditions indicate little difference for the two processes. On the other hand, the E_a for cyclic carbonate production is larger under the reaction conditions involving pure cyclohexene oxide. However, because of the low level of cyclic carbonate production in this instance the E_a is subject to significant uncertainty, i.e., an error of ±10.5 kJ-mol^{-1}. Nevertheless, a higher value for E_a is anticipated based on the low rate of cyclic carbonate formation observed in the absence of a cosolvent. This is explained based on

the backbiting process which leads to cyclic carbonate formation being inhibited in pure cyclohexene oxide. As previously noted, once the reaction medium becomes viscous due to copolymer formation, where chain growth is greatly retarded, the rate of cyclic carbonate production dramatically increases.[67] This is clearly illustrated in Figure 40 for a solventless copolymerization process carried out under typical reaction conditions.

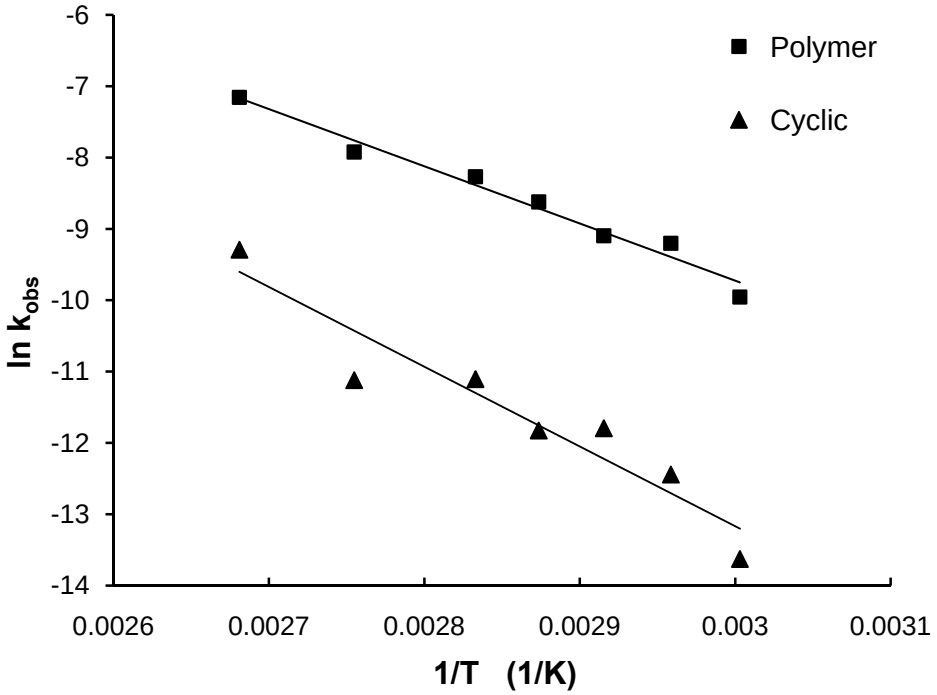

Figure 39. Arrhenius plots for polymer ($R^2 = 0.9747$) and cyclic carbonate ($R^2 = 0.9018$) formation from polymerizations carried out in neat cyclohexene oxide. Conditions: 50 mg (1.16×10^{-4} mol) of **1** and 2 equivalents of $PPNN_3$ in 20 mL of cyclohexene oxide under a CO_2 pressure of 35 bar.

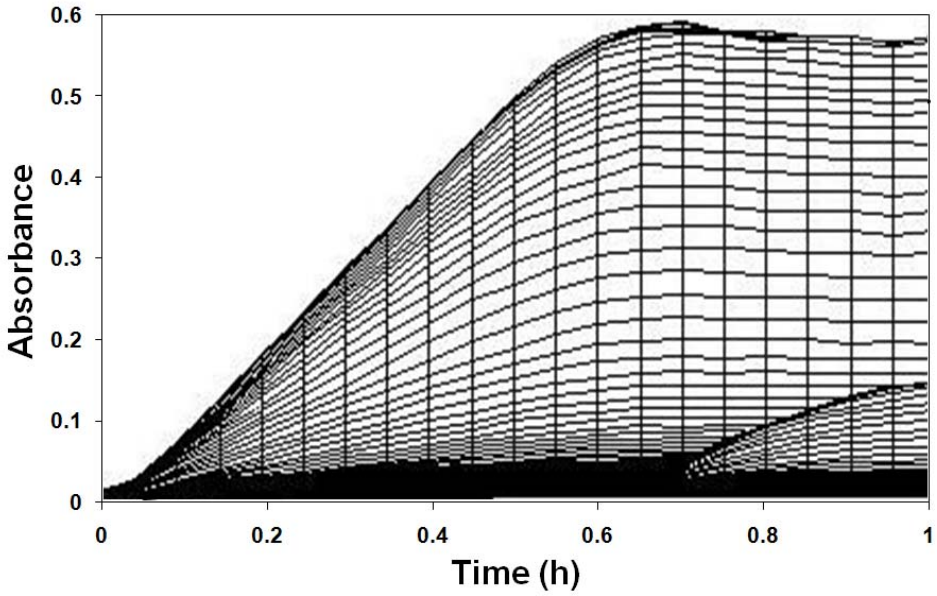

Figure 40. Time-dependent reaction plot for the solventless copolymerization of cyclohexene oxide (20 mL) and CO_2 (35 bar) in the presence of 50mg (0.116 mmol) of **1** and 3 equivalents of $PPNN_3$ at 80 ºC. Note enhancement of cyclic carbonate production at 0.7 h after copolymer formation has reached a plateau.

Copolymerization of epoxides other than cyclohexene oxide. Several other epoxides have been surveyed for their ability to afford copolymer and/or cyclic carbonate in the presence of the Cr(tmtaa)Cl/PPNX catalyst system. These studies were conducted under typical reaction conditions, i.e., 50 mg of **1**, two equivalents of $PPNN_3$ or PPNCl, and 35 bar of CO_2 in the absence of a cosolvent. Because it is well-established that higher temperatures generally lead to enhanced production of cyclic carbonates, these experiments were performed starting at temperatures close to ambient, with subsequent ramping up the temperatures as needed to observe reaction progress. Copolymerization reactions were carried out in a stainless steel reactor and were

monitored by in situ infrared spectroscopy. The epoxides examined were propylene oxide (**A**), styrene oxide (**B**), 1,2-epoxyhexane (**C**), isobutylene oxide (**D**), and 4-vinylcyclohexene oxide (**E**) as depicted in Figure 41.

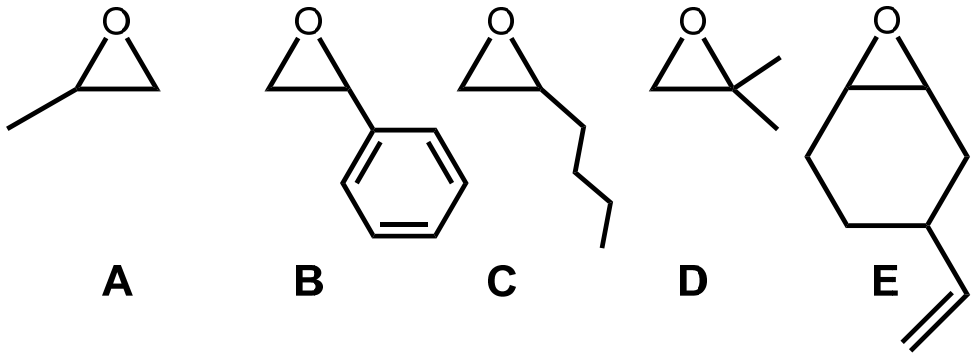

Figure 41. Epoxides surveyed for copolymer production catalyzed by Cr(tmtaa)Cl/$PPNN_3$.

The most widely investigated monomer for the copolymerization with carbon dioxide studied to date, other than cyclohexene oxide, is propylene oxide. The challenge in polymerizing aliphatic epoxides such as ethylene- or propylene oxide is the ease at which these comonomers provide cyclic carbonates as opposed to polycarbonates. Nevertheless, there are several reports for the selective production of poly(propylene carbonate) from propylene oxide and CO_2 in the presence of M(salen)X complexes (M = Cr[75-77] or Co[33,34,69,70,78-81]). In particular, the Co(salen)X complexes in the association with anionic cocatalysts have been shown to provide copolymers with stereo- and regioselectivity. In this study the copolymerization of propylene oxide and carbon

dioxide using complex **1** and two equivalents of $PPNN_3$ at 40 ºC yielded a 21% conversion to product in one hour with 36% of the product being copolymer. Additionally, a 60 ºC run carried out for 3 hours provided 49% conversion where 15% of the product was poly(propylene carbonate). Hence, **1** in the presence of $PPNN_3$ is not a particularly effective catalyst system for this monomer, i.e., much less effective than the M(salen)X derivatives of chromium(III) or cobalt(III).

In an effort to examine an epoxide monomer with two substituents on an isocarbon center, the copolymerization of isobutylene oxide (**D**) with carbon dioxide was investigated. The hope was that **1**, with its metal center being more accessible, would allow for the interaction with this sterically encumbered monomer and facilitate ring-opening. However, after some time at 40 ºC only trace quantities of cyclic carbonate was observed which increased in rate of formation as the temperature was raised to 60 ºC and then to 80 ºC (Figure 42). At no time was there spectral evidence for the formation of polycarbonate. Similar observations were made for reactions performed with 1,2-epoxyhexane (**C**) and carbon dioxide with the exception that cyclic carbonate formation occurred rapidly as the reaction temperature reached 90 ºC (Figure 43). It should be recalled that in the patent literature Jacobsen and coworkers have reported that Cr(salen)Cl in the absence of a cocatalyst was effective at copolymerizing 1,2-epoxyhexane and CO_2 to polycarbonate.[36]

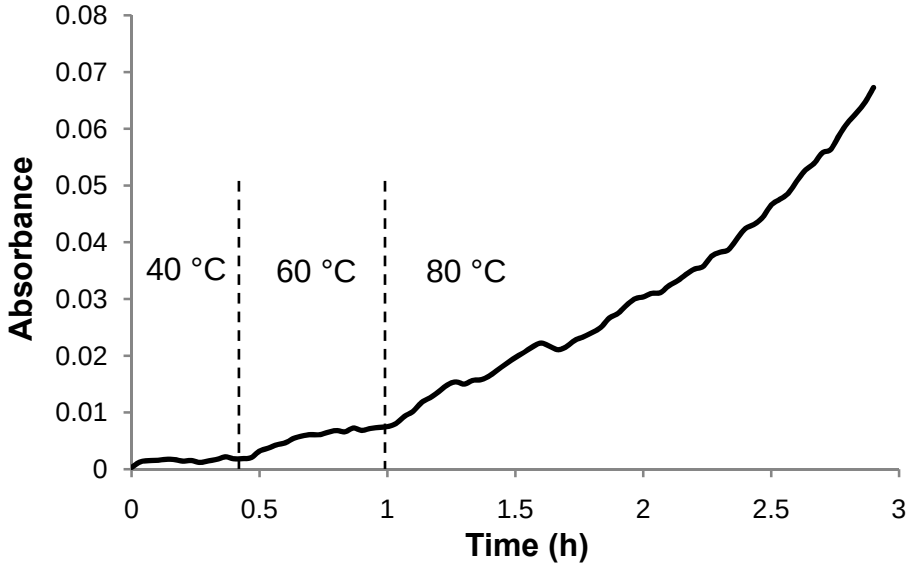

Figure 42. In situ infrared profile of isobutylene carbonate from the attempted copolymerization of isobutylene oxide (20 mL, M/I = 1,940) and CO_2 (35 bar) utilizing 50 mg of **1** and 2 equivalents of PPNCl.

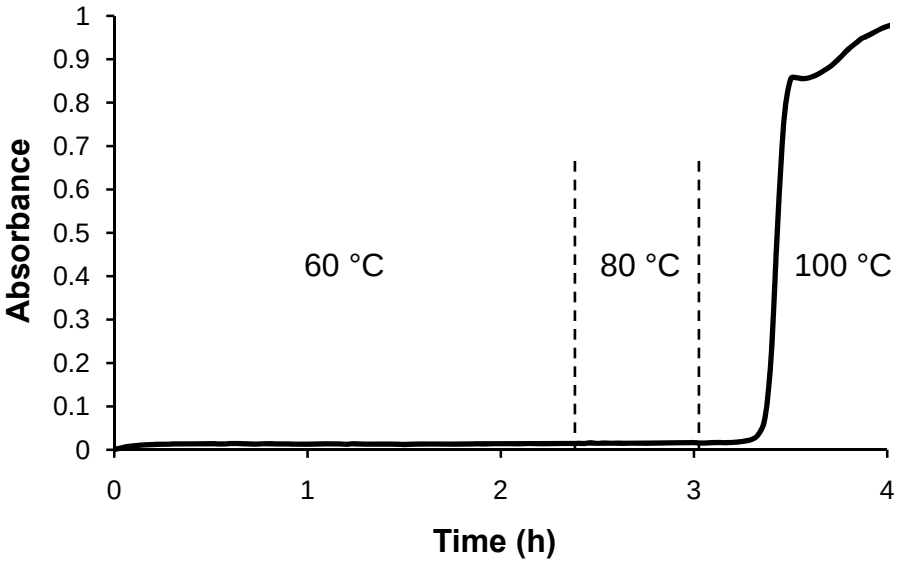

Figure 43. In situ infrared profile of 1,2-hexylene carbonate from the attempted copolymerization of 1,2-epoxyhexane (20 mL, M/I = 1,430) and CO_2 (35 bar) utilizing 50 mg of **1** and 2 equivalents of PPNCl.

Polystyrene has become a widely used commodity thermoplastic as it is colorless, transparent, rigid, economical, and easy to cast. In an effort to build upon the same aromatic functionality of polystyrene while possibly synthesizing a polymer with desirable properties, styrene oxide was subjected to copolymerization with carbon dioxide using the **1** complex as a catalyst. As mentioned *vide supra* pertaining to aliphatic epoxides, the ease of cyclic carbonate formation poses a challenge to affording copolymer. In earlier attempts in the Darensbourg laboratory, the copolymerization of styrene oxide (**B**) and CO_2 utilizing Cr(salen)N_3 and PPNN_3 catalysts resulted in trace quantities of copolymer and moderate amounts of cyclic styrene carbonate.[16] In this study, the reaction was carried out starting at a temperature of 40 °C, under which conditions a small yield of cyclic carbonate was observed. Further increases in temperature to 80 °C and then to 100 °C resulted in increases in cyclic carbonate formation, but no poly(styrene carbonate) was observed via infrared spectroscopy.

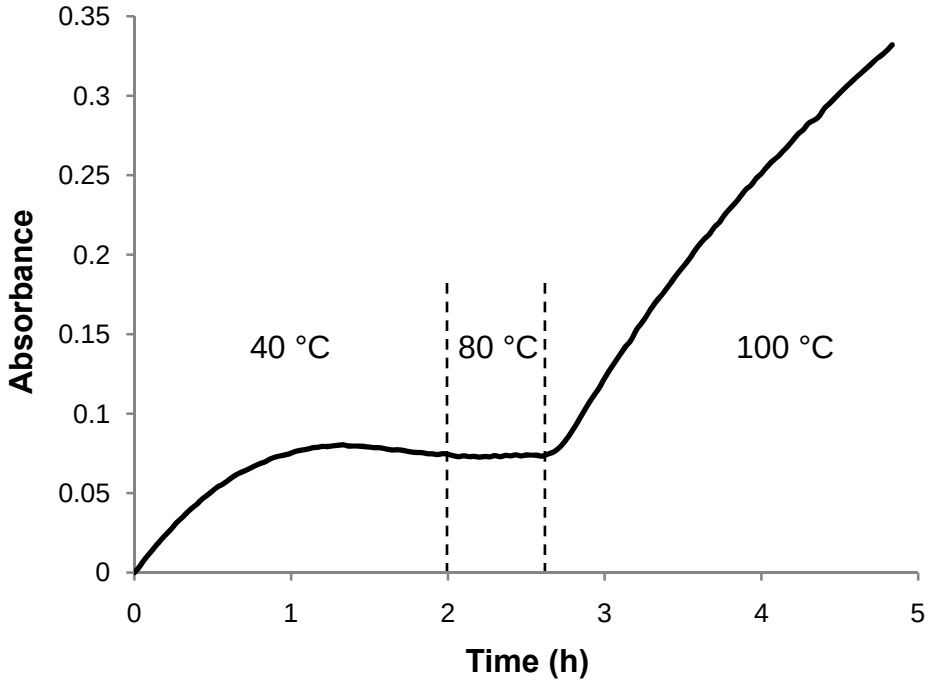

Figure 44. In situ infrared profile of styrene carbonate from the attempted copolymerization of styrene oxide (20 mL, M/I = 1,510) and CO_2 (35 bar) utilizing 50 mg of **1** and 2 equivalents of PPNCl.

Although the cyclohexene oxide monomer has been invaluable for understanding the process of epoxide/carbon dioxide coupling, the inherent properties of the resulting copolymer, poly(cyclohexylene carbonate), make it commercially unattractive.[82] A closely related monomer, 4-vinylcyclohexene oxide (**E**), offers the selective reactivity of an alicyclic epoxide similar to cyclohexene oxide with the advantage of a pendant vinyl functionality that can be post-polymerization-modified. Indeed, studies have shown it to be possible to prepare block copolymers of poly(cyclohexylene carbonate) and poly(4-vinylcyclohexylene carbonate),[83] as well as intramolecular cross-linked terpolymers of cyclohexene oxide, 4-vinylcyclohexene oxide, and carbon dioxide.[84] A similar strategy

has been previously explored for intermolecularly cross-linking a copolymer prepared from [2-(3,4-epoxycyclohexyl)ethyl]trimethoxysilane and CO_2 via silsesquioxane units.[85] Figure 15 represents the reaction profiles for the formation of the copolymer and cyclic carbonate from the coupling of 4-vinylcyclohexene oxide and carbon dioxide as catalyzed by **1** and 2 equivalents of PPNCl at 80 °C. The copolymerization reaction proceeded at a slower rate, that is, ~3 times slower, than the corresponding process with the cyclohexene oxide monomer. Nevertheless, the process was highly selective for copolymer formation, providing a polycarbonate with a molecular weight of 9,300 g mol^{-1} and a narrow polydispersity of 1.12.

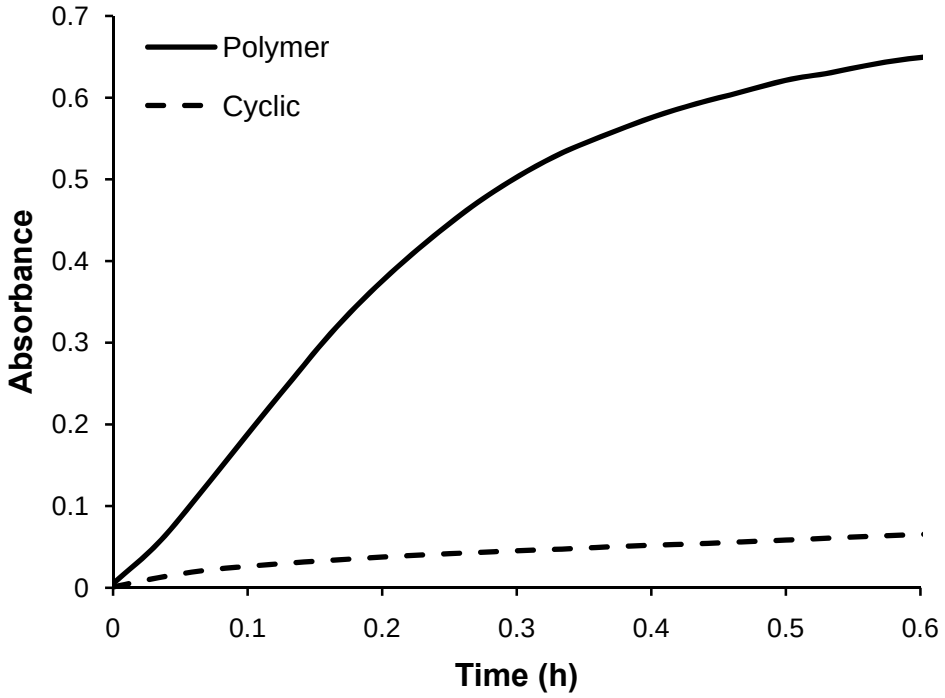

Figure 45. In situ infrared profile of polycarbonate and cyclic carbonate from the copolymerization of 4-vinyl cyclohexene oxide (20 mL, M/I = 1,320) and CO_2 (35 bar) utilizing 50 mg of **1** and 2 equivalents of PPNCl.

Conclusions

In part, the interest in exploring tetraazaannulene chromium(III) derivatives as catalysts for the copolymerization of cyclohexene oxide and carbon dioxide was to compare their activity with the closely related salicylaldimine and porphyrin analogs. Although differences in reaction conditions make it difficult to quantitatively contrast the catalytic activities involving these metal complexes, it is apparent that, under optimal conditions, the Cr(salen)X and Cr(tmtaa)X metal complexes in the presence of anionic cocatalysts display similar activities. For example, Cr(salen)X complexes exhibit a TOF of ~1,150 h^{-1} at 80 °C and provide high molecular weight copolymers (50,000) with low PDIs (1.13).[60] Under identical reaction conditions the Cr(tmtaa)X complexes are somewhat more active with TOF of ~1,500 h^{-1} at 80 °C yielding a copolymer of molecular weight 30,000 with a PDI of 1.07. On the other hand, the complex containing the more expensive N_4^{-2} ligand, Cr(porphyrin)X, afforded a TOF ≈ 150 h^{-1} at 110 °C, yielding a low molecular weight copolymer (Mn ≈ 3,500) with a PDI of 1.19.[11] Hence, the Cr(tmtaa)X complex is slightly more active than the correspondent complex containing the ubiquitous salicylaldimine ligand and is considerably more active than analogous chromium derivatives of the porphyrin ligand. This reactivity trend parallels the expected electron-donating ability of the ligand set about the chromium(III) center, where tmtaa > salen >> porphyrin. Consistent with observations of Cr(salen)Cl derivatives, the addition of electron-donating and electron-withdrawing substituents to the tmtaa ligand affected the catalytic activity of the complexes, resulting in the reactivity trend; Cr(omtaa)Cl ≥ Cr(tmtaa)Cl >Cr(tmtaaCl_4)Cl.

An important observation resulting from this investigation is that the selectivity for formation of the copolymer versus cyclic carbonate is highly dependent on whether cosolvents are used. That is, a comparison of product selectivity under solventless and cosolvent conditions clearly shows that in the absence of a cosolvent the rate of the backbiting process for cyclic carbonate production, either at the metal center or subsequent to chain dissociation, is greatly retarded. Current thoughts on this behavior are that enhanced cyclic carbonate formation is the result of copolymer chain dissociation from the metal center followed by facile cyclization.[33-35,86] The mechanistic aspects of the copolymerization reactions of epoxides and carbon dioxide employing Cr(salen)X and those presented herein for Cr(tmtaa)X correspond intimately to one another and further reinforce the proposed copolymerization mechanism. Finally, these chromium(III)(tmtaa) derivatives, like other closely related complexes, are rather disappointing as catalysts for the copolymerization of aliphatic epoxides and carbon dioxide. However, they were shown to be very effective at copolymerizing other alicyclic epoxides such as 4-vinylcyclohexene oxide.

CHAPTER IV

MECHANISTIC INVESTIGATIONS INTO THE COPOLYMERIZATION OF EPOXIDES AND CARBON DIOXIDE

Introduction

Over the past fifteen years, the Darensbourg group has explored various aspects of the copolymerization of epoxides and carbon dioxide to produce polycarbonate plastics through a more environmentally conscious process than is currently employed in industry. Through this research, several highly active catalyst systems have been developed.

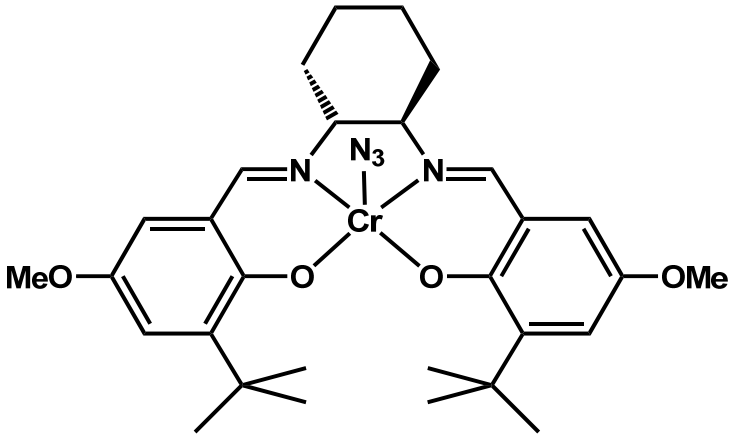

Figure 46. Skeletal representation of a chromium salen catalyst used for the copolymerization of epoxide and carbon dioxide.

The most notable system utilizes a salen-based architecture with a chromium metal center and was inspired by the work of Jacobsen and coworkers.[13,36] As mentioned in previous chapters, the chromium salen system (Figure 46) has been modified to adjust electronic and steric properties, examined with various nucleophilic cocatalysts, and a reliable mechanism has been proposed for the copolymerization reaction through careful observation.[12,14,37,56-59,68,74,85,86] The mechanism, shown in Figure 5, begins by the addition of a nucleophilic cocatalyst. This "activated complex" then initiates the polymerization by ring-opening an incoming epoxide molecule. Carbon dioxide is rapidly inserted into the chromium alkoxide bond resulting in the formation of a carbonate linkage. The catalytic cycle is continued by the alternating insertion of epoxide and carbon dioxide.

A remaining ambiguity of this mechanism is whether or not monomer insertion occurs on both sides of the chromium-centered catalyst (Figure 47). Previous reports studying epoxide/CO_2 copolymerizations using aluminum-, chromium-, and cobalt porphyrin and salen catalysts have proposed that these complexes are dicatalytic single-site catalysts, where polymer chain growth occurs from both sides of the metal center.[23,26,32,33,69] A major drawback to the salen and porphyrin ligand architectures is its difficulty to directly test this mechanistic proposition. Some observations would lead to the belief that the polymerization occurs from both sides of the catalyst while others support chain growth from only one side of the catalyst while a nucleophile, either the added cocatalyst or the preexisting ancillary nucleophile from the initial five-coordinate

complex, occupies the trans coordination site of the metal. These observations and subsequent theories will be discussed in detail herein.

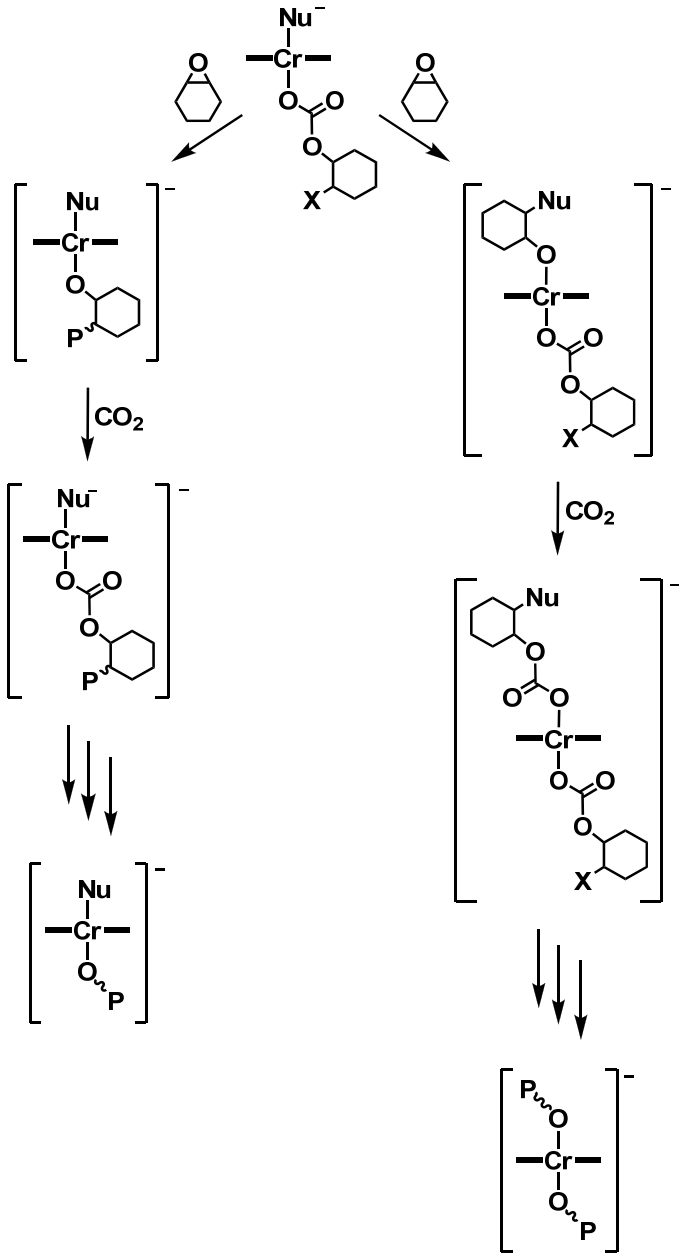

Figure 47. Proposed mechanisms for one-sided monomer insertion (left) vs. monomer insertion occuring on both sides of the chromium catalyst (right).

Another, more recent, highly active catalyst system developed in the Darensbourg group incorporates the tetramethyltetraazaannulene (tmtaa) macrocyclic ligand architecture. This chromium complex, Cr(tmtaa)Cl (**1**) has previously been demonstrated to achieve activities of 1500 turnovers per hour (turnover frequency, TOF = mole epoxide consumed per mole catalyst per hour) while suppressing the formation of cyclic cyclohexene carbonate, concomitantly producing polycyclohexylene carbonate at moderate molecular weights with high CO_2 incorporation and narrow polydispersities.[67,87]

Investigations into the chromium tetramethyltetraazaannulene catalyst system suggest the same mechanism for copolymerization of epoxides and carbon dioxide proposed for the chromium salen catalysts.[67,87] This has allowed for a direct comparison between the two systems. Tetramethyltetraazaannulene complexes do not exhibit the relative ligand planarity inherent to salen and porphyrin complexes, but rather possesses a well pronounced saddle shape (Figure 48). As mentioned *vide supra*, the salen and porphyrin ligand architectures incite difficulty in examining the catalysts' topography with regards to polymer chain growth. It is believed that the tmtaa ligand system will be able to provide evidence to support the copolymerization occurs exclusively from one side of the catalyst.

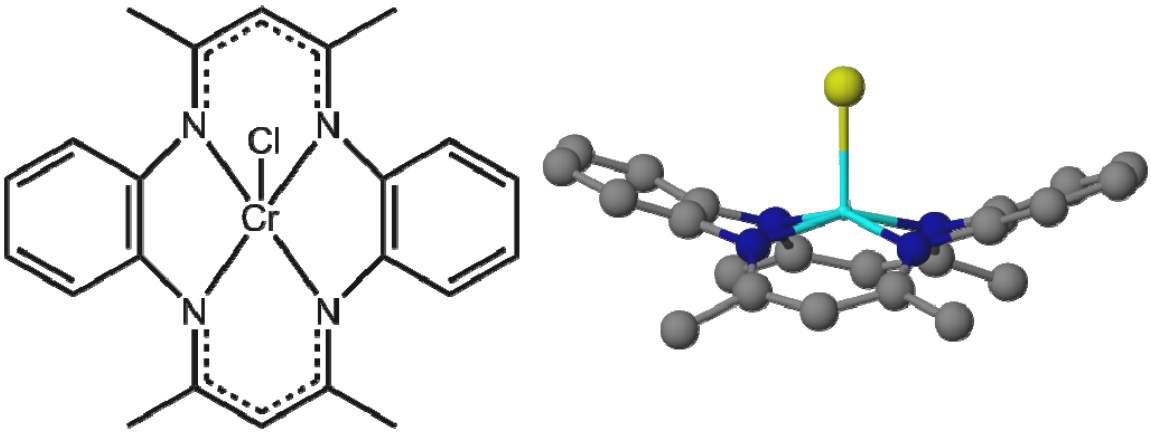

Figure 48. Skeletal (left) and three dimensional (right) representations of **1** used to catalyze the copolymerization of epoxide and carbon dioxide.

Succeeding the work performed by Sakata and coworkers,[88] opposing sides of the ligand have been tethered via a strap running beneath the ligand (Figure 49). This added steric bulk should limit catalytic activity to merely one side of the complex while still leaving enough breadth for the necessary binding of a cocatalyst. If the hypothesis is correct, the chromium tmtaa catalyst featuring the strap moiety, Cr(stmtaa)Cl, would exhibit similar catalytic activity observed for the unsubstituted catalyst, Cr(tmtaa)Cl, while producing a copolymer with similar constitution.

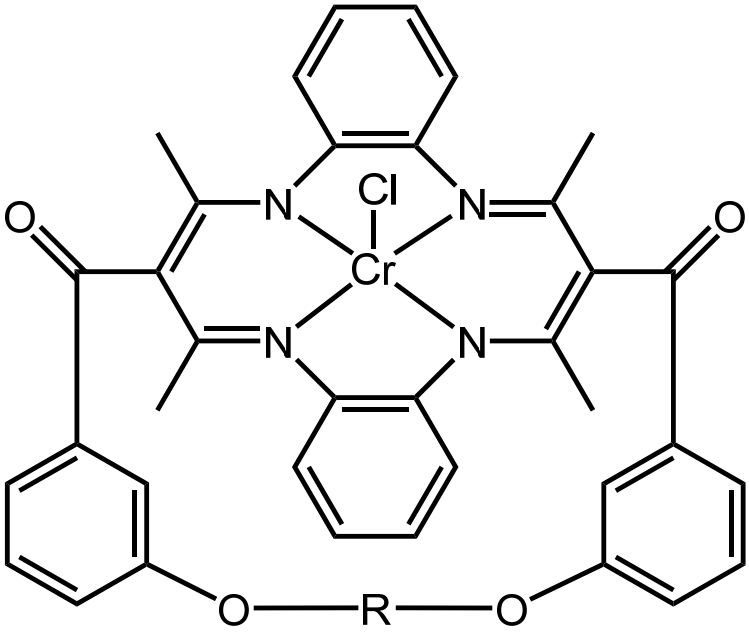

Figure 49. Skeletal representation of a strapped chromium tetramethyltetraazaannulene complex, where R = an alkyl or aromatic linker.

Experimental

Methods and materials. Unless otherwise specified, all manipulations were carried out on a double manifold Schlenk vacuum line under an atmosphere of argon or in an argon-filled Glovebox. Methanol (EMD Chemicals), absolute ethanol (Pharmco-Aaper), 2,4-pentanedione (Aldrich), nickel acetate tetrahydrate (Fisher), chromium(III) chloride (Strem), ammonium hexafluorophosphate (Oakwood), sodium azide (Aldrich), sodium chloride (EMD Chemicals), sodium cyanate (Aldrich), sodium cyanide (Aldrich), potassium hydroxide (EMD Chemicals), N,N-dimethylformamide (Aldrich), 3-hydroxybenzoic acid (Alfa Aesar), *m*-anisic acid (Alfa Aesar), *m*-xylene dibromide (Alfa Aesar), 1,6-dibromohexane (Acros), methyl 3-hydroxybenzoate (Alfa Aesar),

sodium hydride (Alfa Aesar), sulfuric acid (EMD Chemicals), and hydrochloric acid (EMD Chemicals) were used without further purification. Triethylamine (EMD Chemicals) was stored over sodium hydroxide and freshly distilled before use. Thionyl chloride (Aldrich) was distilled prior to use. Bis(triphenylphosphoranylidene)ammonium chloride was recrystalized from methylene chloride/ether. Bis(triphenylphosphoranylidene)ammonium azide was synthesized from a published literature procedure.[49] Methylene chloride, benzene, hexane, tetrahydrofuran, methanol, ethyl ether, and toluene were freshly purified by an MBraun Manual Solvent System packed with Alcoa F200 activated alumina desiccant. The synthesis of H_2tmtaa was conducted following published procedures.[47] Cyclohexene oxide (TCI) was freshly distilled from CaH_2 (Alfa Aesar) prior to use. Acetone (Pharmco-Aaper) was freshly distilled from sodium carbonate (EMD Chemicals) prior to use. Bone dry carbon dioxide (Scott Specialty Gases) was supplied in a high pressure cylinder equipped with a liquid dip-tube. Unless otherwise stated, all other reagents were used without further purification. ^{1}H and ^{13}C NMR spectra were acquired on using a Varian Inova 300 MHz or 500 MHz superconducting NMR spectrometers. Infrared spectra were recorded on using a Bruker Tensor 27 FTIR spectrometer. Molecular weight determinations were carried out on a Viscotek Gel Permeation Chromatograph equipped with refractive index, right-angle and low-angle light scattering detectors.

Synthesis of 3,3'-(1,3-phenylenebis(methylene))bis(oxy)dibenzoic acid. The synthesis was conducted through modification of a reported procedure.[89] 4 g (26.3 mmol) methyl 3-hydroxybenzoate was dissolved in 20 mL THF and added to a slurry of

0.63 g (26.3 mmol) NaH in 10 mL THF. After hydrogen gas evolution had ceased, the clear solution was allowed to stir for an additional 20 minutes. The solvent was removed under reduced pressure and the residue dissolved in 40 mL dry DMF. 3.47 g (13.15 mol) *m*-xylene dibromide was added and the solution refluxed for 10-15 minutes. The DMF was removed under reduced pressure and the tan residue dissolved in a minimal amount of acetone and filtered to remove the precipitated NaBr. The solvent was removed in vacuo and the residue refluxed in 70 mL of 10% KOH solution overnight. The solution was cooled, and the product precipitated as a white solid upon the addition of 40 mL of 6 N HCl. The precipitate was isolated, washed with water, and recrystallized from hot ethanol. Yield: 3.95 g (79.4%). ^{1}H NMR (*d*-DMSO, 300 MHz): δ 7.56-7.23 (m, 12H), 5.17 (s, 4H). ^{13}C{^{1}H} NMR (*d*-DMSO, 300 MHz): δ 167.09, 158.29, 137.09, 132.27, 129.74, 128.62, 127.22, 126.83, 121.82, 119.66, 114.90, 69.23.

Synthesis of 3,3'-(hexane-1,6-diylbis(oxy))dibenzoic acid. The synthesis was conducted by modifying a published procedure.[89] The same procedure outlined above was used with the substitution of 3.2 g (13.14 mmol) 1,6-dibromohexane in place of *m*-xylene dibromide. Yield: 3.15 g (67%). ^{1}H NMR (*d*-DMSO, 300 MHz): δ 7.51-7.15 (m, 8H), 4.01 (t, 4H), 1.74 (p, 4H), 1.48 (p, 4H). ^{13}C{^{1}H} NMR (*d*-DMSO, 300 MHz): δ 167.13, 158.62, 132.13, 129.68, 121.42, 119.34, 114.41, 67.55, 28.54, 25.23.

Synthesis of 5,14-Dihydro-6,8,15,17-tetramethyl-7,16-(3,3'-(2,6-phenylenedimethylenedioxydibenzoylo)dibenzo[b,i][1,4,8,11]tetraazacyclotetradecine (4). This synthesis was modified from a previous report.[88] 1.2 g (3.18 mmol) 3,3'-(1,3-

phenylenebis(methylene))bis(oxy)dibenzoic acid was refluxed in 20 mL thionyl chloride overnight. The thionyl chloride was removed under reduced pressure, the residue dissolved in 20 mL benzene, and removed under reduced pressure to remove any remaining thionyl chloride. This benzene wash was repeated once more and the residue dissolved in 1800 mL toluene. 1.1 g (3.19 mol) of H_2tmtaa and 4.5 mL (32.29 mmol) NEt_3 were added and the solution refluxed for 7 days. The solution was concentrated, filtered through celite to remove triethylamine hydrochloride, and evaporated under reduced pressure. The product was purified by column chromatography over silica gel using dichloromethane as an eluent, collecting the second fraction. Removal of solvent yielded 1.49 g (68% yield) pure product. X-ray quality crystals were obtained through slow evaporation of a chloroform solution. ^{1}H ($CDCl_3$, 500 MHz): δ 14.34 (s, 2H), 8.07 (s, 1H), 7.81 (t, 2H), 7.77 (d, 2H), 7.52 (t, 2H), 7.36 (t, 1H), 7.23 (m, 4H), 7.00 (m, 8H), 5.14 (s, 4H), 2.13 (s, 12H). $^{13}C\{^1H\}$ ($CDCl_3$, 500 MHz): δ 201.03, 158.51, 141.78, 137.26, 137.07, 130.18, 128.44, 126.18, 123.82, 123.79, 123.40, 120.73, 120.09, 115.60, 109.84, 69.58, 19.89.

Synthesis of 5,14-Dihydro-6,8,15,17-tetramethyl-7,16-(3,3'hexamethylene-dioxydibenzoylo)dibenzo[b,i][1,4,8,11]tetraazacyclotetradecine (H_2stmtaa, 5). The synthesis was conducted by modifying published procedures[88,90] and follows the procedure outlined above for **4** using 1.0 g (2.79 mmol) 3,3'-(hexane-1,6-diylbis(oxy))dibenzoic acid in place of 3,3'-(1,3-phenylenebis(methylene))-bis(oxy)-dibenzoic acid. Yield: 1.02 g (55%). X-ray quality crystals were obtained through slow evaporation of a chloroform solution. ^{1}H NMR ($CDCl_3$, 500 MHz): δ 14.36 (s, 2H),

7.66 (d, 2H), 7.54 (s, 2H), 7.42 (t, 2H), 7.05 (d, 2H), 7.01 (s, 8H), 4.02 (t, 4H), 2.13 (s, 12H), 1.81 (p, 4H), 1.62 (p, 4H). $^{13}C\{^{1}H\}$ ($CDCl_3$, 500 MHz): δ 199.88, 159.81, 159.06, 142.21, 137.16, 130.04, 124.03, 123.62, 120.64, 117.60, 117.23, 110.23, 68.19, 28.66, 25.98, 20.28.

Synthesis of 5,14-Dihydro-6,8,15,17-tetramethyl-7,16-bis((3-methoxy-phenyl)methanone)dibenzo[b,i][1,4,8,11]tetraazacyclotetradecine (H_2s^mtmtaa, 6). Modifying a previously reported procedure,[91] 6 g (15 mmol) Ni(tmtaa) was dissolved in 100 mL benzene and 7 mL (50.2 mmol) triethylamine. *m*-anisoyl chloride (5.12 g, 30 mmol) was added and the solution refluxed for 1.5-2 hours and allowed to stand at room temperature overnight. The solvent was removed under reduced pressure and the residue washed with hot water, isolated, and dried in vacuo. The neutral disubstituted ligand was obtained by bubbling anhydrous hydrogen chloride gas through the suspension of the crude nickel complex in dry acetone with vigorous stirring. Over the course of 2 hours, an orange/yellow precipitate formed and the flask stirred overnight. The precipitate was isolated, washed with acetone, and dried. The collected material was returned to a flask and stirred vigorously with cold dilute (1:10) hydrochloric acid, filtered and washed with hot water followed by acetone to remove nickel chloride and the hydrochloride salt of the unsubstituted and mono-substituted ligands. The isolated γ,γ'-disubstituted hydrochloride ligand salt was transferred to a flask, dissolved in methanol, and neutralized by addition of excess triethylamine, resulting in precipitation of the pure, light green product. Yield: 4.317 g (47%). X-ray quality crystals were obtained through slow evaporation of a dichloromethane solution. MS (ESI): m/z

613.27 (M+H). ^{1}H NMR ($CDCl_3$, 300 MHz): δ 14.27 (s, 2H), 7.61 (d, 2H), 7.56 (s, 2H), 7.42 (t, 2H), 7.14-7.00 (m, 10H), 3.88 (s, 6H), 1.99 (s, 12H). $^{13}C\{^{1}H\}$ ($CDCl_3$, 300 MHz): δ 198.63, 160.81, 159.99, 142.44, 137.59, 129.75, 124.31, 122.57, 119.46, 112.84, 109.22, 109.00, 55.48, 19.28.

Synthesis of 5,14-Dihydro-6,8,15,17-tetramethyl-7,16-(3,3'hexamethylenedi-oxydibenzoylo)dibenzo[b,i][1,4,8,11]tetraazacyclotetradecinato chromium chloride (Cr(stmtaa)Cl, 7). The chromium complex was synthesized following the procedure reported by Cotton for Cr(tmtaa)Cl (**1**).[48] 1.07 g (1.61 mmol) **5** was refluxed in 400 mL benzene for 2 weeks in the presence of 1 equivalent anhydrous chromium(III) chloride (0.255 g, 1.61 mmol) and 2 equivalents (0.5 mL, 3.6 mmol) freshly distilled triethylamine. Over the course of the reaction, the solution turned from yellow to burgundy, after which, the solution was filtered hot to remove triethylammonium chloride and concentrated under reduced pressure. The crude product was precipitated upon addition of hexanes, allowed to settle, and the supernatant decanted. This recrystallization procedure was repeated with dichloromethane/hexanes until the supernatant remained colorless. The product was dried in vacuo and stored in an argon-filled glovebox until use. Yield: 0.269 g (22%). X-ray quality crystals were obtained from a standing solution of DMSO. Anal. calcd (%) for $C_{42}H_{40}ClCr\ N_4O_4 \cdot 6H_2O$: C, 59.89; H, 5.98; N, 6.65; found: C, 59.77; H, 5.98; N, 6.63.

Synthesis of 5,14-Dihydro-6,8,15,17-tetramethyl-7,16-bis((3-methoxyphe-nyl)methanone)dibenzo[b,i][1,4,8,11]tetraazacyclotetradecinato chromium chloride

(Cr(s^{m}tmtaa)Cl, 8). The chromium complex was synthesized following the procedure reported by Cotton for Cr(tmtaa)Cl (**1**).[48] 1.1 g (1.8 mmol) **6** was refluxed in 350 mL benzene for 1 week in the presence of 1 equivalent anhydrous chromium(III) chloride (0.285 g, 1.8 mmol) and 2 equivalents (0.5 mL, 3.6 mmol) freshly distilled triethylamine. Over the course of the reaction, the solution turned from yellow to burgundy, after which, the solution was filtered hot to remove triethylammonium chloride and concentrated under reduced pressure. The crude product was precipitated upon addition of hexanes, allowed to settle overnight, and the supernatant decanted. While allowed to settle overnight, crystals of the unreacted ligand were found on the flask's sides. A minimal amount of dichloromethane was carefully added to the bottom of the flask to dissolve the product, which was transferred to another flask. This recrystallization procedure was repeated with dichloromethane/hexanes, dichloromethane/ether, and THF/ether until the unreacted ligand was no longer observed. The product was dried in vacuo and stored in an argon-filled glovebox until use. Yield: 0.169 g (13.4%). Anal. calcd (%) for $C_{38}H_{34}ClCrN_4O_4 \cdot 2H_2O \cdot CH_2Cl_2$: C, 57.19; H, 4.92; N, 6.84; found: C, 56.89; H, 4.93; N, 7.67.

Copolymerization of cyclohexene oxide and carbon dioxide. High pressure measurements of the copolymerization processes were carried out using a stainless steel Parr autoclave modified with a SiComp window to allow for attenuated total reflectance infrared spectroscopy (ASI ReactIR 1000 in situ probe). The catalyst and cocatalyst were dissolved in 10 mL of dichloromethane, allowed to stir for 30 minutes, and then dried in vacuo. The "activated" catalyst/cocatalyst mixture was then dissolved in 20 mL

of neat cyclohexene oxide and injected into the autoclave via injection port and cannula, after which a single 128-scan background spectrum was collected. The autoclave was then charged with 35 bar carbon dioxide and a single 128-scan spectrum was taken every 2 minutes during the reaction period. Profiles of the absorbances at 1750 cm^{-1} (polycarbonate) and 1810 cm^{-1} (cyclic carbonate) vs. time were recorded after baseline correction. After cooling and venting of the autoclave, the reaction was extracted with dichloromethane. The solution was dried overnight under a stream of compressed air to remove excess dichloromethane. The polymer residue was then dissolved in a minimum amount of dichloromethane and slowly added to a stirred beaker containing a 1 M HCl methanolic solution to remove the catalyst and precipitate the polycarbonate product. The supernatant solution containing the catalyst, cyclic carbonate, and any remaining cyclohexene oxide was decanted and the purified polymer dried in vacuo overnight. The dried polymer was collected and weighed to determine yield and the corresponding TONs and TOFs. The polymers were analyzed by ^{1}H NMR where the amount of ether linkages was determined by integrating the peaks corresponding to the methine protons of polyether at ~3.45 ppm and polycarbonate at ~4.6 ppm. Molecular weight determinations were carried out on a Viscotek Gel Permeation Chromatograph equipped with refractive index, right-angle light scattering, and low-angle light scattering detectors.

X-ray structure studies. A Leica microscope, equipped with a polarizing filter, was used to identify suitable crystals from a sample of crystals of the same habit. The representative crystal was coated in a cryogenic protectant, such as paratone, and affixed

to a nylon sample loop attached to a copper mounting pin. The mounted crystals were then placed in a cold nitrogen stream (Oxford) maintained at 110 or 293 K on either a Bruker SMART 1000, GADDS, or APEX 2 three circle goniometer. The X-ray data were collected on either a Bruker CCD, GADDS, or an APEX 2 diffractometer and covered more than a hemisphere of reciprocal space by a combination of three (or nine in the case of the GADDS) sets of exposures; each exposure set had a different φ angle for the crystal orientation and each exposure covered 0.3° in ω. Crystal data and details on collection parameters are given in Table 1. The crystal-to-detector distance was 5.0 cm for all crystals. Crystal decay was monitored by repeating the data collection for 50 initial frames at the end of the data set and analyzing the duplicate reflections; and found to be negligible. The space group was determined based on systematic absences and intensity statistics.[50] The structure was solved by direct methods and refined by full matrix least-squares on F^2. All non-H atoms were refined with anisotropic displacement parameters. All H atoms attached to C and N atoms were placed in idealized positions and refined using a riding model with aromatic C-H = 0.93 Å, methyl C-H = 0.96 Å, amine N-H = 0.86 Å and with fixed isotropic displacement parameters equal to 1.2 (1.5 for methyl H atoms) times the equivalent isotropic displacement parameter of the atom to which they are attached. The methyl groups were allowed to rotate about their local 3-fold axis during refinement.

For all structures: data reduction, SAINTPLUS (Bruker[50]); program used to solve structures, SHELXS (Sheldrick[51]); program used to refine structures, SHELXL-97

(Sheldrick[52]); molecular graphics and preparation of material for publication, SHELXTL-Plus version 5.0 (Bruker[53]) and XSEED (Barbour[54]).

Results and discussion

Initial observations with both the chromium salen and tmtaa complexes have provided enough evidence to support the assumption that the copolymerization reaction utilizing these compounds proceeds via a monocatalytic single-site mechanism. That is to say the copolymer is produced from only one side of the metal center. This assumption is based on isolated polymer samples and the peak profiles obtained by recording the absorbance values vs. time for the stretching band of the polymer's carbonate functionality in the infrared throughout the course of the copolymerization reactions. The turnover frequencies obtained from the isolated copolymers emphasized that different anions, provided by the cocatalysts, resulted in different catalytic activities, with the azide and chloride anions providing the highest catalytic activities.[56,87] If polymer chain growth does occur from both sides of the chromium center, the rates of polymer formation would be identical after initiation considering both sides of the metal would contain identical substituents, exemplified by the mechanism shown on the right in Figure 47. This would infer that the only difference in the polymerization activities when different cocatalyst anions were used would be in the rate of the initial ring-opening step. This is certainly not the case as cyclohexene oxide ring-opening occurs rapidly, even at room temperature.[58] The differences in the slopes of the polymer

infrared peak traces observed during the polymerizations with various cocatalyst anions suggests dissimilar polymerization rates, further supporting the theory that the polymerization occurs exclusively from one side of the catalyst.

Opponents to this theory have found support for polymer chain growth occurring from both sides of the catalyst through analysis of the produced polycarbonates by gel permeation chromatography (GPC).[23,26,32,33,69] The refractive index-monitored (RI) GPC profiles indicated a distinct bimodal distribution in the polymer chain population. In each case, the higher-molecular-weight copolymer was twice as large as that of the lower-molecular-weight one. They attributed this to the presence of two active species; one with two active sites and a polymer growing in two directions, and the other which propagated from an active end.

In 2005, Inoue and coworkers probed deeper into this facet of the mechanism by employing an ultraviolet-active nucleophile, occupying the fifth coordination site of an aluminum salen catalyst, as well as a quaternary ammonium salt cocatalyst containing the same ultraviolet-active functionality.[32] When the polymers were analyzed by an ultraviolet detector-equipped GPC, the polymer chain end groups could more clearly be identified. The results of the study were inconclusive in determining the nature of the RI bimodal molecular weight distribution. MALDI-TOF mass spectrometry revealed the presence of hydroxyl end groups, indicating the bimodal distribution was most likely a product of chain termination by trace water contamination, a well known occurrence in this immortal copolymerization process.[9] After drying the hygroscopic Et_4NOAc

cocatalyst at 130 °C in vacuo, the corresponding obtained polymer exhibited a unimodal GPC profile with a very small shoulder on the higher molecular weight region. This phenomenon, also observed with the chromium salen and tmtaa systems using the more hydrophobic PPNX cocatalysts, further supports the theory of one directional polymer chain growth and illustrates the detrimental effect water plays on polymerization control.

A steric approach to mechanistic elucidation. In an effort to investigate whether polymer chain growth occurs from one or both sides of the metal center, two ligands were synthesized with straps linking the γ and γ' methine carbons on the diiminato positions of the tmtaa ligand. These ligands were synthesized following or modifying the reports of Sakata and coworkers[88,90] and feature straps that allow enough space for the binding of a cocatalyst, but have sufficient steric bulk to block polymer growth. The solid state structures and crystallographic data of these ligands obtained by X-ray diffractometry are shown in Figure 50 and Table 14. Solid state structures of **4** and **5** have previously been reported to the Cambridge Structural Database in 2005, but were refined with less accuracy and possessed a different unit cell (**5**).[92,93] As illustrated, the two strapped ligands contain different linking groups that span the underside of the compound. The first, shown on the top, contains a *m*-xylylene group connecting the benzoyl functionalities on opposing sides of the ligand, with the second (bottom) being bridged by a more flexible hexylene chain. Table 15 lists distances of key atoms in the straps from the N_4 donor plane that illustrate the similar cavity sizes shared by the two ligands, where the closest contact is over 3.5 Å while the longest is 7.25 Å away from the nitrogen core.

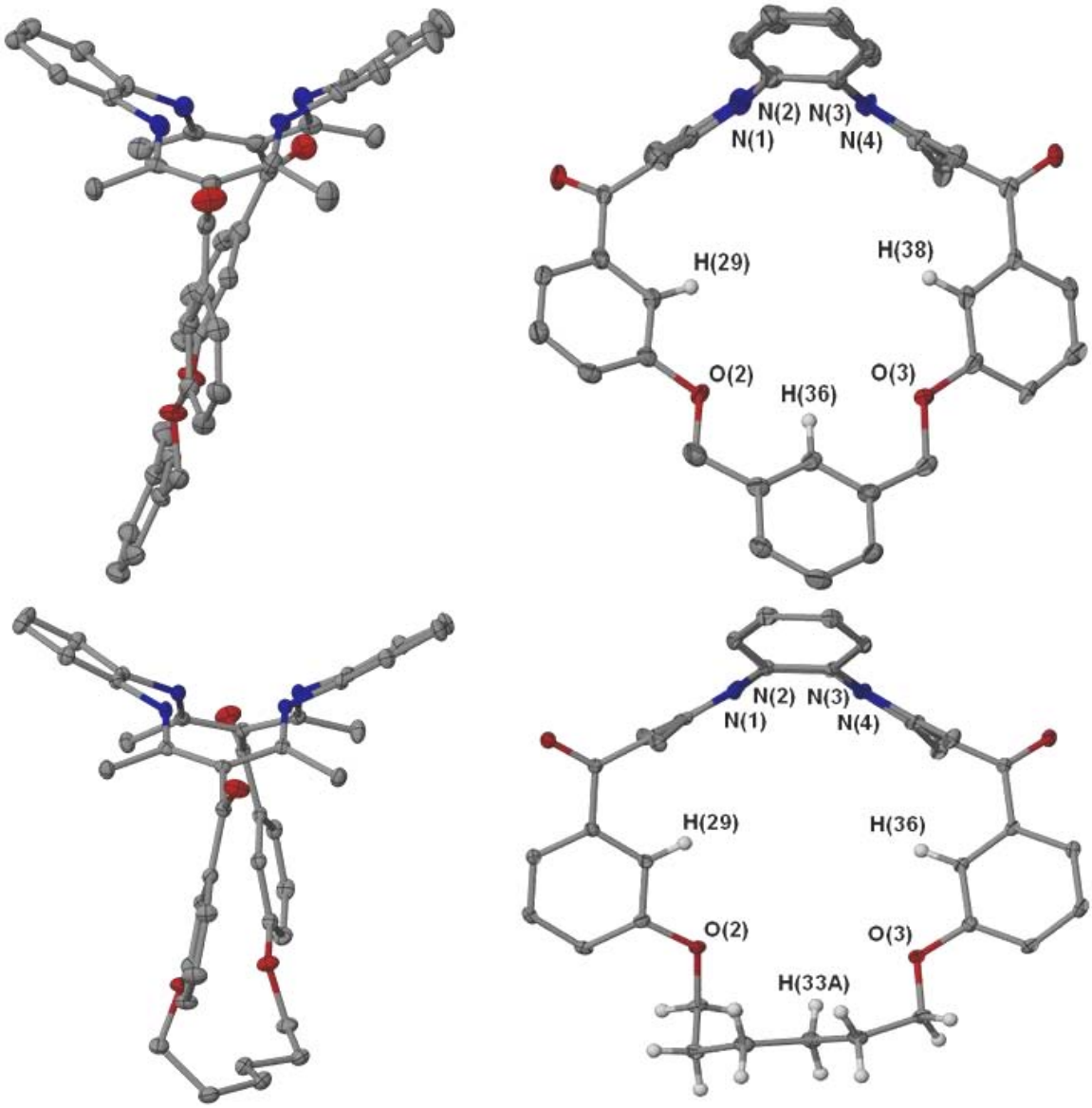

Figure 50. X-ray crystal structures of **4** (top) and **5** (bottom), showing both side-on and end-on perspectives. Thermal ellipsoids are shown at the 50% probability level with selected hydrogens and solvent molecules omitted for clarity.

Table 14. Crystal Data and Structure Refinement for **4**, **5**, and **6**.

	4·CHCl$_3$	**H$_2$stmtaa (5)·4CHCl$_3$**	**H$_2$s^{m}tmtaa (6)**
Empirical formula	$C_{45}H_{39}Cl_3N_4O_4$	$C_{46}H_{46}Cl12N_4O_4$	$C_{38}H_{36}N_4O_4$
Formula wt, g/mol	806.15	1144.27	612.71
Temp (K)	110(2)	110(2)	210(2)
Wavelength (Å)	0.71073	0.71073	0.71073
Crystal system	monoclinic	monoclinic	monoclinic
Space group	$P2_1/n$	$P2_1/c$	$P2_1/c$
a (Å)	12.699(3)	11.8052(14)	11.039(7)
b (Å)	22.317(5)	18.600(2)	20.966(13)
c (Å)	14.771(4)	22.863(3)	14.447(9)
α (deg)	90	90	90
β (deg)	110.666(3)	97.3580(10)	109.086(11)
γ (deg)	90	90	90
Cell volume (Å^3)	3917.0(16)	4978.7(10)	3160(3)
Z	4	6	4
Density (calcd)	1.386	2.290	1.288
Absorb coeff (mm^{-1})	0.285	1.073	0.085
Obsd no. of reflcns	34993	56833	26387
No. of unique reflcns ($I > 2\sigma$)	8634	11961	7163
GooF	1.000	1.000	1.000
R,[a] % [$I > 2\sigma$]	6.45	3.35	6.93
R_w,[a] % [I > 2σ]	12.04	8.57	14.33

[a] $R = \sum||F_o| - |F_c||/\sum|F_o|$. $R_w = \{[\sum w(F_o^2 - F_c^2)^2]/[\sum w(F_o^2)^2]\}^{1/2}$.

Table 15. Selected Contact Distances from the N_4 Donor Plane for **4** and **5**.

	4 (Å)	**H_2stmtaa (5)** (Å)
N_4 – H29	3.8401	3.5525
N_4 – H36	6.5509	3.648
N_4 – H38	3.5368	------
N_4 – O2	6.0389	5.938
N_4 – O3	6.0074	6.1051
N_4 – H33A	------	7.2520

It has been previously shown for both the chromium salen and tmtaa systems that alteration of the electronic environment of the ligands by the addition of electron-withdrawing substituents resulted in diminished polymerization activities.[58,87] The nature of the strapped complex is such that it is electronically unequal to the underivatized Cr(tmtaa)Cl complex and renders direct comparison impossible. To overcome this hurdle, ligand alteration was needed that retained the electronic constraints of H_2stmtaa (**5**) without possessing its steric restrictions. Suitable ligand derivation was found upon reviewing the work of Eilmes and coworkers[91,94] and modified slightly to afford a strap "mimic" ligand, H_2S^mtmtaa (**6**), with an electronic environment that was comparable to **5**. As seen in Figure 51, **6** contains arms that exhibit rotational freedom, exemplified in the solid state structure where the arms are twisted to leave the underside of the ligand accessible, once metallated, to molecules associated with the copolymerization process. In support the rotational freedom of **6**, polymorphism has been observed and fully characterized in a similar complex.[95]

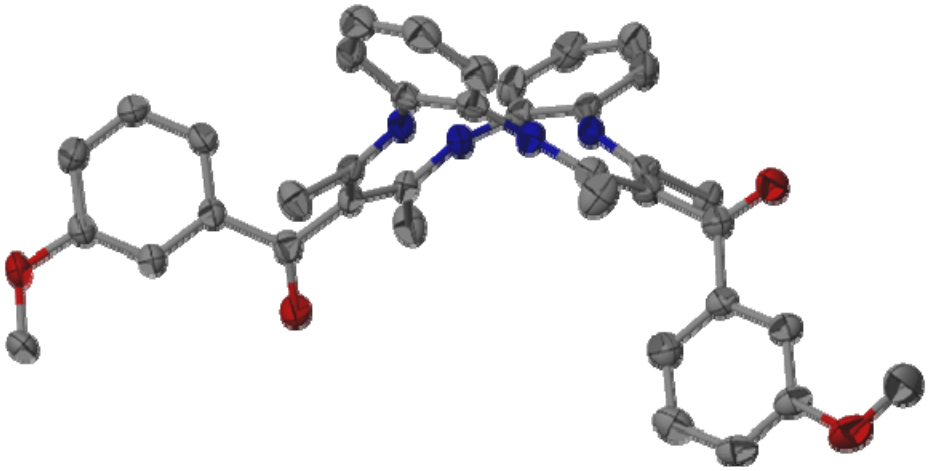

Figure 51. X-ray crystal structures of **6**, illustrating the flexibility of the anisoyl arms to expose the underside of the complex. Thermal ellipsoids are shown at the 50% probability level with hydrogens omitted for clarity.

Cocatalyst binding to Cr(stmtaa)Cl and Cr(s^{m}tmtaa)Cl. Synthesis of the corresponding chromium complexes of **5** and **6** was conducted following the reported procedure for **1** by Cotton and coworkers.[39] The hexylene-linked ligand, **5**, was chosen over that of the xylylene-linked, **4**, for metallation due to the greater flexibility in the strap and ease of synthesis.

Since epoxide/CO_2 catalysts incorporating tetradentate ligand systems, such as porphyrin, salen, and tmtaa, require binding to occur at both of the ancillary sites to

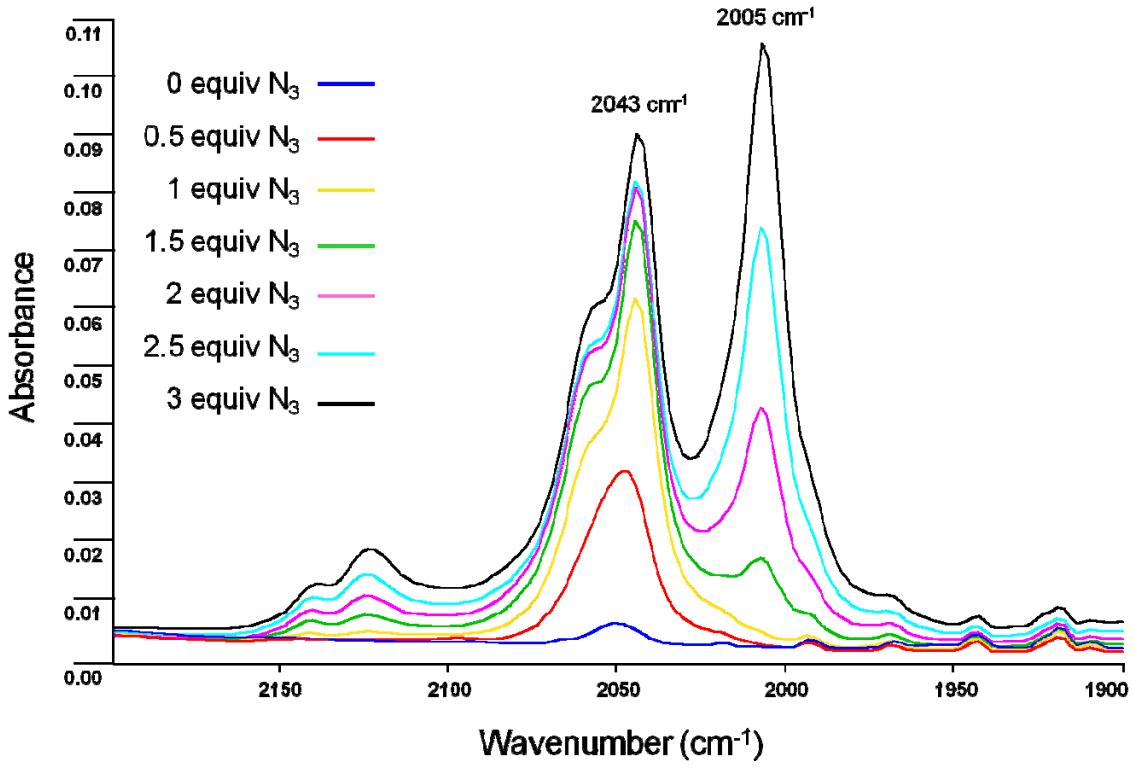

Figure 52. Infrared spectra from the titration of complex **7** with $PPNN_3$.

achieve high activity; therefore, complete blockage of one of these sites would not be beneficial. With that in mind, the strapped complex, Cr(stmtaa)Cl (**7**), and the corresponding strap mimic complex, Cr(s^mtmtaa)Cl (**8**), must not be so sterically encumbering to prevent the binding of a cocatalyst anion. To determine the catalysts' ability to bind cocatalyst, titrations were conducted in which sequential additions of $PPNN_3$ were added to complexes **7** and **8** and the ν_{N_3} monitored by infrared spectroscopy. As can be seen from the overlay of infrared spectra for the addition of $PPNN_3$ to **7** in Figure 52, a metal-bound azide stretching band is observed at 2043 cm^{-1}.

This band continues to grow in intensity until the [N_3^-] reaches 1 equivalent, after which, a further increase can be explained by a concentration effect and is supported by the increased noise above 2100 cm^{-1}. When the [N_3^-] reaches 1.5 equivalents, the observance of a stretching band at 2005 cm^{-1}, corresponding to free N_3^- is apparent, indicating coordinative saturation after binding only 1 equivalent of cocatalyst. From a previous cocatalyst binding study (Figure 20), the stretching band observed at 2043 cm^{-1} in Figure 52 corresponds to a six-coordinate chromium species, but unlike the previous study, **1** was found to bind 2 equivalents of N_3^- anion by displacing the originally bound chloride.[67] With these results, a proposed azide cocatalyst binding scheme is shown in Figure 53 where the sterically hindered underside of complex **7** is too encumbered to allow the azide anion access to the chromium center and instead, displaces the chloride ligand. Interpreting the observance of a six-coordinate chromium azide complex and only 1 equivalent of azide uptake from Figure 52 suggests that the cavity is large enough to allow smaller ligands access to the metal center, such as the azide-displaced chloride, but restricting enough to impede the binding of the slightly larger azide anion.

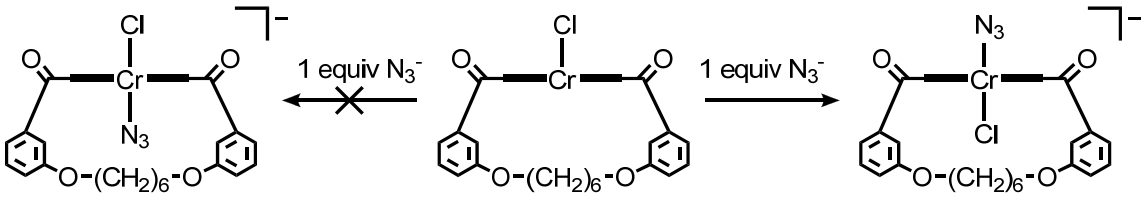

Figure 53. Proposed cocatalyst binding scheme between **7** and $PPNN_3$.

Further support for selective access to the cavity of the strapped complex is provided by the solid state crystal structure (Table 16) obtained from a solution of DMSO, where the apical chloride has been displaced by a solvent molecule and recoordinated to the open site of the chromium center, within the strap cavity (Figure 54).

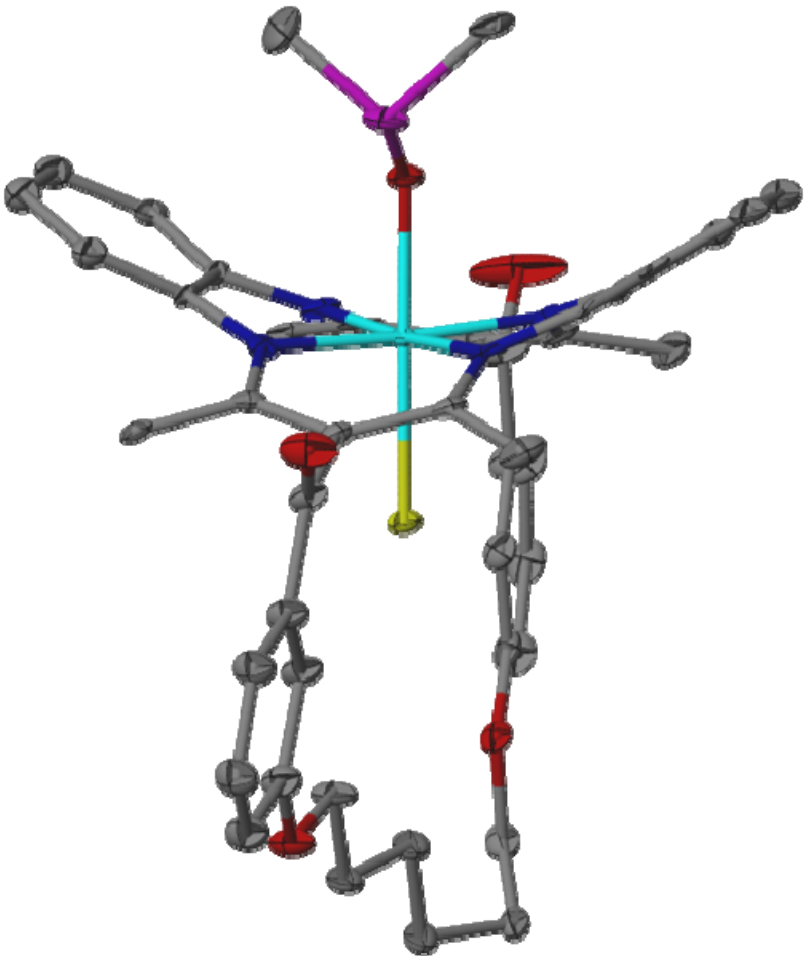

Figure 54. X-ray crystal structure of **7**, illustrating the ability of the chloride to bind within the cavity of the strap. Thermal ellipsoids are shown at the 50% probability level with hydrogens and interstitial solvent molecules omitted for clarity.

Table 16. Crystal Data and Structure Refinement for **7**.

	Cr(stmtaa)Cl(DMSO)·1.5DMSO (7)
Empirical formula	$C_{44}H_{46}ClCrN_4O_5S{\cdot}C_3H_9O_{1.5}S_{1.5}$
Formula wt, g/mol	947.55
Temp (K)	110(2)
Wavelength (Å)	0.71073
Crystal system	triclinic
Space group	P-1
a (Å)	11.540(12)
b (Å)	12.128(13)
c (Å)	17.192(18)
α (deg)	75.31(2)
β (deg)	89.25(2)
γ (deg)	77.71(2)
Cell volume ($Å^3$)	2272(4)
Z	2
Density (calcd)	1.385
Absorb coeff (mm^{-1})	0.480
Obsd no. of reflcns	16063
No. of unique reflcns ($I > 2\sigma$)	7346
GooF	1.011
R,[a] % [$I > 2\sigma$]	9.51
R_w,[a] % [$I > 2\sigma$]	15.12

[a] $R = \sum||F_o| - |F_c||/\sum|F_o|$. $R_w = \{[\sum w(F_o^2 - F_c^2)^2]/[\sum w(F_o^2)^2]\}^{1/2}$.

A comparison of **7** and **1** reveal little structural difference between the tetraazaannulene cores of the two complexes. As shown in Table 17 and illustrated in Figure 55 below, the coordination of DMSO trans to the chloride has increased the chromium-chloride bond length slightly. Interestingly, the out-of-plane distortion of the

chromium from the nitrogen donor plane changed from 0.4235 Å above the plane in **1** to 0.0821 Å below the plane in **7**, concomitantly causing an enlargement in the chromium nitrogen bond angles. Also shown in Figure 55 are spheres representing the van der Waals radii of selected atoms to illustrate the steric allowances of the strap moiety. From the distances listed in Table 17, the closest contact to the chloride is 3.015 Å, well outside the sum of the van der Waals radii for hydrogen and chlorine of 2.84 Å, supporting the ability of a chloride anion from the required cocatalyst to bind to the chromium center within the steric confines of the strap.

Table 17. Selected Bond and Contact Distances and Angles for **1** and **7**.

	Cr(tmtaa)Cl (1)[a]	**Cr(stmtaa)Cl·DMSO (7)**
Cr – N1 (Å)	1.9881(18)	1.964(7)
Cr – N2 (Å)	1.9745(17)	1.984(7)
Cr – N3 (Å)	1.9900(18)	1.951(7)
Cr – N4 (Å)	1.9716(17)	1.985(8)
Cr – Cl (Å)	2.2607(7)	2.346(3)
Cr – O5 (Å)	------	2.033(5)
Cr – H29 (Å)	------	4.367
Cr – H30B (Å)	------	5.228
Cr – H36 (Å)	------	4.488
Cl – H29 (Å)	------	3.015
Cl – H30B (Å)	------	3.143
Cl – H36 (Å)	------	3.252
N1 – Cr – N2 (deg)	92.98(7)	94.3(3)
N2 – Cr – N3 (deg)	81.76(7)	84.7(3)
N3 – Cr – N4 (deg)	92.96(7)	96.4(3)
N1 – Cr – N4 (deg)	81.78(7)	84.3(3)
Cr – N_4 (Å)	0.4235	-0.0821

[a]Data taken from structure determination in ref. [67].

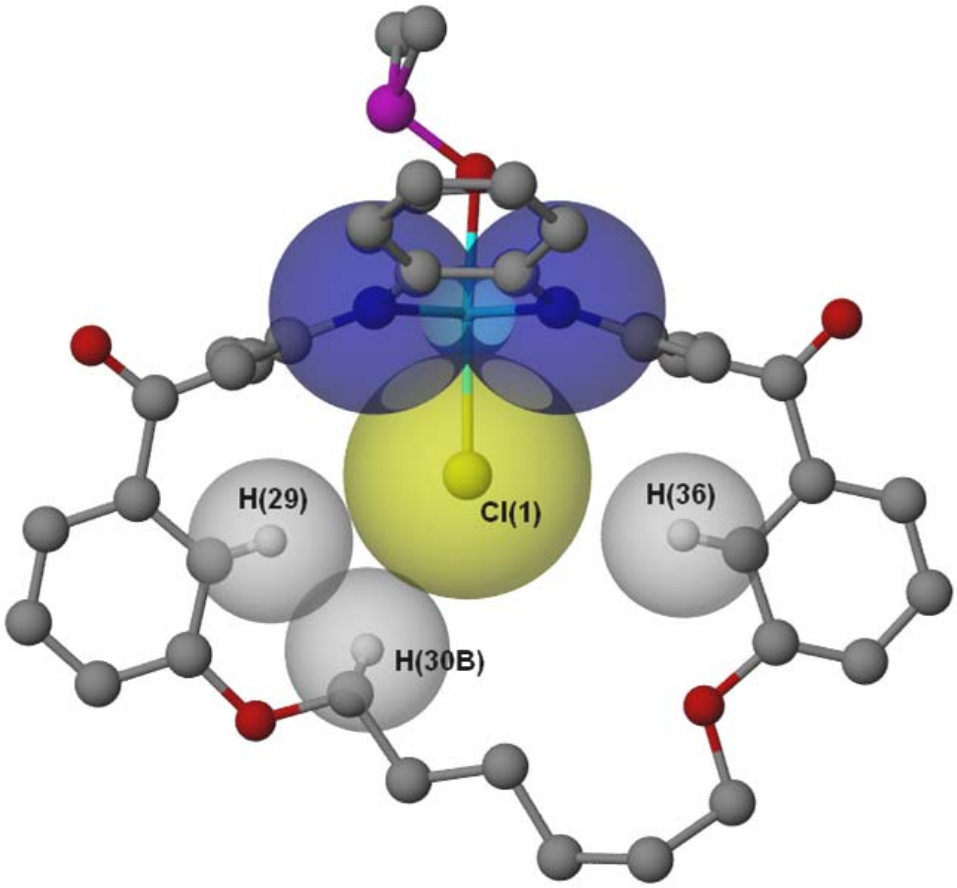

Figure 55. Three-dimensional representation from the X-ray crystal structure of **7**. The spheres represent the van der Waals radii of the selected atoms, illustrating the strict steric allowances of the strap moiety.

To investigate the ability of complex **8**, acting as a strap mimic, to bind cocatalyst, a titration mirroring those previously completed for complexes **1** and **7** was conducted. Figure 56 shows an overlay of the infrared spectra of **8** as sequential amounts of $PPNN_3$ was added. As seen previously with **1**, as the $[N_3^-]$ was increased, an absorbance band at 2043 cm^{-1} was observed, which grew in intensity until 2 equivalents of N_3^- was reached. At $[N_3^-]$ above 2 equivalents, complex **8** became saturated with

azide, apparent by the observance of an absorption band at 2005 cm^{-1}, indicative of free azide anion in solution. This study proves the strap mimic to behave, as predicted, like complex **1** rather than **7** and presumably retain the ability to undergo polymerization from both sides of the metal center, if necessary.

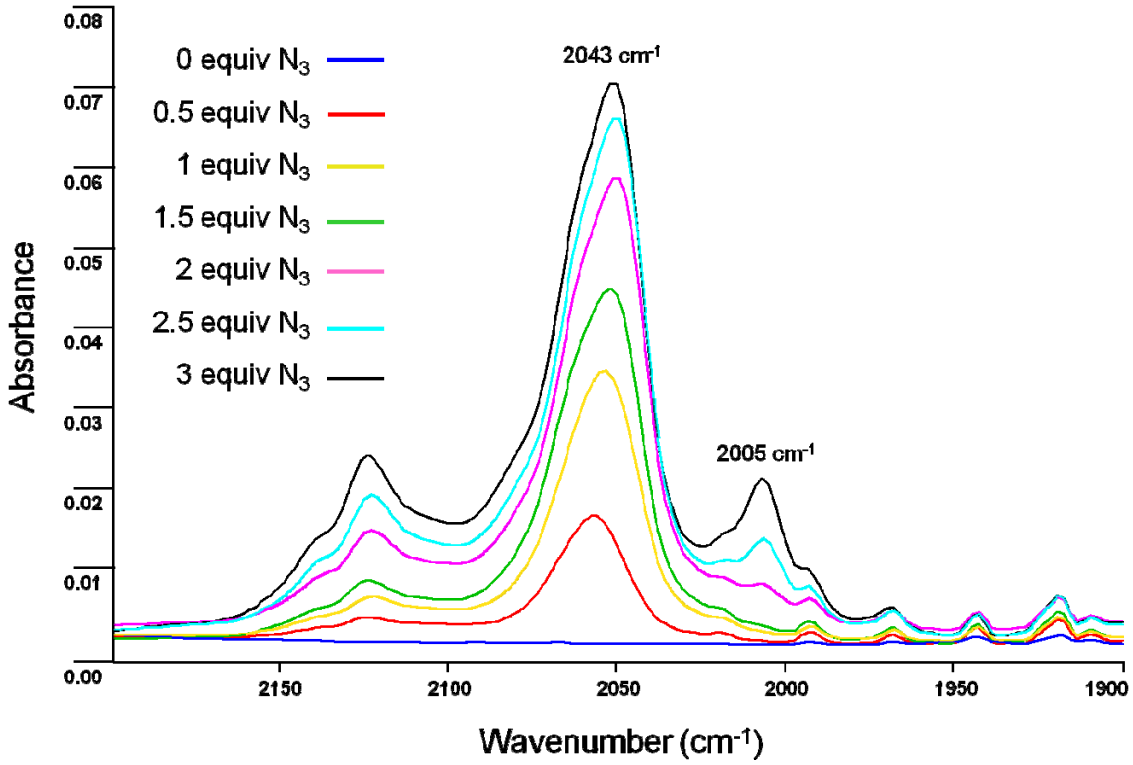

Figure 56. Infrared spectra from the titration of complex **8** with $PPNN_3$.

Copolymerizations catalyzed by Cr(stmtaa)Cl and Cr(s^{m}tmtaa)Cl. With the cocatalyst binding behavior of the strap (**7**) and strap mimic (**8**) complexes understood,

the question of whether these complexes act as mono- or dicatalytic single-site catalysts for the epoxide/CO_2 copolymerization could finally be addressed. To reiterate the discussion *vide supra*, the strap moiety of complex **7** provides sufficient steric constraint to bind select cocatalysts to the underside of the metal center while complex **8** does not exhibit such selectivity. If these complexes are able to catalyze the copolymerization of cyclohexene oxide and carbon dioxide at a similar rate and produce copolymers with similar molecular weights and polydispersities, rationale would point to these complexes operating through the monocatalytic single-site pathway in which polymer chain propagation occurs from only one side of the catalyst. To accurately investigate the ability of these complexes to polymerize cyclohexene oxide with carbon dioxide, both compounds were employed as catalysts under the same conditions utilized for copolymerizations using **1** discussed in previous reports.[67,87]

The copolymerizations employing **7** and **8** as catalysts were conducted in 20 mL of cyclohexene oxide, 2 equivalents of PPNCl, and the appropriate amount of catalyst to achieve an M/I ratio ~ 1700. After the reaction mixture reached 80 °C, the reactor was charged with 35 bar CO_2 and allowed to react for a standard comparison time of 1 hour. Figure 57 displays an overlay of the reaction profiles obtained from the copolymerization reactions, illustrating polycarbonate and cyclic carbonate production for both the strap and strap mimic catalysts. It is easily seen from these profiles that formation of both polymer and cyclic carbonate occur at nearly identical rates for the two different catalysts. This leads to the assumption that the polymers were formed by the same mechanism. It follows previous observations about the steric constraints of the

strap moiety that chain growth occurred from only one side of the metal center. After the polymers were isolated and weighed, the TOFs were determined to be 807 h^{-1} for the strap catalyst (**7**) and 797 h^{-1} for the strap mimic catalyst (**8**). The ^{1}H NMR spectra of the purified polymers indicate > 99% CO_2 incorporation while the GPC profiles calculated number average molecular weights of 11,431 and 12,003 as well as polydispersity indices of 1.108 and 1.048 for **7** and **8**, respectively. The similarities in the amounts and properties of the isolated polymers, with the polydispersity index being lower for the catalyst with

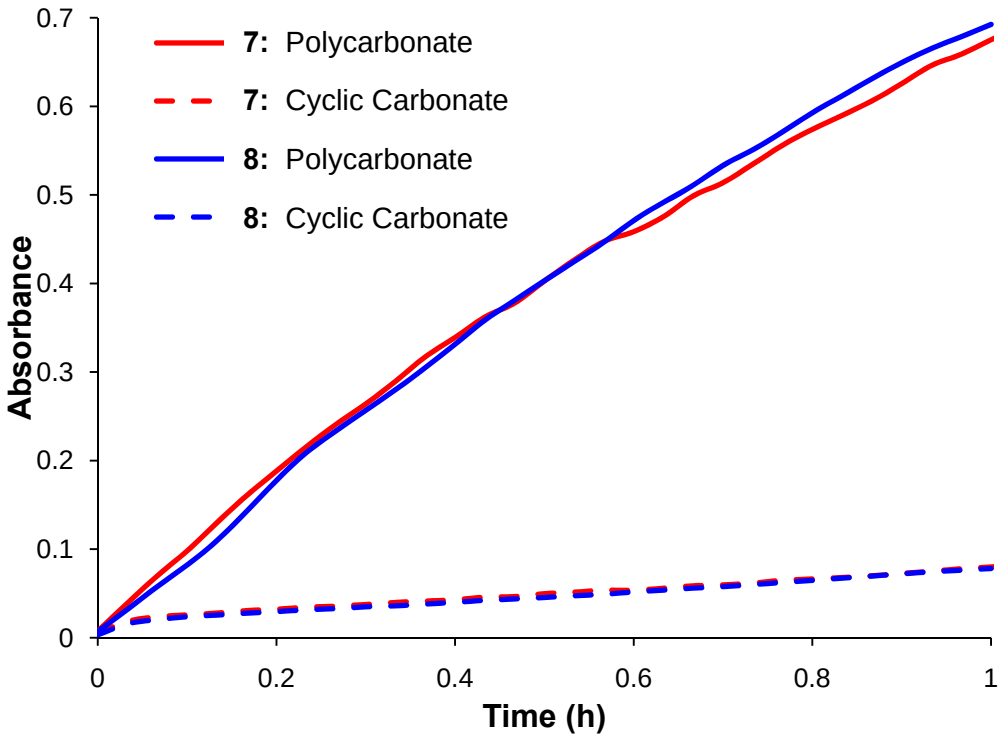

Figure 57. Reaction profiles indicating polycarbonate and cyclic carbonate formation with time for the copolymerization of cyclohexene oxide and CO_2, catalyzed by complexes **7** and **8** in the presence of 2 equivalents of PPNCl and 35 bar carbon dioxide at 80 ºC.

the potential to simultaneously grow two independent polymer chains further supports the theory of a monocatalytic single-site mechanism. These results, as well as other reaction parameters, are listed in Table 18 below.

Table 18. Data Comparing the Results of the Copolymerizations of CHO and CO_2 for Catalysts **7** and **8**.[a]

	Cr(stmtaa)Cl (7)	**Cr(s^{m}tmtaa)Cl (8)**
M/I	1709	1704
Time (h)	1.0	1.0
Polymer (g)	13.26	13.15
TON	806.6	797.3
TOF (h^{-1})	806.6	797.3
% CO_2[b]	> 99%	> 99%
M_n[c] ($g \cdot mol^{-1}$)	11,431	12,003
M_w[c] ($g \cdot mol^{-1}$)	12,664	12,584
PDI[d]	1.108	1.048

[a]Copolymerization reactions were conducted with 20 mL CHO, 87 mg and 81 mg of **7** and **8**, respectively, and 2 equivalents of PPNCl at 80 ºC and under 35 bar CO_2 pressure for 1 h. [b]Determined by ^{1}H NMR. [c]Determined by GPC. [d]M_n/M_w.

Conclusions

In the interest of gaining insight into the mechanism of the copolymerization of epoxides with carbon dioxide, two new catalysts were developed based upon the chromium tetramethyltetraazaannulene system previously reported to be highly active and selective towards the production of poly(cyclohexylene carbonate).[67,87] These catalysts were designed to elucidate whether copolymer formation occurs from a single

side of the metal center or two independent polymer chains were produced simultaneously. Previous efforts to address this ambiguity have focused on GPC analysis, where bimodal distributions where thought to be the result of two different active species, but findings were inconclusive as to whether the different molecular weight distributions were caused by dual catalysis at the active site or from chain termination caused by the presence of trace water during the reaction.[23,26,32,33,69] Reported herein is a different approach taken to address this mechanistic uncertainty; one that employs the concept of steric hindrance at the active site to control polymerization behavior. The first catalyst, Cr(stmtaa)Cl, contained a strap, tethering opposing sides of the complex and providing steric bulk under the metal center that limits polymer chain propagation to one side of the catalyst. Since the alterations to the complex would in turn alter the electronic environment around the chromium active site and make direct comparison to the parent complex, Cr(tmtaa)Cl, inapplicable, a similar catalyst, Cr(s^mtmtaa)Cl, with the same electronic features was designed to mimic the strapped complex while allowing the opportunity for double-sided catalysis to occur.

The cavity on the underside of Cr(stmtaa)Cl created by the strap moiety was found to be large enough to accommodate the chloride anion, but too small to allow the azide anion to bind to the chromium center, while Cr(s^mtmtaa)Cl retained the ability to bind both the chloride and azide cocatalysts. This leads to the conclusion that the cavity of the strapped catalyst is large enough to allow binding of the cocatalyst, but too sterically encumbered to allow epoxide binding and polymerization to occur.

Both catalysts were able to copolymerize cyclohexene oxide and carbon dioxide to produce polymers with near identical reaction profiles and activities, achieving turnover frequencies of 807 h^{-1} and 797 h^{-1} for Cr(stmtaa)Cl (**7**) and Cr(s^mtmtaa)Cl (**8**), respectively. These copolymers produced also contained essentially indistinguishable molecular weights and molecular weight distributions of 11,431 $g \cdot mol^{-1}$ and 1.108 for Cr(stmtaa)Cl and 12,003 $g \cdot mol^{-1}$ and 1.048 for Cr(s^mtmtaa)Cl. Although the activities of these catalysts are, as expected, less than that of Cr(tmtaa)Cl, the copolymers contain molecular weight distributions that coincide exactly with copolymers obtained from the underivatized catalyst. Despite the observance of a slight shoulder in the higher molecular weight region of the GPC profiles, the infrared binding data, X-ray crystal structure, in situ infrared reaction profiles, and copolymer properties all support the conclusion that copolymerization of cyclohexene oxide with carbon dioxide occurs from only one side of the catalyst via a monocatalytic single-site mechanism.

CHAPTER V

VARIOUS SOLID STATE X-RAY CRYSTAL STRUCTURES RELEVANT TO THE TETRAMETHYLTETRAAZAANNULENE SYSTEM AND/OR THE COPOLYMERIZATION OF CARBON DIOXIDE AND EPOXIDES

Introduction

This dissertation reports the development of the chromium tetramethyltetraazaannulene catalyst system. Along the way, several compounds were synthesized and characterized that are relevant to either the chromium complex or the copolymerization of cyclohexene oxide and carbon dioxide. Reported here are the synthesis and characterization of two ligand derivatives that were synthesized with the intent of metallation and catalytic investigation, but were deemed unsuitable due to high reagent cost and low yields. Also reported are the synthesis and X-ray crystal structures of two cocatalysts utilized in the copolymerization studies, $PPNN_3$ and PPNBr.

Experimental

Methods and materials. Unless otherwise specified, all manipulations were carried out on a double manifold Schlenk vacuum line under an atmosphere of argon or in an argon-filled Glovebox. Methanol (EMD Chemicals), absolute ethanol (Pharmco-

Aaper), 2,4-pentanedione (Aldrich), nickel acetate tetrahydrate (Fisher), chromium(III) chloride (Strem), ammonium hexafluorophosphate (Oakwood), sodium azide (Aldrich), sodium chloride (EMD Chemicals), potassium bromide (Fisher), *p*-toluenesulfonyl cyanide (Aldrich), n-butyllithium (1.6 M in hexanes) (Alfa Aesar), sodium sulfate (EMD Chemicls), and hydrochloric acid (EMD Chemicals) were used without further purification. Triethylamine (EMD Chemicals) was stored over sodium hydroxide and freshly distilled before use. Methylene chloride, hexane, acetonitrile, tetrahydrofuran, methanol, and ethyl ether were freshly purified by an MBraun Manual Solvent System packed with Alcoa F200 activated alumina desiccant. The synthesis of H_2tmtaa was conducted following published procedures.[47] ^{1}H NMR spectra were acquired on using a Varian Inova 300 MHz superconducting NMR spectrometer. Infrared spectra were recorded on using a Bruker Tensor 27 FTIR spectrometer.

Synthesis of 5,14-Dihydro-6,8,15,17-tetramethyl-7-cyanodibenzo[b,i]-[1,4,8,11]tetraazacyclotetradecine, H_2tmtaaCN (9). This synthesis was modified from a previous report.[96] 0.86 g (2.5 mmol) H_2tmtaa was dissolved in 30 mL THF and cooled to -78 °C, followed by dropwise addition of 3.2 mL (5.12 mmol) *n*-butyllithium (1.6 M in hexanes) and allowed to stir for 10 minutes. Stirring was continued for 1 hour at room temperature and the solution was recooled to -78 °C. 1 g (5.52 mmol) *p*-toluenesulfonyl cyanide was dissolved in 30 mL THF and cooled to -78 °C and added dropwise to the solution containing the dilithiated compound and allowed to stir at room temperature overnight. After solvent removal in vacuo, the residue was dissolved in dichloromethane and washed with brine, dried over Na_2SO_4, and filtered. The solvent

was removed in vacuo and the residue recrystallized from ethanol. Yield was not determined. X-ray quality crystals were obtained through slow evaporation of a dichloromethane solution. MS (ESI): m/z 370.20 (M+H). FTIR $\nu_{C\equiv N}$: 2195 cm^{-1} in dichloromethane. ^1H ($CDCl_3$, 300 MHz): δ 14.32 (s, 2H), 7.16 (m, 4H), 7.07 (m, 4H), 4.91 (s, 1H), 2.42 (s, 12H).

Synthesis of 5,14-Dihydro-6,8,15,17-tetramethyl-7,16-biscyanodibenzo[b,i]-[1,4,8,11]tetraazacyclotetradecine, H_2tmtaa$(CN)_2$ (10). This synthesis was modified from a previous report.[96] 1 g (2.9 mmol) H_2tmtaa was dissolved in 40 mL THF and cooled to -78 °C, followed by dropwise addition of 4 mL (6.4 mmol) *n*-butyllithium (1.6 M in hexanes) and allowed to stir for 5 minutes. Stirring was continued for 1 hour at room temperature and the solution was recooled to -78 °C. 1.57 g (6.67 mmol) *p*-toluenesulfonyl cyanide was dissolved in 40 mL THF and cooled to -78 °C and added dropwise to the solution containing the dilithiated compound and allowed to stir at room temperature for 3 days. After solvent removal in vacuo, the residue was dissolved in dichloromethane and washed with brine, dried over Na_2SO_4, and filtered. Ether was added and a grey solid removed by filtration. The solvent was removed in vacuo and the product extracted with acetonitrile. Yield was not determined. X-ray quality crystals were obtained through slow evaporation of a dichloromethane solution. MS (ESI): m/z 395.2 (M+H). FTIR $\nu_{C\equiv N}$: 2195 cm^{-1} in dichloromethane. ^1H ($CDCl_3$, 300 MHz): δ 14.32 (s, 2H), 7.16 (m, 4H), 7.07 (m, 4H), 2.43 (s, 12H).

Synthesis of bis(triphenylphosphoranylidene)ammonium azide. The syntheses was conducted following the reported procedure.[49] 15 g (26 mmol) bis(triphenylphosphoranylidene)ammonium chloride was stirred overnight with 1 equivalent (1.7 g, 26 mmol) of NaN_3 in 250 mL absolute ethanol. The solution was filtered and the filtrate dried in vacuo. The residue was dissolved in acetonitrile and filtered to remove any remaining sodium chloride. The solution was concentrated and recrystallized upon layering with ether. Yield: 13 g (80%). FTIR ν_{N_3}: 2005 cm^{-1} in dichloromethane.

Synthesis of bis(triphenylphosphoranylidene)ammonium bromide. The syntheses was conducted through modification of the reported procedure.[49] 15 g (26 mmol) bis(triphenylphosphoranylidene)ammonium chloride was stirred overnight with 1 equivalent (3.1 g, 26 mmol) of KBr in 250 mL absolute ethanol. 30 mL of water was added to aid in the solubility of KBr and the suspension allowed to stir for an additional day. The solution was filtered and the filtrate dried in vacuo. The residue was dissolved in acetonitrile and filtered to remove any remaining sodium chloride. The solution was concentrated and recrystallized upon layering with ether. Yield: 15.5 g (85.1%).

X-ray structure studies. A Leica microscope, equipped with a polarizing filter, was used to identify suitable crystals from a sample of crystals of the same habit. The representative crystal was coated in a cryogenic protectant, such as paratone, and affixed to a nylon sample loop attached to a copper mounting pin. The mounted crystals were then placed in a cold nitrogen stream (Oxford) maintained at 110 or 293 K on either a

Bruker SMART 1000, GADDS, or APEX 2 three circle goniometer. The X-ray data were collected on either a Bruker CCD, GADDS, or an APEX 2 diffractometer and covered more than a hemisphere of reciprocal space by a combination of three (or nine in the case of the GADDS) sets of exposures; each exposure set had a different φ angle for the crystal orientation and each exposure covered 0.3° in ω. Crystal data and details on collection parameters are given in Table 1. The crystal-to-detector distance was 5.0 cm for all crystals. Crystal decay was monitored by repeating the data collection for 50 initial frames at the end of the data set and analyzing the duplicate reflections; and found to be negligible. The space group was determined based on systematic absences and intensity statistics.[50] The structure was solved by direct methods and refined by full matrix least-squares on F^2. All non-H atoms were refined with anisotropic displacement parameters. All H atoms attached to C and N atoms were placed in idealized positions and refined using a riding model with aromatic C-H = 0.93 Å, methyl C-H = 0.96 Å, amine N-H = 0.86 Å and with fixed isotropic displacement parameters equal to 1.2 (1.5 for methyl H atoms) times the equivalent isotropic displacement parameter of the atom to which they are attached. The methyl groups were allowed to rotate about their local 3-fold axis during refinement.

For all structures: data reduction, SAINTPLUS (Bruker[50]); program used to solve structures, SHELXS (Sheldrick[51]); program used to refine structures, SHELXL-97 (Sheldrick[52]); molecular graphics and preparation of material for publication, SHELXTL-Plus version 5.0 (Bruker[53]) and XSEED (Barbour[54]).

Results and discussion

Cyanation of H_2tmtaa. In an attempt to investigate the effect derivatization of the γ and γ' positions on the ligand had on the catalytic activity of the chromium tetramethyltetraazaannulene system towards the copolymerization of epoxide and carbon dioxide, the addition of cyano groups was explored (Figure 58). This work was inspired by the highly active zinc β-diiminate catalyst (upper right of Figure 4), able to achieve catalytic activities of ~2300 h^{-1}, developed by Coates and coworkers.[97] Previous ligand modifications, with the goal of optimization, have been centered on the addition of electron-withdrawing or -donating groups to the phenylene moieties. The results of these modifications on catalytic activity were somewhat inconclusive and were attributed to the aromatic stabilization of the phenylene rings restricting communication with the metal center. In contrast, the addition of electron-withdrawing benzoyl moieties at the γ and γ' positions of the ligand, as discussed for the complexes in Chapter IV, resulted in decreased catalytic activities. The electronic sensitivity this position has on the metal center exists because both are part of a six-membered, psuedoaromatic metallocycle, allowing electron density alterations at the ligand to communicate back to the metal.

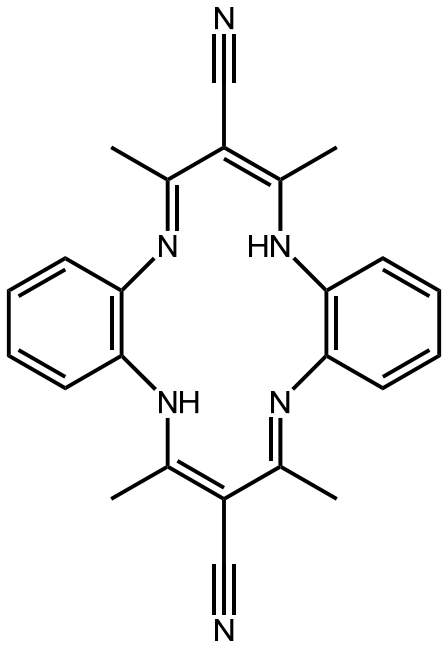

Figure 58. Skeletal representation of H_2tmtaa$(CN)_2$ (**10**).

The addition of cyano groups to the ligand was modeled after the synthesis reported by Coates for the analogous β-diiminate modification.[96] Unfortunately, the synthesis of H_2tmtaa$(CN)_2$ (**10**) did not proceed as straightforwardly as reported for the β-diiminate ligand system. Attempts at product purification lead to the isolation of the mono-cyanated complex, H_2tmtaaCN (**9**), in very low yield. Modification of the synthesis with longer reaction times and a more extensive workup yielded a small quantity of **10**. X-ray solid state crystal structures were obtained for complexes **9** and **10** with the crystallographic data and thermal ellipsoid plots shown in Table 19 and Figure 59.

Table 19. Crystal Data and Structure Refinement for **9** and **10**.

	H_2tmtaaCN (9)	**H_2tmtaa$(CN)_2$ (10)**
Empirical formula	$C_{23}H_{23}N_5$	$C_{24}H_{22}N_6$
Formula wt, g/mol	369.46	394.48
Temp (K)	110(2)	110(2)
Wavelength (Å)	1.54178	0.71073
Crystal system	monoclinic	orthorhombic
Space group	$P2_1/c$	Pnma
a (Å)	21.900(3)	11.957(9)
b (Å)	10.3129(17)	18.362
c (Å)	18.608(3)	18.362(14)
α (deg)	90	90
β (deg)	111.926(7)	90
γ (deg)	90	90
Cell volume ($Å^3$)	3898.8(11)	4032(4)
Z	8	8
Density (calcd)	1.259	1.300
Absorb coeff (mm^{-1})	0.605	0.081
Obsd no. of reflcns	29912	31522
No. of unique reflcns ($I > 2\sigma$)	5742	4687
GooF	1.000	1.010
R,[a] % [$I > 2\sigma$]	5.31	6.42
R_w,[a] % [$I > 2\sigma$]	7.26	12.94

[a] $R = \sum||F_o| - |F_c||/\sum|F_o|$. $R_w = \{[\sum w(F_o^2 - F_c^2)^2]/[\sum w(F_o^2)^2]\}^{1/2}$.

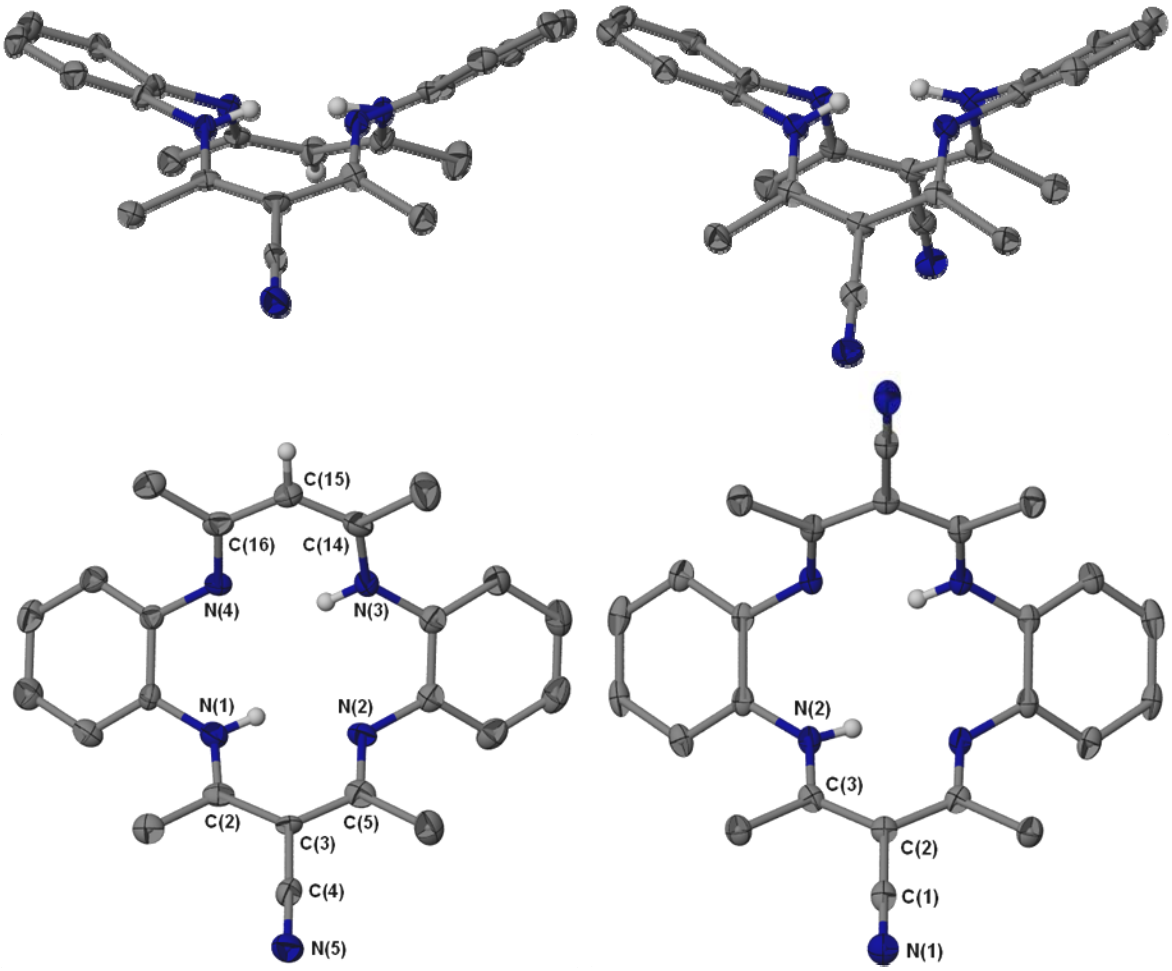

Figure 59. X-ray crystal structures of **9** (left) and **10** (right). Thermal ellipsoids are shown at the 50% probability level with hydrogens omitted for clarity with the exception of those selected.

The asymmetry of complex **9** and electron-withdrawing nature of the cyano group causes the imine and amine bond distances to vary from one side of the ligand to the other. Listed in Table 20 are selected bond distances and angles for complex **9**, illustrating the imine and amine bond lengths on the cyano-substituted side of the ligand

being ~ 0.02 Å shorter than the corresponding bonds of the underivatized side. Symmetry characteristics of the structure obtained for complex **10** make direct comparison to **9** difficult, but the analogous bond lengths for both imine and amine bonds correspond very closely to those of the substituted side of **9**. Both complexes contain near-linear cyano groups with typical carbon-nitrogen bond lengths and connectivity angles ranging from 116.45-118.04 Å to the diiminato portions of the ligand.

Table 20. Selected Bond Distances and Angles for Complex **9**.

	H_2tmtaaCN (9)
C2 – N1 (Å)	1.321(3)
C5 – N2 (Å)	1.313(3)
C14 – N3 (Å)	1.342(3)
C16 – N4 (Å)	1.330(3)
C4 – N5 (Å)	1.161(3)
C2 – C3 – C4 (deg)	116.6(3)
N5 – C4 – C3 (deg)	178.1(3)

Bis(triphenylphosphoranylidene)ammonium azide and bromide. The synthesis of $PPNN_3$ and PPNBr involve a metathesis reaction between PPNCl and the desired product anion as a sodium or potassium salt. The PPN moiety is a large, bulky, non-interacting, and hydrophobic cation that has proven invaluable as a cocatalyst for the copolymerization of carbon dioxide and epoxides.[56] Its phenyl rings shield access to the cationic nitrogen, providing an essentially "free" anion to bind to an open site on a

metal complex. The hydrophobicity of the cation make PPN salts easier to prepare anhydrous than the analogous tetraalkylammonium salts. This is important as the presence of water in the copolymerization reactions leads to early chain termination, lower molecular weight polymers, and broader polydispersities.

Table 21. Crystal Data and Structure Refinement for $PPNN_3$ and PPNBr.

	$PPNN_3$·MeCN	**PPNBr·2MeCN**
Empirical formula	$C_{38}H_{33}N_5P_2$	$C_{32}H_{28.80}Br_{0.80}N_{2.40}P_{1.60}$
Formula wt, g/mol	621.63	560.45
Temp (K)	110(2)	110(2)
Wavelength (Å)	0.71073	0.71073
Crystal system	orthorhombic	monoclinic
Space group	Pbca	$P2_1/c$
a (Å)	19.7959(18)	9.6223(9)
b (Å)	16.1534(15)	19.8880(19)
c (Å)	20.1733(19)	18.8039(18)
α (deg)	90	90
β (deg)	90	98.7230(10)
γ (deg)	90	90
Cell volume ($Å^3$)	6450.8(10)	3556.8(6)
Z	8	5
Density (calcd)	1.280	1.308
Absorb coeff (mm^{-1})	0.171	1.278
Obsd no. of reflcns	68803	38592
No. of unique reflcns ($I > 2\sigma$)	7275	7922
GooF	1.003	1.000
R,[a] % [$I > 2\sigma$]	5.22	4.65
R_w,[a] % [$I > 2\sigma$]	14.92	11.61

[a] $R = \sum||F_o| - |F_c||/\sum|F_o|$. $R_w = \{[\sum w(F_o^2 - F_c^2)^2]/[\sum w(F_o^2)^2]\}^{1/2}$.

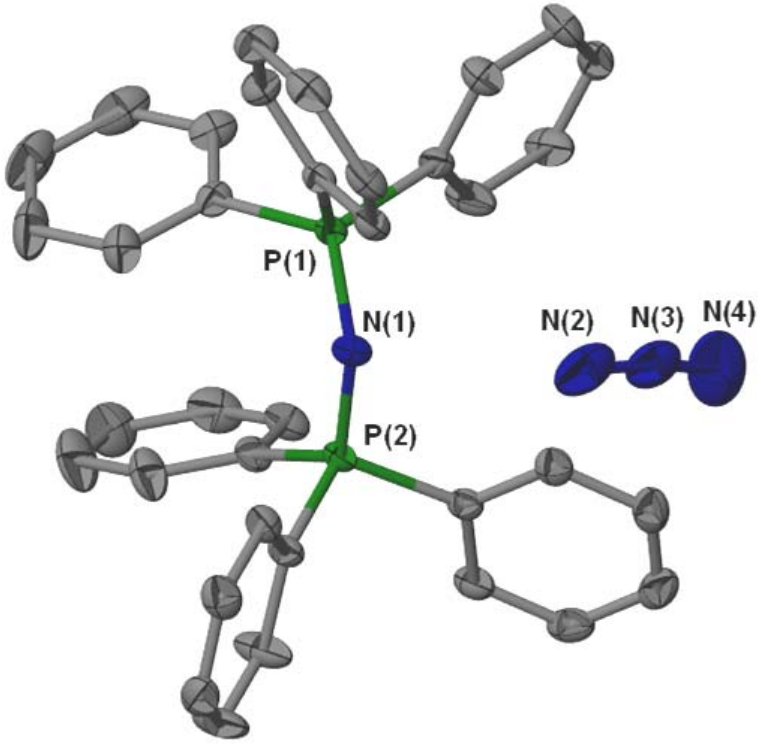

Figure 60. X-ray crystal structures of $PPNN_3$. Thermal ellipsoids are shown at the 50% probability level with hydrogens and solvent molecule omitted for clarity.

The solid state crystal structure of $PPNN_3$ in Figure 60 illustrates the near uninhibited freedom of the azide anion due to the steric bulk around the positively charged ammonium nitrogen of the PPN cation (Table 21). In the solid state, the azide anion resides 4.424 Å from the ammonium nitrogen and 2.608 Å from the nearest phenyl group on the cation. In contrast, the solid state crystal structure of PPNBr (Table 21) packs in an arrangement such that the bromide anion is 4.693 Å away from the nearest ammonium nitrogen and is most closely contacted by a phenyl group of a neighboring PPN cation at a distance of 2.950 Å (Figure 61). In both structures the loose ion pairing

of between the PPN cation and its anion is clearly seen. These and other structural characteristics are listed in Table 22.

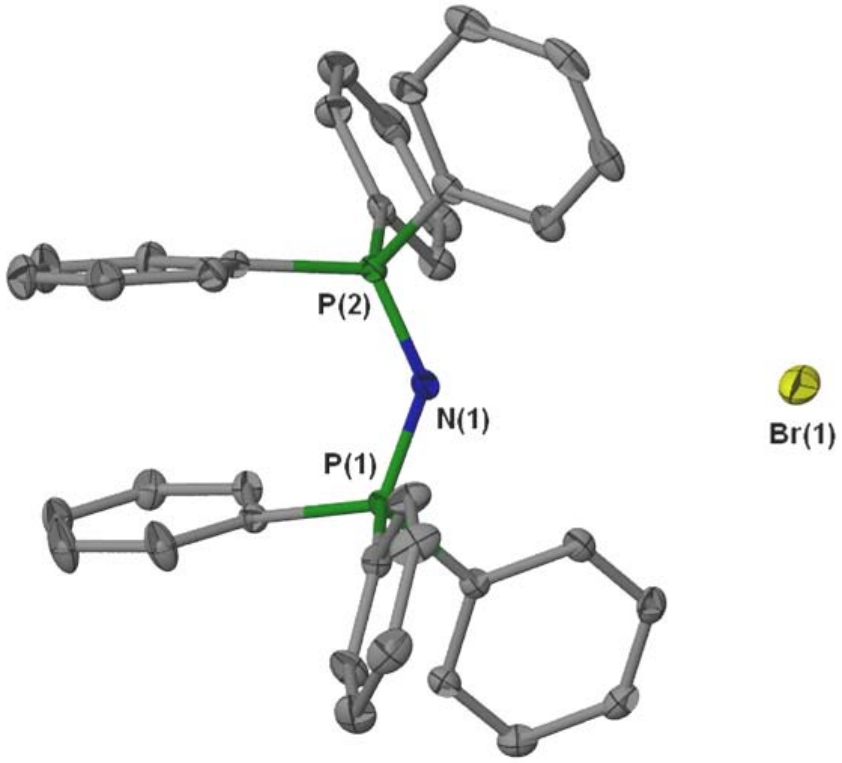

Figure 61. X-ray crystal structures of PPNBr. Thermal ellipsoids are shown at the 50% probability level with hydrogens and solvent molecules omitted for clarity.

Table 22. Selected Bond Distances and Angles for $PPNN_3$ and PPNBr.

	$PPNN_3$	**PPNBr**
N1 – N2 (Å)	4.424	------
N1 – Br (Å)	------	4.693
N2 – N3 (Å)	1.098(3)	------
N3 – N4 (Å)	1.213(4)	------
N1 – P1 (Å)	1.5748(15)	1.583(2)
N1 – P2 (Å)	1.5770(15)	1.578(2)
P1 – N1 – P2 (deg)	142.66(11)	135.69(14)
N2 – N3 – N4 (deg)	168.0(3)	------

Conclusions

Although the chromium complexes incorporating the cyanated ligands, H_2tmtaaCN (**9**) and H_2tmtaa$(CN)_2$ (**10**), were never synthesized, important experimental experience and structural insight was gained. The knowledge gained has lead to the inspiration of other ligand ideas as well as a better understanding of the electronic environment of the tetramethyltetraazaannulene framework. Ongoing efforts are being made to further investigate the derivatization potential at the γ and γ' positions and their electronic effect on the metal, with the goal of developing an even more efficient catalyst for the copolymerization of carbon dioxide and epoxide.

The use of PPN salt cocatalysts to aid the formation of polycarbonates from epoxide and carbon dioxide has been an unquestionable milestone in the development of highly active catalyst systems. Their straightforward synthesis, hydrophobicity, and non-interacting nature are all well understood. Presented herein, to augment previous

understanding of other PPN complexes is the structural details for $PPNN_3$ and PPNBr explaining the nature of the ion pair interaction and the PPN cation's ability to deliver a "free" anion.

CHAPTER VI

CONCLUSIONS

With ever-growing concern for the environment, there is a significant push from society for scientists to develop products and services that have a more green impact on the planet. One such process under scrutiny for its use of harmful chemicals is the production of poly(bisphenol A carbonate), a high-strength thermoplastic that has become ubiquitous in today's marketplace. An alternative route to the formation of polycarbonate plastics while avoiding the use of phosgene, bisphenol A, and chlorinated solvents is through the copolymerization of epoxides and carbon dioxide. Pioneered by Inoue in 1969 and later developed by key scientists such as Darensbourg, Kruper and Holmes, Coates, Nozaki, and Lee, the field of environmentally benign polycarbonate formation utilizing CO_2 has exploded in the areas of catalyst design, monomer availability, and process development. For the majority of the Darensbourg group's investigation of this process, efforts have focused on understanding and developing the mechanism of chromium salen catalyst system.

In continuation of this convention, the goal of this work was to develop a new catalyst system for the copolymerization of epoxides and carbon dioxide. The catalyst's framework, a Schiff base tetraazaannulene macrocycle, was selected for its numerous reports in the literature, straight forward and inexpensive synthesis, and its similarity to the architecture of the salen ligand. The entirety of this dissertation was devoted to the

structural and mechanistic study of the chromium tetramethyltetraazaannulene catalyst system. Initial results for the parent complex, Cr(tmtaa)Cl, showed it to be a highly active catalyst for the copolymerization of cyclohexene oxide and carbon dioxide to produce poly(cyclohexylene carbonate) with molecular weights ranging from 10,000 to nearly 30,000 $g \cdot mol^{-1}$, near quantitative CO_2 incorporation, and narrow polydispersities (≤ 1.1). Further optimization of the catalyst lead to activities of 1500 turnovers per hour, about 25% faster than the most active chromium salen catalyst. Another advantage over the chromium salen system was discovered when investigating the affect of cocatalyst on Cr(tmtaa)Cl. In the presence of several equivalents of excess PPNCl or $PPNN_3$ cocatalyst, only trace amounts of the cyclic cyclohexylene carbonate byproduct was observed. This is in contrast to analogous polymerizations conducted with a chromium salen catalyst where the cyclic byproduct was more prevalent, although selectivity towards copolymer formation was still highly favored.

After achieving a basic understanding of the chromium tetramethyltetraazaannulene system, other aspects were investigated, such as the effects of various cocatalyst anions, CO_2 pressure, adjusting the electronic environment of the ligand, and the employment of epoxides other than cyclohexene oxide. Copolymerization reactions were conducted using halides, such as chloride and bromide, pseudohalides, such as azide and cyanide, and the pentafluorobenzoate anion as cocatalysts. The catalytic activity of Cr(tmtaa)Cl (**1**) did not exhibit a preference for either the chloride or azide anions, achieving TOFs of nearly 1500 h^{-1}. The cyanide anion facilitated the third most active cocatalyst with a TOF of ~1160 h^{-1}, followed by

bromide and pentafluorobenzoate with TOFs of ~800 and 660 h^{-1}, respectively. These results indicate complex **1** favors hard, nucleophilic cocatalyst anions over the larger and softer anions, like bromide and pentafluorobenzoate, which are less able to donate electron density to the metal center. Similar behavior was observed with the chromium salen system[56] with the exception that **1** exhibits higher catalytic activities and reduced sensitivity towards the anion species. Pressure dependence studies were conducted to investigate the catalyst's tolerance to various pressures of carbon dioxide, with the hope that **1** would sustain activity at lower, more industrially advantageous conditions. The studies revealed that while the catalyst is most active under 35 bar CO_2, **1** still maintained considerable activity at pressures as low 1 bar. The infrared reaction profile did reveal a large decrease in activity as carbon dioxide was consumed, but it is believed that the initial copolymerization rate could be maintained if the pressure was replenished and maintained at 1 bar. In efforts to optimize the catalytic activity, electron-withdrawing and -donating substituents were added to the phenylene moieties and the corresponding polymerization activities compared to those obtained for **1**. While the methyl-derivatized catalyst, Cr(omtaa)Cl (**3**), performed at rates marginally different than **1**, the copolymerization activity of the chloro-derivatized complex, Cr(tmtaaCl_4)Cl (**2**), was decreased. From these results, **1** was determined the optimal catalyst. It was hypothesized that the > 0.4 Å elevation of the chromium metal over the nitrogen donor plane would allow the activation of epoxides with greater steric bulk. These monomers include epoxides that might afford polycarbonates with desirable properties based on known commodity plastics, such as styrene oxide, as well as several aliphatic epoxides

and those derived from natural, renewable resources, like limonene oxide and α-pinene oxide. Unfortunately, **1** was unable to copolymerize these epoxides, but varying degrees of cyclic carbonate were observed via infrared spectroscopy. Complex **1** was able to rapidly copolymerize 4-vinylcyclohexene oxide with a rate close to polymerizations conducted employing cyclohexene oxide. Poly(4-vinylcyclohexylene carbonate) is of interest due to the potential for post-polymerization transformations into a wide variety of products. Investigations into the scope of such transformations are currently underway in the Darensbourg labs.

The desire to thoroughly understand the chromium tetramethyltetraazaannulene system has lead to kinetic investigations in both neat cyclohexene oxide and in the presence of a cosolvent. The use of dichloromethane as a cosolvent afforded a quantitative conversion of cyclohexene oxide by preventing the significant viscosity increase that limits mass transfer of monomer to catalyst observed in polymerizations conducted in neat epoxide. Unfortunately, the activity of **1** was severely retarded when dichloromethane was present in the reaction mixture and cyclic carbonate formation was much more significant. A range of reaction temperatures was explored and the activation energies for poly(cyclohexylene carbonate) and cyclohexylene carbonate were estimated using the enthalpy of activation values from an Eyring analysis and found to be 65.2 and 80.3 $kJ \cdot mol^{-1}$, respectively. Similarly, the polymerizations conducted in neat cyclohexene oxide were analyzed by the method of initial rates, where the reaction rate was measured before any significant changes in concentration or viscosity could occur. This allowed for the activation energies for poly(cyclohexylene carbonate) and

cyclohexylene carbonate to be directly determined through application of the Arrhenius equation, and were found to be 67.1 ± 4.2 and 91.2 ± 10.5 kJ-mol^{-1}, respectively. The higher activation barrier for cyclic carbonate formation in neat epoxide than in the presence of a cosolvent, 91.2 vs. 80.3 kJ-mol^{-1}, is evident from the reaction profiles, where trace formation is observed throughout the course of the reaction until polymer formation ceases due to viscosity effects.

In the interest of gaining insight into the mechanism of the copolymerization of epoxides with carbon dioxide, two new catalysts were developed to investigate an aspect of the process that has remained unanswered. The goal of this study was to elucidate whether polymer chain propagation proceeded from one side of the catalyst in a monocatalytic single-site manner or from both sides via a dicatalytic single-site mechanism. Prior studies have speculated a double sided process, concluded from analysis of the polymers by GPC.[23,26,32,33] However, support for a one-sided propagation mechanism was present by interpreting the in situ infrared reaction rate profiles which monitored polymer formation throughout the course of the reaction. To investigate these conflicting theories, the newly developed catalyst, based on the chromium tetramethyltetraazaannulene system, was designed to test the copolymerization mechanism from a steric approach, where access to one side of the metal center would be restricted by a strap connecting opposite sides of the ligand framework. Previous catalysts utilizing porphyrin or salen ligands do not possess a feasible geometry to assess the copolymerization mechanism by these means. Infrared and X-ray data affirmed the cavity on the underside of the strapped chromium complex, Cr(stmtaa)Cl (**7**), was large

enough to allow binding of a chloride cocatalyst, but restricting enough to forbid an azide anion. In order to mimic **7** for control purposes, the second catalyst, Cr(s^mtmtaa)Cl (**8**), contained a similar electronic environment without the steric bulk provided by the tether and was confirmed by infrared spectroscopy to unselectively bind cocatalyst in the same manner as **1**. Comparative copolymerizations between **7** and **8** resulted in the production of poly(cyclohexylene carbonate) at near identical rates, achieving TOFs of 807 and 797 h^{-1}, respectively. The isolated polymers from these reactions were found to contain > 99% carbonate linkages and have molecular weights and polydispersity indices of 11,431 $g \cdot mol^{-1}$ and 1.108 for **7** and 12,003 $g \cdot mol^{-1}$ and 1.048 for **8**. The similarity in catalytic activity, infrared and X-ray data, and polymer properties obtained from this study and their agreement with properties of polymers obtained using **1** as a catalyst all strongly support a monocatalytic single-site mechanistic pathway where copolymer formation proceeds from only one side of the catalyst.

Future development of this catalyst system could be concentrated in areas of more extensive ligand derivatization, polymer/catalyst separation, and the use of different monomers to produce polycarbonates with new properties. Thus far, modifying the ligand to investigate the effect on catalytic activity has been limited to the phenylene moieties. Exploring methods to add electron-donating substituents to the γ and γ' positions could increase catalyst activity through greater communication with the metal center. Substitution of the phenylene moieties for enantiomerically pure cyclohexylene groups would result in a chiral complex and possible stereocontrol of the polymer

products. Other modifications, such as the addition of cationic arms, have greatly increased the activity of cobalt salen towards propylene oxide and carbon dioxide copolymerization and provided a means for catalyst recyclability[35] and could possibly provide the same benefits to the tetraazaannulene system. Catalyst separation could also be explored using methods shown previously to work for chromium salen, such as switchable polarity solvents and the addition of low molecular weight isobutylene groups to facilitate polymer extraction through solvent phase separation.[98,99] Despite the limited success in producing polycarbonates from various epoxides discussed *vide supra*, further investigation into other monomers is also worth exploring. Since epoxides are synthesized from a wide variety of synthetic and naturally occurring olefins, they are an attractive feedstock for the production of commercial plastics. Chromium tetramethyltetraazaannulene's success with cyclohexene oxide and 4-vinyl cyclohexene oxide warrants trials with other alicyclic epoxides such as norbornene oxide, among others.

In summary, it is with hope that this dissertation has demonstrated the time and effort that has gone into the development of the chromium tetramethyltetraazaannulene catalyst system, both structurally and mechanistically. Although the ligand system has been around for 40 years, with numerous transition metal and derivatized compounds reported, these complexes have rarely been applied in catalytic processes. This work presents a complex that was developed into the fastest and most selective known chromium catalyst to date. It has also provided valuable mechanistic details for the copolymerization of cyclohexene oxide and carbon dioxide previously unexplored. In

the past decade, the number of reports involving this ligand system has been much decreased. Hopefully this dissertation will rekindle interest in this unique ligand, remind others of the importance of catalyst development and embolden them to explore directions inspired by this work.

REFERENCES

(1) De Simone, J. In *Greenhouse Gas Control Technol., Proc. Int. Conf. 6th* **2003**, p 33.

(2) Vansant, J. In *Recovery and Utilization of Carbon Dioxide*; Aresta, M., Ed.; Klumer Academic Publishers: The Netherlands, 2003; pp.3-50.

(3) Vom Saal, F. S.; Hughes, C. *Environ. Health Perspect.* **2005**, *113*, 926-933.

(4) ICIS *Polycarbonate Uses and Market Data*; http://www.icis.com/v2/chemicals/9076146/polycarbonate/uses.html (Accessed December 2008), Reed Business Information Limited, Surrey, 2008.

(5) Legrand, D. G.; Bendler, J. T. *Handbook of Polycarbonate Science and Technology*; Marel Dekker, Inc.: New York, 2000.

(6) Stevens, P. M., Ed. *Polymer Chemistry: An Introduction*; 3rd ed.; Oxford University Press: New York, 1999.

(7) Darensbourg, D. J.; Holtcamp, M. W. *Macromolecules* **1995**, *28*, 7577-7579.

(8) Inoue, S.; Koinuma, H.; Tsuruta, T. *J. Polym. Sci., Part C: Polym. Lett.* **1969**, *7*, 287-292.

(9) Inoue, S. *J. Polym. Sci., Part A: Polym. Chem.* **2000**, *38*, 2861-2871.

(10) Cheng, M.; Lobkovsky, E. B.; Coates, G. W. *J. Am. Chem. Soc.* **1998**, *120*, 11018-11019.

(11) Mang, S.; Cooper, A. I.; Colclough, M. E.; Chauhan, N.; Holmes, A. B. *Macromolecules* **2000**, *33*, 303-308.

(12) Darensbourg, D. J.; Yarbrough, J. C. *J. Am. Chem. Soc.* **2002**, *124*, 6335-6342.

(13) Hansen, K. B.; Leighton, J. L.; Jacobsen, E. N. *J. Am. Chem. Soc.* **1996**, *118*, 10924-10925.

(14) Darensbourg, D. J.; Mackiewicz, R. M.; Phelps, A. L.; Billodeaux, D. R. *Acc. Chem. Res.* **2004**, *37*, 836-844.

(15) Nakano, K.; Nozaki, K.; Hiyama, T. *Macromolecules* **2001**, *34*, 6325-6332.

(16) Mackiewicz, R. M. Ph.D. Dissertation, Texas A&M University, 2005.

(17) Takeda, N.; Inoue, S. *Makromol. Chem.* **1978**, *179*, 1377-1381.

(18) Aida, T.; Inoue, S. *Macromolecules* **1981**, *14*, 1162-1166.

(19) Aida, T.; Inoue, S. *Macromolecules* **1981**, *14*, 1166-1169.

(20) Aida, T.; Inoue, S. *Macromolecules* **1982**, *15*, 682-684.

(21) Aida, T.; Inoue, S. *J. Am. Chem. Soc.* **1983**, *105*, 1304-1309.

(22) Aida, T.; Inoue, S. *J. Am. Chem. Soc.* **1985**, *107*, 1358-1364.

(23) Aida, T.; Ishikawa, M.; Inoue, S. *Macromolecules* **1986**, *19*, 8-13.

(24) Qin, Y.; Wang, X.; Zhao, X.; Wang, F. *Chin. J. Polym. Sci.* **2008**, *2*, 241-247.

(25) Sugimoto, H.; Ohshima, H.; Inoue, S. *J. Polym. Sci., Part A: Polym. Chem.* **2003**, *41*, 3549-3555.

(26) Qin, Y.; Wang, X.; Zhang, S.; Zhao, X.; Wang, F. *J. Polym. Sci., Part A: Polym. Chem.* **2008**, *46*, 5959-5967.

(27) Kruper, W. J.; Dellar, D. V. *J. Org. Chem.* **1995**, *60*, 725-727.

(28) Pfeiffer, P.; Breith, E.; Lübbe, E.; Tsumaki, T. *Liebigs Ann.* **1933**, *503*, 84-130.

(29) Diehl, H.; Hach, C. C.; Bailar, J. C. In *Inorganic Syntheses*; Ludwig, F. A., Ed.; McGraw-Hill: New York, 1950; Vol. 3, pp.196-201.

(30) Lu, X.-B.; Feng, X.-J.; He, R. *Appl. Catal., A* **2002**, *234*, 25-33.

(31) Lu, X.-B.; He, R.; Bai, C.-X. *J. Mol. Catal. A: Chem.* **2002**, *186*, 1-11.

(32) Sugimoto, H.; Ohtsuka, H.; Inoue, S. *J. Polym. Sci., Part A: Polym. Chem.* **2005**, *43*, 4172-4186.

(33) Nakano, K.; Kamada, T.; Nozaki, K. *Angew. Chem., Int. Ed.* **2006**, *45*, 7274-7277.

(34) Noh, E. K.; Na, S. J.; S, S.; Kim, S. W.; Lee, B. Y. *J. Am. Chem. Soc.* **2007**, *129*, 8082-8083.

(35) S, S.; Min, J. K.; Seong, J. E.; Na, S. J.; Lee, B. Y. *Angew. Chem., Int. Ed.* **2008**, *47*, 7306-7309.

(36) Jacobsen, E. N.; Tokunaga, M.; Larrow, J. F. PCT Int. Appl. WO 2000009463, 2000.

(37) Darensbourg, D. J.; Frantz, E. B. *Inorg. Chem.* **2007**, *46*, 5967-5978.

(38) Frantz, E. B. Ph.D. Dissertation, Texas A&M University, 2008.

(39) Cotton, F. A.; Czuchajowska, J. *Polyhedron* **1990**, *9*, 2553-2566.

(40) Mountford, P. *Chem. Soc. Rev.* **1998**, *27*, 105-116.

(41) Goedken, V. L.; Pluth, J. J.; Peng, S.-M.; Bursten, B. *J. Am. Chem. Soc.* **1976**, *98*, 8014-8021.

(42) Weiss, M. C.; Bursten, B.; Peng, S.-M.; Goedken, V. L. *J. Am. Chem. Soc.* **1976**, *98*, 8021-8031.

(43) De Angelis, S.; Solari, E.; Gallo, E.; Floriani, C.; Chiesi-Villa, A.; Rizzoli, C. *Inorg. Chem.* **1992**, *31*, 2520-2527.

(44) Solari, E.; De Angelis, S.; Floriani, C.; Chiesi-Villa, A.; Rizzoli, C. *Inorg. Chem.* **1992**, *31*, 96-101.

(45) E.-G. Jäger *Z. Anorg. Chem.* **1969**, *364*, 177-191.

(46) Goedken, V.; Molin-Case, J.; Whang, Y. *Chem. Comm.* **1973**, *1973*, 337-338.

(47) Goedken, V. L.; Weiss, M. C. *Inorg. Synth.* **1980**, *20*, 115-119.

(48) Cotton, F. A.; Czuchajowska, J.; Falvello, L. R.; Feng, X. *Inorg. Chim. Acta* **1990**, *172*, 135-136.

(49) Demadis, K. D.; Meyer, T. J.; White, P. S. *Inorg. Chem.* **1998**, *37*, 3610-3619.

(50) *SAINT-Plus*, version 6.02; Bruker: Madison, WI, 1999.

(51) *SHELXS-86*, Sheldrick, G.: Institut fur Anorganische Chemie der Uniseritat Gottingen: Gottingen, Germany, 1986.

(52) *SHELXL-87*, Sheldrick, G.: Institut fur Anorganische Chemie der Uniseritat Gottingen: Gottingen, Germany, 1987.

(53) *SHELXTL*, version 5.0; Bruker: Madison, WI, 1999.

(54) Barbour, L. J. *J. Supramol. Chem.* **2001**, *1*, 189-191.

(55) Hao, S.; Edema, J. H. H.; Gambarotta, S.; Bensimon, C. *Inorg. Chem.* **1992**, *31*, 2676-2678.

(56) Darensbourg, D. J.; Mackiewicz, R. M. *J. Am. Chem. Soc.* **2005**, *127*, 14026-14038.

(57) Darensbourg, D. J.; Yarbrough, J. C.; Ortiz, C.; Fang, C. C. *J. Am. Chem. Soc.* **2003**, *125*, 7586-7591.

(58) Darensbourg, D. J.; Mackiewicz, R. M.; Rodgers, J. L.; Fang, C. C.; Billodeaux, D. R.; Reibenspies, J. H. *Inorg. Chem.* **2004**, *43*, 6024-6034.

(59) Darensbourg, D. J.; Mackiewicz, R. M.; Rodgers, J. L.; Phelps, A. L. *Inorg. Chem.* **2004**, *43*, 1831-1833.

(60) Darensbourg, D. J.; Mackiewicz, R. M.; Billodeaux, D. R. *Organometallics* **2005**, *24*, 144-148.

(61) Darensbourg, D. J. *Chem. Rev.* **2007**, *107*, 2388-2410.

(62) L'Eplattenier, F. A.; Pugin, A. *Helv. Chim. Acta* **1975**, *58*, 917-929.

(63) Place, D. A.; Ferrara, G., P.; Harland, J. J.; Dabrowiak, J. C. *J. Heterocycl. Chem.* **1980**, *17*, 439-443.

(64) Jäger, E.-G. *Z. Anorg. Chem.* **1969**, *364*, 177-191.

(65) Alcock, N. W.; Cannadine, J. C.; Errington, W.; Moore, P.; Wallbridge, M. G. H. *Acta Crystallogr., Sect. C: Cryst. Struct. Commun.* **1994**, *50*, 2037-2039.

(66) Buzatu, D. A.; Nolan, S. P.; Stevens, E. D. *Acta Crystallogr., Sect. C: Cryst. Struct. Commun.* **1995**, *51*, 1855-1857.

(67) Darensbourg, D. J.; Fitch, S. B. *Inorg. Chem.* **2007**, *46*, 5474-5476.

(68) Darensbourg, D. J.; Moncada, A. I. *Inorg. Chem.* **2008**, *47*, 10000-10008.

(69) Cohen, C. T.; Chu, T.; Coates, G. W. *J. Am. Chem. Soc.* **2005**, *127*, 10869-10878.

(70) Cohen, C. T.; Coates, G. W. *J. Polym. Sci., Part A: Polym. Chem.* **2006**, *44*, 5182-5191.

(71) Cohen, C. T.; Thomas, C. M.; Peretti, K. L.; Lobkovsky, E. B.; Coates, G. W. *Dalton Trans.* **2006**, 237-249.

(72) Darensbourg, D. J.; Niezgoda, S. A.; Draper, J. D.; Reibenspies, J. H. *J. Am. Chem. Soc.* **1998**, *120*, 4690-4698.

(73) Darensbourg, D. J.; Holtcamp, M. W.; Struck, G. E.; Zimmer, M. S.; Niezgoda, S. A.; Rainey, P.; Robertson, J. B.; Draper, J. D.; Reibenspies, J. H. *J. Am. Chem. Soc.* **1999**, *121*, 107-116.

(74) Darensbourg, D. J.; Wildeson, J. R.; Lewis, S. J.; Yarbrough, J. C. *J. Am. Chem. Soc.* **2002**, *124*, 7075-7083.

(75) Eberhardt, R.; Allmendinger, M.; Rieger, B. *Macromol. Rapid Commun.* **2003**, *24*, 194-196.

(76) Chisholm, M. H.; Zhou, Z. *J. Am. Chem. Soc.* **2004**, *126*, 11030-11039.

(77) Darensbourg, D. J.; Phelps, A. L. *Inorg. Chem.* **2005**, *44*, 4622-4629.

(78) Qin, Z.; Thomas, C. M.; Lee, S.; Coates, G. W. *Angew. Chem., Int. Ed.* **2003**, *42*, 5484-5487.

(79) Lu, X.-B.; Wang, Y. *Angew. Chem., Int. Ed.* **2004**, *43*, 3574-3577.

(80) Lee, B. Y.; Kwon, H. Y.; Lee, S. Y.; Na, S. J.; Han, S.-i.; Yun, H.; Lee, H.; Park, Y.-W. *J. Am. Chem. Soc.* **2005**, *127*, 3031-3037.

(81) Paddock, R. L.; Nguyen, S. T. *Macromolecules* **2005**, *38*, 6251-6253.

(82) Koning, C.; Wildeson, J.; Parton, R.; Plum, B.; Steeman, P.; Darensbourg, D. J. *Polymer* **2001**, *42*, 3995-4004.

(83) Hsu, T.-J.; Tan, C.-S. *Polymer* **2002**, *43*, 4535-4543.

(84) Cherian, A. E.; Sun, F. C.; Sheiko, S. S.; Coates, G. W. *J. Am. Chem. Soc.* **2007**, *129*, 11350-11351.

(85) Darensbourg, D. J.; Rodgers, J. L.; Fang, C. C. *Inorg. Chem.* **2003**, *42*, 4498-4500.

(86) Darensbourg, D. J.; Bottarelli, P.; Andreatta, J. R. *Macromolecules* **2007**, *40*, 7727-7729.

(87) Darensbourg, D. J.; Fitch, S. B. *Inorg. Chem.* **2008**, *47*, 11868-11878.

(88) Sakata, K.; Ueno, A.; Jibuta, T.; Hashimoto, M. *Synth. React. Inorg. Met.-Org. Chem.* **1993**, *23*, 1107 - 1115.

(89) Elwahy, A. H. M.; Abbas, A. A. *Tetrahedron* **2000**, *56*, 885-895.

(90) Sakata, K.; Saitoh, Y.; Kawakami, K.; Nakamura, N.; Hashimoto, M. *Synth. React. Inorg. Met.-Org. Chem.* **1995**, *25*, 1279 - 1293.

(91) Eilmes, J. *Polyhedron* **1985**, *4*, 943-946.

(92) Alcock, N. W.; Busch, D. H.; O'Brien, J. (2005) Private communication to the Cambridge Structural Database, deposition number CCDC 286491.

(93) Alcock, N. W.; Busch, D. H.; O'Brien, J. (2005) Private communication to the Cambridge Structural Database, deposition number CCDC 286494.

(94) Eilmes, J.; Ptaszek, M.; Zielinska, K. *Polyhedron* **2001**, *20*, 143-149.

(95) Sliwinski, J.; Eilmes, J.; Oleksyn, B. J.; Stadnicka, K. *J. Mol. Struct.* **2004**, *694*, 1-19.

(96) Allen, S. D.; Moore, D. R.; Lobkovsky, E. B.; Coates, G. W. *J. Organomet. Chem.* **2003**, *683*, 137-148.

(97) Moore, D. R.; Cheng, M.; Lobkovsky, E. B.; Coates, G. W. *Angew. Chem. Int. Ed.* **2002**, *41*, 2599-2602.

(98) Hongfa, C.; Tian, J.; Andreatta, J.; Darensbourg, D. J.; Bergbreiter, D. E. *Chem. Comm.* **2008**, 975-977.

(99) Phan, L.; Andreatta, J. R.; Horvey, L. K.; Edie, C. F.; Luco, A.-L.; Mirchandani, A.; Darensbourg, D. J.; Jessop, P. G. *J. Org. Chem.* **2008**, *73*, 127-132.

VITA

Shawn Brendan Fitch was born at Harris Methodist Hospital in Fort Worth, TX in January 1982. At the age of five, he moved with his family to Weatherford, TX where he graduated from Weatherford High School in 2000. He then attended Texas A&M University in College Station, TX where he graduated with a Bachelors of Science in chemistry with an American Chemical Society Certification in May 2004. In June of the same year he continued his education by starting his graduate program under the guidance of Drs. Donald J Darensbourg and Marcetta Y. Darensbourg and graduated with a Doctorate of Philosophy in May 2009. Questions and comments may be directed to Dr. Donald J. Darensbourg at MS 3255, Department of Chemistry, Texas A&M University, College Station, TX 77843-3255.